The determination and modelling of the brittle structures of the Kumpula Campus Drill hole

Riikka Valtonen
December, 2018
Master's Thesis
Department of Geosciences and Geography
Division of Geology
University of Helsinki

Tiedekunta – Fakultet – Faculty	Koulutusohjelma – Utbildningsprogram – Degree programme
Faculty of Science	Geology

Tekijä – Författare – Author	
Riikka Olga Maria Valtonen	

Työn nimi – Arbetets titel – Title		
The determination and modelling of the brittle structures of the Kumpula Campus Drill hole		

Työn laji – Arbetets art – Level	Aika – Datum – Month and year	Sivumäärä – Sidoantal – Number of pages
Master's Thesis	December 2018	86+28

Tiivistelmä – Referat – Abstract

A 370 meter deep drill hole was drilled on the Kumpula Campus of the Univerity of Helsinki for teaching purposes at the end of the year 2015. This work deals with fragile structures in the borehole, which have been compared with existing research data from the Helsinki area and nearby outcrop data.

Natural breaks were observed and measured from the drill core and that data was compared to the acoustic and optical images of the drill hole in the Wellcad software. The drill core was not oriented, so the dip direction and dip of the breaks were measured in the Wellcad software and the final correction was made in Excel. depth, possible filling, surface roughness, and slickenside feature of the breaks were recorded. A preliminary RQD value was also measured, which was excellent (94%). Five filling samples, which differed in color and texture, were subjected to XRD analysis. Approximately 700 natural breaks plus two crushed zones, with hearth loss were found found in the drill core. About 11% of the breaks were classified as slickensides. Most of the other break points were filled with minerals. a fracture group in which the gap was not open in the core was observed on the basis of the acoustic image. These kinds of fractures were about 11% of the natural breaks.

Comparative field work was carried out on Kumpula campus and surroundings. There were altogether ten outcrops, three of them were road cuts. In addition to the location and direction and dipping, the visible length of the fracture, possible filling of surfaces, surface roughness, and density of the parallel fractures were observed. Observations were greatly affected by the quality and freshness of the outcrops.

The main processing of the results was carried out in software Move in 3D, in which the fractures of the drill hole and the collected outcrop fracture data were compared, and the locations of the crushed zones were examined more closely. Both drill hole fractures and the fractures from the outcrops have one main dip direction to the northeast (ie the strike towards the NW), which is in line with previous studies in the Helsinki area. The study also revealed that the strikes of the fractures differ in the northern and southern sides on the hill: the main direction on the south side was in NW-SE, while on the north side it was in E-W direction. To further reinforce this finding, more data is needed, e.g. a comparative borehole on the north side of the hill would provide extra exposure for this possible direction. Another interesting research topic would be the more accurate classification of the drill hole fractures with the help of fillings. The preliminary studies show that slickensides differ from other filled fractures in both the orientation and filling and there are at least four different fillings as well. Such studies could help in estimating the relative ages of the brittle structures.

Avainsanat – Nyckelord – Keywords
Kumpula, Fracture, slickenside, Fracture filling, Helsinki, Structural geology

Säilytyspaikka – Förvaringställe – Where deposited
University of Helsinki

Muita tietoja – Övriga uppgifter – Additional information

Tiedekunta – Fakultet – Faculty		Koulutusohjelma – Utbildningsprogram – Degree programme	
Matemaattis-luonnontieteellinen		Geologia	
Tekijä – Författare – Author			
Riikka Olga Maria Valtonen			
Työn nimi – Arbetets titel – Title			
Kumpulan kairasydämen hauraiden rakenteiden määritys ja mallinnus			
Työn laji – Arbetets art – Level	Aika – Datum – Month and year		Sivumäärä – Sidoantal – Number of pages
Pro Gradu	joulukuu 2018		86+28

Tiivistelmä – Referat – Abstract

Kumpulan kampukselle kairattiin vuoden 2015 lopulla 370 metriä syvä kairareikä opetustarkoitukseen. Tämä työ käsittelee kairareiän hauraita rakenteita, joita on verrattu jo olemassa olevaan tutkimustietoon Helsingin alueelta sekä ympäristön paljastumilta.

Kairasydämestä kerättiin perustieto katko kohdista, joita verrattiin Wellcad-ohjelmassa kairareiästä kuvattuun akustiseen ja optiseen kuvaan. Kairasydän ei ollut suunnattu, joten katkoskohtien kaadesuunta ja kaade saatiin mitattua Wellcad-ohjelmassa ja lopullinen suuntakorjaus tehtiin Excelissä laskien. Katkoskohdista kirjattiin ylös syvyys, mahdollinen rakotäyte, pinnan karheus sekä haarniskapinnan- ominaisuudet. Myös alustava RQD-arvo mitattiin, joka oli erinomainen (94%). Viidestä rakotäytteestä, jotka erosivat toisistaan väriltään ja tekstuuriltaan, tehtiin XRD-analyysi. Luonnollisia katkoksia laskettiin olevan kairasydämessä noin 700 kappaletta sekä kaksi selkeää ruhjetta, joissa oli sydänhukkaa. Noin 11 % katkoksista luokiteltiin haarniskaraoiksi. Suurin osa raoista oli täytteisiä. Akustisen kuvan perusteella havaittiin rakoryhmä, jossa raot eivät olleet avoinna kairasydämessä, mutta erottuivat akustisessa kuvassa selkeästi. Näitä oli myös noin 11 % luonnollisesta katkossummasta.

Vertailevat kenttätyöt suoritettiin Kumpulan kampusmäellä ja ympäristössä. Paljastumia oli yhteensä kymmenen, joista kolme oli tieleikkauksia. Paljastumilta mitattiin sijainnin ja suunnan ja kaateen lisäksi raon näkyvä pituus, mahdollinen rakotäyte, pinnan karheus sekä samansuuntaisten rakojen tiheys. Havaintojen tekemistä vaikeutti huomattavasti kalliopaljastumien huono kunto.

Tulosten pääasiallinen käsittely suoritettiin Move 3D-ohjelmalla, jossa kairasydämen rakojen ja paljastumien rakodataa verrattiin toisiinsa ja kairasydämen ruhjeiden paikkaa tutkittiin lähemmin. Sekä kairasydämen raoissa että paljastumilla tuli esiin rakojen kaadesuunta koilliseen (eli kulku kohti luodetta), joka on linjassa aikaisempien tutkimusten kanssa Helsingin alueelta. Tutkimuksissa tuli myös ilmi, että Kumpulan kalliopaljastumien rakosuunnat eroavat pohjois-eteläsuunnassa: mäen eteläpuolella rakojen pääasiallinen kulkusuunta oli akselilla NW-SE, kun taas pohjoispuolella nousi esiin E-W-kulku suunta. Tämän huomion vahvistamiseen tarvittaisiin vielä enemmän rakodataa, joten esimerkiksi toinen kairareikä pohjoispuolella mäkeä antaisi lisävalotusta tähän mahdolliseen rakosuunnan kääntymiseen pelkästään mäen alueella. Toinen mielenkiintoinen jatko tutkimusaihe olisi kairasydämen rakojen tarkempi luokittelu rakotäytteiden avulla. Nyt alustavissa tutkimuksissa huomattiin, että esimerkiksi haarniskaraot eroavat muista täytteisistä raoista niin kulun kuin täytteen perusteella, sekä että täytteisissä raoissa esiintyy ainakin neljää eri täytettä. Tällaisella tutkimuksella voitaisiin parhaimmassa tapauksessa saada lisää tietoa hauraiden rakenteiden ikäsuhteista.

Avainsanat – Nyckelord – Keywords	
Kumpula, rako, haarniskarako, rakotäyte, Helsinki, rakennegeologia	
Säilytyspaikka – Förvaringställe – Where deposited	
Helsingin yliopisto	
Muita tietoja – Övriga uppgifter – Additional information	

CONTENTS

Appendix I: The depth stations of the drill hole

Appendix II. The complete drill hole fracture data

Appendix III. The complete outcrop fracture data

Appendix IV. The engineering geological values

Appendix V: The XRD-diffractograms

Appendix VI. The 3D-images from the drill hole and dip direction fractures of the outcrops

Appendix VII: The 2D-map of the crushed zones and 3D image from
the crossing point of the crushed zones

Appendix VIII: The 3D-images from different fracture groups in the drill hole

1. INTRODUCTION

One of the leading trends in the modern world is urbanization and people are being packed into increasingly smaller areas. Because the areas of cities are limited, the cities must expand underground and upwards. People are travelling in subways and living in skyscrapers.

Helsinki is also one of the growing cities. The first subway line of Helsinki was opened in 1982, when population of the area was under 500 000 now it is over 600 000. The subway line is extending to the west and cars in the city centre have been increasingly directed underground. However, the city is also growing upwards: the first skyscrapers of Helsinki are under construction.

In order to be able to build cities, the local bedrock must be examined before construction. The main concern are planes of weakness (fractures and faults), which may have to be supported. Not much research, especially in point of view of structural geology, has been done from the bedrock of Helsinki, although such are the base of large-scale construction projects.

One way to investigate brittle structures of the bedrock is to drill. They can then be mapped from the drill core and the drill hole. The drill hole data, however, gives an 1D-image of the fracturing and is always lacking or overrepresented some fracture directions or overrepresenting others. That is why the drill hole observations should be complemented with ground mapping data or, if possible, with tunnel mapping data. Based on these observations and data, it is possible to create and examine a 3D-model of the bedrock, which could expose the problematic zones of the bedrock better. It is also necessary to evaluate the relationships of the brittle structures larger tectonic context, if the structure is supposed to last for hundreds of thousands of years like in the case of the nuclear waste disposal site in Olkiluoto.

This master thesis is related to the Kumpula Campus drill hole (see next chapter) and its aim is to study brittle structures from the drill core and nearby outcrops and make an estimation of rock fragmentation using RQD and Q' parameters, study the fracture fillings, classify brittle structures based on their character and orientation, and finally also

compare these results to the previous studies of brittle structures from the Helsinki area. The results are presented in 3D-model of the Kumpula hill. Besides this study there are two more master thesis projects related to the drill hore. One is related to petrology, which is being prepared by Penttilä (in prep.) and other is related to geochemistry and has been made by Räisänen (2018). These three master theses complete each other, while focusing on different aspects of the drill hole.

1.1. Research area

Research area is situated in southern Finland (Figure 1) in urbanized Helsinki area. The Faculty of Science of the University of Helsinki are situated at the top of the Kumpula hill. The Kumpula hill direction is NE-SW so that is bounded by Kustaa Vaasa road in the east, Kumpula Botanic Garden in the south, Limingantie in the west, and Intiantie in the north (Figure 2). Length in NE-SW direction is about 700 m and width in the NW-SE direction is 500 m. The maximum height of the hill is around 30 meter above sea level.

There are six major outcrops around the Kumpula hill and next to Kustaa Vaasa road there are road cuttings. The Kumpula campus drill hole has been drilled on one of the outcrops on the hill (Figure 2).

In previous studies of Pajunen et al. (2001) has been found out that the nearest brittle zones around the Kumpula located at the eastern side, between Kumpula hill and Arabia and the valley of the Vallila (Figure 3). Structures on the west side of the hill has been classified only slightly weathered. The valley of the Vallila situated at the WNW-ESE axis and the eastern brittle zone located almost in N-S axis. The fracture density on the Kumpula hill is around > 0.5-1.
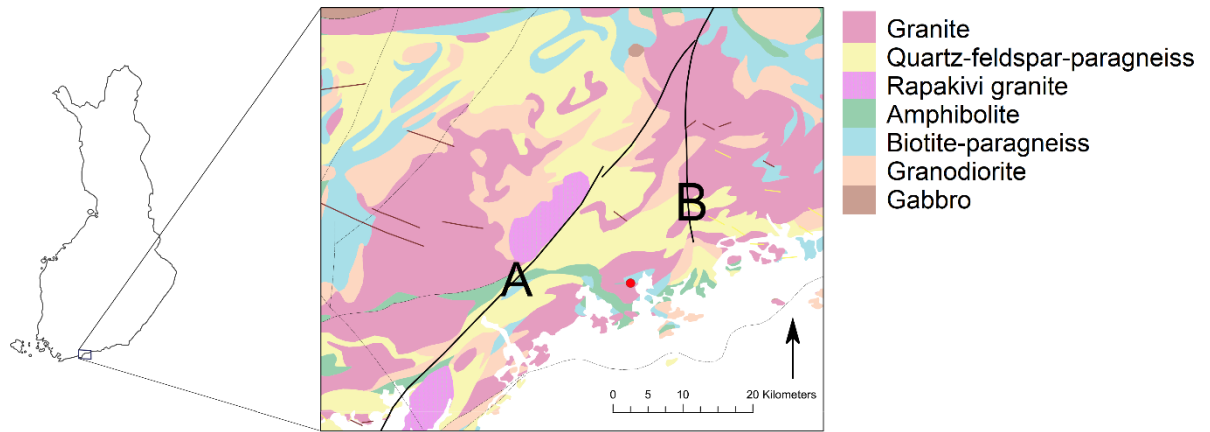
Figure 1. The map of the Finland and around Helsinki area. The location of the research area is marked in the geological map as a red circle. Two largest fault zones (Porkkala-Mäntsälä and Vuosaari-Korso) are indicated with letters A and B. The geological map has been modified after general map of Finland from National Land Survey of Finland.
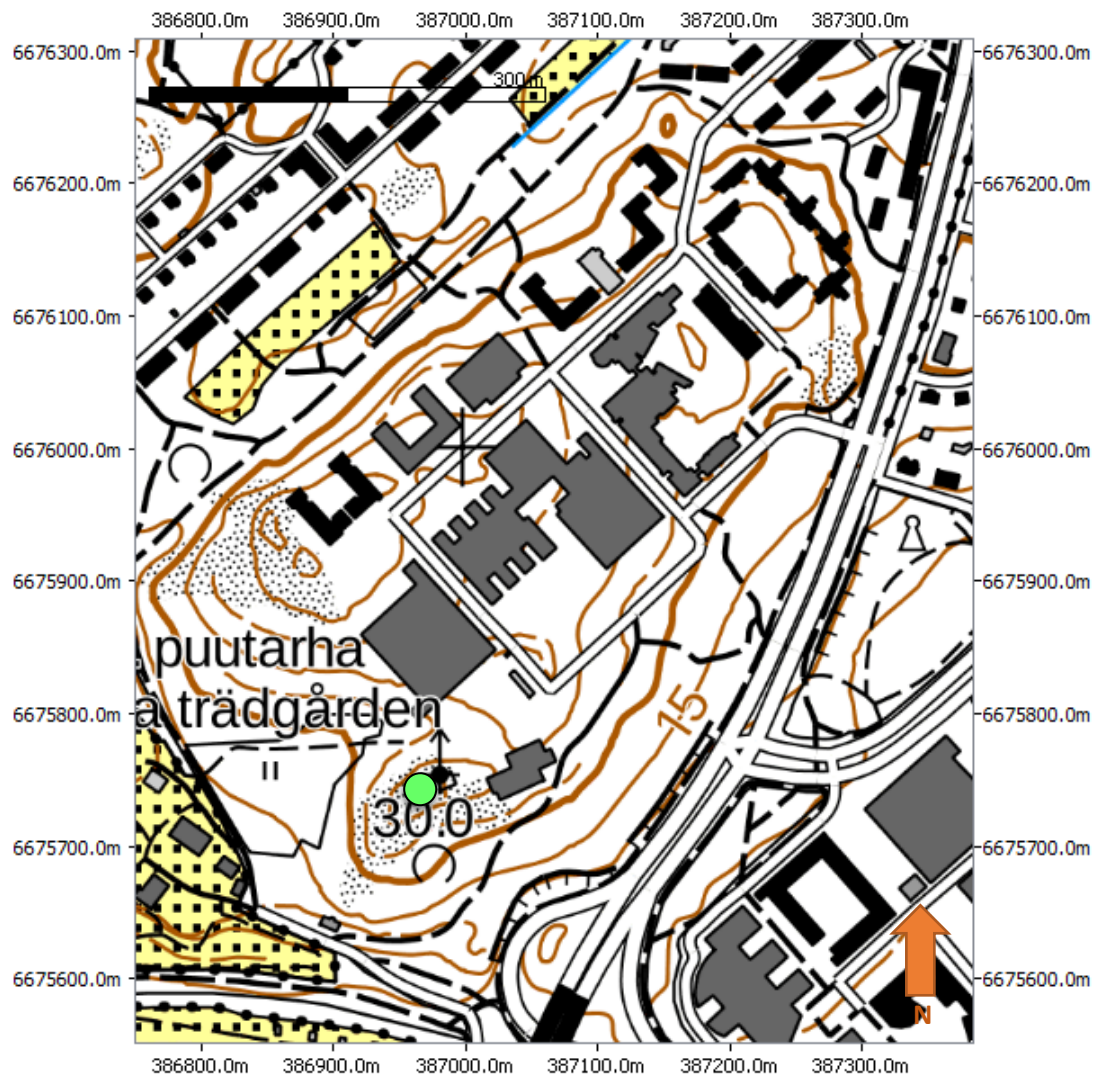
Figure 2. The detailed map of the Kumpula area. The place of the Kumpula drill hole is marked on green circle. the Kustaa Vaasa road is seen on the eastern side and on the western side of the hill is seen habitation of the Kumpula suburban. Modified from the general raster map 1:100 000 from National Land Survey of Finland.

Rock quality

▬▬▬ 1. Unweathered or only little weathered (Rp0-1)

▬▬▬ 2. Little or in abundance weathered (Rp1-2)

▬▬▬ 3. In abundance or fully weathered (Rp2-3)

Fracture density

A Fracture density over 1 m, fracture length under 10 m, fracture headings two in max

B Fracture density over 0.5-1, fracture length under 10 m, two or three fracture headings and random directions

▬▬▬ Thickness of the soil cover over 17 m

▬▬▬ Probably broken zone of the rock

Rock type

● Amphibolite, alkaline volcanic rock
● Intermediate volcanite
● Quartz-feldspar gneiss, acid volcanic rock
● Micagneis
● Gabbro
● Granodiorite
● Granite
● Rapakivi

Foliation (strike and dip)

+ 0-5°

▲ 6-89°

+ Vertical

Figure 3. Modified 1:50 000 constructability map of Kumpula area after Pajunen et al. 2002b. The Kumpula hill is marked on black circle to the map. The original legends of the map are in finnish, so beneath the map has been translated the main points in shorter versions. The map represented the most brittle zones of the bedrock around the Kumpula area.

1.1.1.   Kumpula Campus drill hole

Kumpula campus drill hole was drilled on the Kumpula hill in December 2015. The starting point of drill hole is situated at an outcrop 26.9 m above sea level. The main purpose of the drill hole is research and there is intention to keep drill hole open for decades. The drilling was carried out by the company Suomen Malmi Oy and it was executed with a diamond drill.

The plunge direction of the drill hole is 45 degrees and the plunge are 70 degrees (Kukkonen et al. 2016). The diameter of the drill hole is about 75 mm and length along plunge is 370 m (Kukkonen et al. 2016). There are 81 boxes of the drill core in total. The drill core diameter is 50 mm.

The geophysical measurements have been done by GRM-services Oy right after drilling. The measurements comprise information about the drill hole: optical image, acoustic image, rock resistivity, self-potential, IP-effect, magnetic susceptibility, gamma ray spectroscopy, total gamma, gamma-gamma density, fluid temperature, and fluid electrical conductivity. The optical and acoustic data are used for confirmation of fractures in the drill hole in this study.

1.1.2.   Lithology

Kumpula area rock types have been determinate first time in the 1960's by Laitala (1967). Then it was found out that Kumpula area consist primary of amphibolite/-hornblende gneiss, granite, tonalite, and mica gneiss. Based on the bedrock map of the area, the drill hole has been drilled in the tonalitic part of the bedrock.

The rock types of the drill core have been studied based on drill core and logging and petrography (in prep. Penttilä) and geochemistry (Räisänen 2018). Preliminary logging studies have found at least 13 rock types in the drill core (Figure 4) (Penttilä 2016), whereas with the help of geochemistry, the rock types of the drill core have been divided into the five different classes (Figure 4) (Räisänen 2018).

Major rock types defined with the help of geochemistry, are amphibolite, granite, actinolite-rock, diopside-actinolite skarn, and migmatite/ granite gneiss. They have been analysed based on WD-XRF Omnian scans, P-XRF-device during logging, and petrographical examination of the drill core and surroundings (Räisänen 2018). The rock types vary relative to depth and all rock types are found throughout the drill core (Räisänen 2018). According to Räisänen (2018) the granite is composed mainly of SiO_2, AlO_2, and minor Na_2O and K_2O. The least amount silica (< 50 wt. %) was found from actinolite-rock. The actinolite-rock is rich in magnesium, whereas diopside-actinolite skarn is rich in CaO.

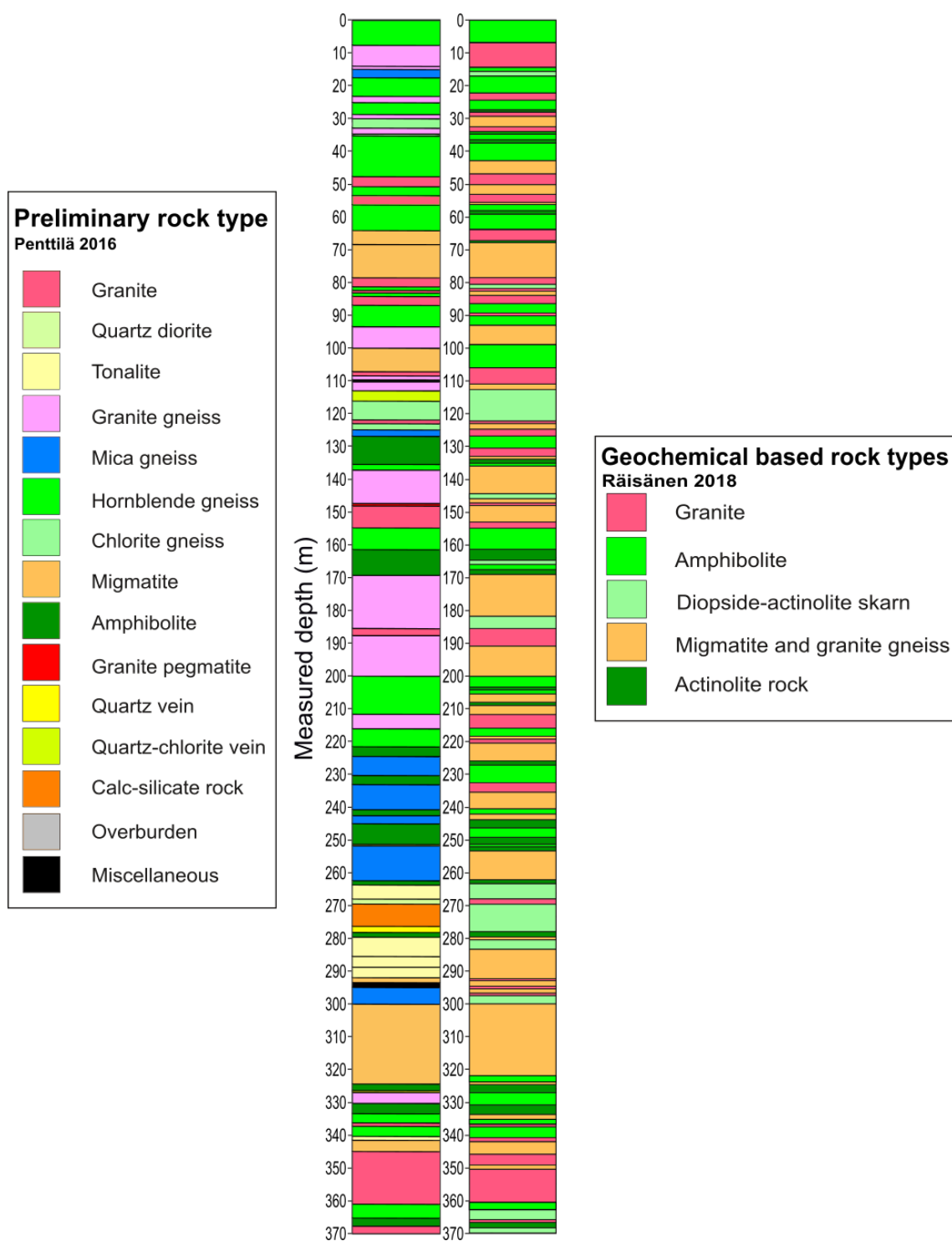Figure 4. Lithological columns of the Kumpula drill hole. On the left are the rock types after Penttilä (2016) and on the right rock types after Räisänen (2018). The rock types on the left have been determined based on preliminary logging of the drill core and the rock types on the right have been determined based on thin sections, measurements with the portable X-ray fluorescence device, and laboratory X-ray fluorescence device.

2. BRITTLE DEFORMATION OF THE BEDROCK

Under brittle deformation, the rock breaks instead of behaving in a plastic way. The breaking of the rock is called fracturing, which could lead to faulting. Fracture is a small planar discontinuity of rock, along which significant block movement has not happened. A fault is a fracture, along which displacement of more than a meter has happened. The terms are not straightforward and different characterizations exist. According to Schultz and Fossen (2008), the fracture is more like general term for a brittle structure, which means a weak structure, along which there is possibility for fluid movement. Terms like joint and anticrack define the mode of the opening so they are more specified terms for weak structures (Schultz and Fossen 2008). Schultz and Fossen (2008) further consider the term fault to be usable when visible movement has happened between the blocks and separated structures like fault core and damage zone can exist. Joint, anticrack, and fault are all fractures as specified by Schultz and Fossen (2008) but based on kinematic sense all these structures are different. Terms fracture and faults are used in this study to distinguish structures without relative block movement, respectively.

Brittle formations are an efficient storage of fluids, but they could also act as a barrier (Singhal and Gupta 1999). Fractures are important preservers of ground water or even hydrothermal and metamorphic fluids (Twiss and Moores 2001). In addition, fractures and faults are important structures for oil and gas industry (Twiss and Moores 2001). On the other hand, when bedrock is used for construction or being mined, brittle formations weaken the bedrock (Niini and Ärmänen 2000). Brittle formations are also carefully investigated in the nuclear waste disposal site (e.g. Niinimäki 2004).

2.1. Fractures

Fractures develop when the stress component exceeds the internal strength of the rock body (Niini and Ärmänen, 2000). These stresses are for example tectonic stresses, residual stresses, the cooling of the magma chamber causing contraction due to shrinkage, the surficial movements like glaciers and weathering (Singhal and Gupta 1999). Non-porous rocks respond to the stress by fracturing, whereas more porous rock responds to the stress by granular flow (Fossen 2010). The latter means that in microscopical perspective the grains translate and rotate more than they break down (Fossen 2010). In

the case of non-porous rocks, the stress breaks grains and this leads eventually to fracturing (Fossen 2010).

In a larger scale, more porous rocks in the brittle regime generate deformation bands, which can be thick zones of differing behaviour (Fossen, et al. 2007). Deformation bands are important, e.g. for petroleum research (Fossen 2010), but in this study, focus is more on non-porous rock behaviour under brittle conditions. Non-porous igneous and metamorphic rock types are more typical in Finland.

2.1.1. Fracture types

Fractures can be classified based on their geometry into systematic fractures and non-systematic fractures (Singhal and Gupta 1999). Systematic fractures are planar, whereas non-systematic fractures are more irregular (Twiss and Moores 2001). Fractures can also be divided based on apparent stress field into shear fractures and opening/extension fractures (Fossen 2010). In the hydrological point of view this categorization is important, because usually extension fractures possess more fluids than shear ones (Singhal and Gupta 1999). Extension fractures typically form in the upper-most few hundred meters of the crust under deformation of only little or no stress (Fossen, 2010). Shear fractures form in conjugate pairs in 20–30 degree angles from the main stress direction σ_1 (Fossen 2010). Shear fractures usually form in upper crust PT-environments, but they can also develop near brittle-plastic transition zones (Fossen 2010).

Based on the relative displacement, fractures can be divided into four classes, which are mode I, II, III and IV (Figure 5) (Fossen 2010). In mode I, the relative movement has happened perpendicular to fracture, whereas in mode II and mode III the relative movement has happened parallel to the fracture (Figure 5) (Twiss and Moores 2001). Mode IV represent fracturing caused by contractional forces and is often called stylolite (Fossen 2010). If fracture has features from both Mode I and Mode II or III, it is called a hybrid fracture (Fossen 2010).
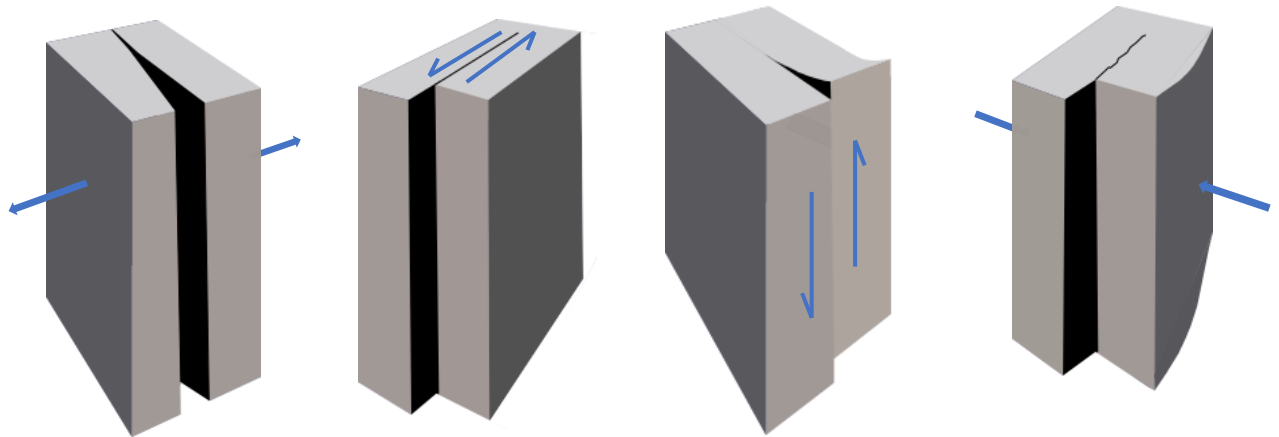
Figure 5. Fracture types based on the relative displacement (after Fossen 2010) a. Mode I is extension fracture with perpendicular to σ_3, force vectors against to the fracture walls, b. Mode II is shear fracture, oblique to σ_3, force vectors sliding parallel to the fracture c. Mode III is shear fracture with oblique to σ_3, force vectors sliding on the edge of the fracture and d. Mode IV is closing fracture, perpendicular to σ_3, force vectors facing each other.

2.1.2. *Focus points on fracture investigation*

Fractures are investigated in four aspects, which are 1. the geometrical features between fractures and other structural features, for example foliation, 2. the relative relationship of different fracture systems, for example does fractures in one direction end clearly to the other fracture system in the different direction, 3. the geometry of the fracture system and 4. features of the fracture surfaces (Twiss and Moores 2001). Fractures with roughly the same orientation and dip belong to the same fracture set, whereas multiple fracture sets create a fracture network (Singhal and Gupta 1999). Points 1 and 3 are examined in a fracture set basis, point 2 is examined in a fracture network basis, and point 4 is examined inside a fracture set from individual fractures.

Parameters like block unit, number of sets, volumetric fracture count, and area and shape of the outcrop are defined in a fracture network scale (Table 1) (Singhal and Gupta 1999, Twiss and Moores, 2001), whereas spacing, and the density parameters are determined in a fracture set scale (Table 1) (Singhal and Gupta 1999, Twiss and Moores, 2001). Parameters like shape, length, filling, aperture, roughness, and orientation are defined from individual fractures (Table 1) (Singhal and Gupta 1999, Twiss and Moores, 2001).

Fractures can be compared to other geometrical features like faults and regional schistosity, but also to folding, intrusive contact or bedding (Twiss and Moores, 2001), and this way it is also possible to date fractures (relative age). For example, if a fracture

crosscuts an intrusive contact or a bedding plane it is younger than that formation (Twiss and Moores 2001). Sometimes near faults, fractures are associated with a conjugate pairs of shear fractures that have 60 degrees angles between them (Twiss and Moores 2001). One fracture set is usually almost parallel with the fault and another is 65 degrees from that first fracture set (Twiss and Moores 2001). Fractures can form in folds as well, so that there are possibly five different sets of fractures, which occur at different part of the folds. There are fractures, which are perpendicular to the bedding plane, and some sets are parallel with the fold axis. Fractures perpendicular to the bedding plane are found on fold limbs, whereas fractures perpendicular to bedding plane and parallel with fold axis are found on the convex side of the fold. One set is usually found in the concave sides of the folds as well. (Twiss and Moores 2001).

Table 1. Important fracture investigation parameters after Twiss & Moores (2001), Singhal & Gupta (1999) and Dershowitz & Einstein (1988).

Features observed on fracture system scale	Meaning
Block unit	Size and shape of a piece of a rock, which is generated in a fracture network. The shape could be prismatic, cubical, or tabular.
Number of sets	Number of fracture sets in a fracture network.
Volumetric fracture count	The number of fractures to the directions within one cubic meter of rock
Area and shape	Summary of the observed outcrop and shape of the area
Features observed on fracture set scale	**Meaning**
Spacing	Space between two fractures of the same set perpendicular to fracture set direction
Density	The number of fractures in certain unit length. Can be also examined in areal and/or volumetric scale.
Features observed from individual fractures	**Meaning**
Orientation	Could be expressed as strike and dip, dip direction and dip or pole orientation with spherical coordinates. Measured from individual fractures, but fractures which continue in the same direction (same orientation) determine a fracture set.
Scale	In the direction of dip and strike. Usually difficult to determine in both directions.
Shape of the fracture	In 2D the fracture is compared to a planar shape. Waviness means fracture shape crosses over 1mm scale.
Roughness	Fracture surface feature (under 1mm scale)
Aperture	Space between walls of the fracture
Fracture filling	Texture and colour of the filling. Important if it is not possible to determine the composition of the filling.

2.2. Faults

Fault is a fracture or a narrow zone, where visible displacement has happened (Fossen 2010). Movement in fault is larger (on a scale of meters) than in fractures (zero or on a scale of centimetre) (Twiss & Moores 2001).

Faults are important from a hydrological perspective, because they affect the flow of groundwater: they could a barrier or a conduit zone depending on the physical characteristics of the surrounding rock and fault rock (Singhal and Gupta 1999, Twiss and Moores, 2001). For example, whereas a breccia zone is an excellent conduit of water, a fault wax acts as a barrier (Twiss and Moores, 2001).

2.2.1. *Growth and structure of fault*

Faults in non-porous rocks grow from small-scale shear fractures, when shear movement happens (Fossen 2010, Singhal and Gupta 1999). In these small-scale shears, tensile and hybrid fractures must connect for the fault to generate (Fossen 2010). The surface of the incipient fault is irregular, and this leads to grinding and fracturing (Fossen 2010).

On a kilometre scale, faults consist of a one big fault, but on smaller scales faults consist of many small shear displacements next to each other (Fossen 2010). A fault consists of a fault core and the surrounding damage zone (Fossen 2010). A fault core can consist of only one slip surface or it can be a zone of cataclastic rocks (Table 2) (Fossen 2010). The origin depth of the fault can be determined from the fault rock (Twiss and Moores 2001). Cataclastic rocks are generated in faults, whose origin of depth is under 10 km, while faults, whose origin of depth is more than 10 km, generate mylonitic fault rocks (Twiss and Moores 2001). Fault rock terminology is variable, and it differs between geologists and in literature (Twiss and Moores 2001).

Table 2. Fault rock structures according to Higgins (1971) and Wise et al. (1984). Table based on that of Pajunen et al. 2001.

Trending	Fault structure	Amount of porfyroclasts or -blasts, or fragments	Grain size of the matrix	Cohesion
Oriented	gneiss	matrix has recrystallized to the grainsize of the protolith or larger than that		cohesive
	blastomylonite augengneiss	some porfyroclasts or -blasts	> 0.5 mm	
	proto- and ultramylonite	porfyroklasts > 10 %	< 0.5 mm	
	ultramylonite	porfyroclasts < 10 %	< 0.5 mm	
Unoriented	pseudotachylite	glass or recrystallized glass		non-cohesive
	breccia	fragments >30 %	finegrain matrix	
	microbreccia	fragments <30 %	finegrain matrix	
	fault breccia	angular fragments > 30 %	finegrain matrix	
	fault wax	fragments <30 %		

2.2.2. Fault types

A fault cuts rock into two halves: hanging wall and footwall. Movement can happen to any direction along the fault surface and basically there are three groups of faults: normal, thrust, and strike-slip (Singhal and Gupta 1999). Based on the relative movement the faults, they can be divided into four categories: dip-slip faults, strike-slip faults, oblique slip faults, and rotational faults (Twiss and Moores 2001). Within these classes the dip-slip faults are divided into normal, and thrust faults, strike-slip faults to dextral, and sinistral faults, and oblique-slip faults to the sinistral-normal and sinistral-reverse faults (Figure 5) (Twiss & Moores 2001).

In the dip-slip fault category, the footwall of a normal fault moves up relative to the hanging wall, whereas in a thrust fault the hanging wall moves up relative to the footwall (Twiss and Moores 2001). The movement can be either right-handed or left-handed in strike-slip faults (Grotzinger and Jordan 2010). Oblique slip faults have characteristics of both strike-slip and dip-slip faults (Twiss and Moores 2001). In rotational faults dislocation changes in horizontal direction (Twiss and Moores 2001).

2.3. Brittle structures in a drill core environment

Drill core gives an opportunity to investigate a rock body in depth, but the downside is that the diameter of the core is usually few centimetres, which gives a very narrow image of the rock body (Marjoribanks 2002). It is difficult to transform drill core data into a 3D environment and due to drill hole having a certain plunge, there is usually a shadow zone that is perpendicular to the drill hole (Davy et al. 2006). Drilling is widely used, however, because it is a rather cheap way to get some impression of the rock in depth (AREVA Resources Canada Inc. 2010).

Drill core can be used for different purposes in geology and one purpose is to evaluate the fragmentation of the rock. The fracture data is used to evaluate fragmentation of the rock mass before construction (AREVA Resources Canada Inc. 2010) and data can be used for creating fracture networks (for example Fox et al. 2012).

Both natural fractures and those that are created during drilling can usually be seen in the drill core. Fractures, which are created during drilling are recognized based on freshness of the surface, unfilled fracture surface, roughness and an alpha angle that is perpendicular to the core axes (AREVA Resources Canada Inc. 2010).

The natural fractures of the drill core are classified in different groups based on intention of the investigation (AREVA Resources Canada Inc. 2010). For example, in a nuclear waste repository, the discontinuities are grouped based on filling into open, tight, filled, filled slickenside, grain–filled, and clay–filled fractures (Niinimäki 2004). On a wider scale, fractures are grouped to the joint, shear/fault, shear/fault zone and fracture (AREVA Resources Canada Inc. 2010). The recognition is based on the individual character of the structure (see last section in Table 1).

2.3.1. *Characteristics of individual fractures*

There are number of individual parameters used in classifying fractures and some of them are already discussed in section 2.1. in general, but some of the parameters are useless in drill core environment: for example, length, waviness, and orientation to some extend (Palmström 1995). The observations in drill core environment are limited almost only to fracture surface and orientation.

Based on core logging manual of AREVA Resources Canada Inc. (2010), the observations, which can be collected from the fracture surfaces, are fillings, roughness, shape, and hardness and alteration. The type, width, spacing, and continuity can also be observed (AREVA Resources Canada Inc. 2010).

The surface of the fracture can be rough, smooth, or slickenside and within these classes they can be undulating or planar (NGI 2013). Lineal shape of the fracture can be also evaluated. Fillings of the fracture can further be classified based on composition, thickness, and hardness (AREVA Resources Canada Inc. 2010).

Fracture fillings form in fractures where fluid interacts with fracture and precipitates solid materials between fracture walls. The type of the fracture filling material (or absence of it) affect to the construction features of the rock negatively or positively or they can be

used to study paleohydrology (Wallin and Peterman 1999) or ground water paths. The important factors of fillings are the material of the filling and its thickness, which together with roughness of the fracture shearing along fracture plane (NGI 2013).

Fracture fillings consist of different minerals. The common filling minerals are biotite, chlorite, calcite, hematite, sericite, quartz, talc, gypsum, and set of clay minerals. The filling could also consist of gravel, sand or silt (AREVA Resources Canada Inc., 2010). Some clay minerals are problematic, because if they get in contact get contact with water, they can expand, and in this way reduce the stability of the rock mass (NGI 2013).

2.3.2. Fault recognition in drill core

Drill core gives only a limited glimpse of information on structures, and fault and shear zones are recognized based on the movement along the fracture walls (AREVA Resources Canada Inc. 2010). In drill core, shears or faults are recognized based on different parameters that indicate movement along a natural break in the drill core. Such indicators could be slickensides, couges, mylonites, or breccias. A slickenside, for example, differs from the other breaks (fractures) so that usually its surfaces are polished, indicating movement. The natural breaks are classified fault or shear zones if there are many parallel or sub-parallel breaks (AREVA Resources Canada Inc. 2010), but large-scale brittle faults appear in drill core as broken zones with core loss and clay filling (Marjoribanks 2002).

2.3.3. Parameters of the rock mass quality assessment

The parameters, which are used to evaluate rock mass in tunnels or outcrops, are also applied to drill cores. There are number of different parameters to evaluate the fragmentation of the rock. One of the first parameters is Rock Quality Designation (RQD), which is used mainly for boreholes (Deere and Deere 1988). The RQD parameter is used so that lengths of all parts of core that are intact for over ten cm are summed together. This number is divided with the whole length of the drill core and then multiplied with 100 to achieve a percentage value (Deere and Deere 1988). The best value in terms of rock quality is 100 % and the worst is 0 % (Table 3) (Deere and Deere 1988).

$$RQD = \frac{\sum length\ of\ parts\ over\ 10\ cm}{total\ length} \times 100\ \%$$
[1]

Table 3. Rock quality designation (RQD) percent and the verbal correlation (Deere & Deere, 1988).

RQD (%)	Description of rock quality
0–25	very poor
25–50	poor
50–75	fair
75–90	good
90–100	excellent

Because the RQD-value is limited descriptor of the rock body. Other parameters have been developed, e.g., the Q-method (Barton et al. 1974). Method is more versatile, because it takes account more parameters than RQD-method and it can be used not only in boreholes. but also, in tunnels (Barton et al. 1974). The Q-value is based on calculation of more parameters than RQD. The parameters are: the number of joint sets (J_n), joint roughness (Jr), joint alteration or filling (Ja), joint water leakage or pressure (Jw), rock stress condition (SRF), and the RQD-value, which in here indicates the mean degree of jointing (Grimstad and Barton 1993). The Q-value varies from 0.001 to 1000, where a value of 1000 means exceptionally good and a value of 0.001 means exceptionally poor rock quality (Grimstad and Barton 1993).

$$Q = \frac{RQD}{J_n} \times \frac{J_r}{J_a} \times \frac{J_w}{SRF}$$
[2]

The RQD/J_n measures the block size, J_r/J_a measures the internal friction and J_w/SRF measure active stresses (NGI 2013). Sometimes (especially in boreholes) the last factor evaluated to be 1 so that the Q-value function diminishes to the Q'-value:

$$Q' = \frac{RQD}{J_n} \times \frac{J_r}{J_a}$$
[3]

The Q-system is easiest to use in tunnel environment, but in can also be applied to core logging and field mapping, even though the parameters do then not give as exact values as in tunnels (NGI 2013). According to NGI (2013), the main limitations in drill core environments, concern parameters Jr, Ja, and Jn. The drill core is only few centimetres in diameter, which means that roughness of fractures on a scale of meter is difficult to estimate. In addition, some of the fillings may have been washed out with water used in drilling. The orientation of the drill core also affects to the fracture directions, which are calculated from the drill core and this, in turn, affects the fracture set calculations.

The Engineering Geological Rock Mass Classification has been developed in Finland to for national purposes (Niini and Ärmänen 2000). It is more descriptive, and it can be used more widely than the other two mentioned previously (Niini and Ärmänen 2000). The classification system consists of three parts: Analytical part, Synthetic part and Descriptive part (Table 4) (VTT 1974, 1976). The rock type, its quality, and basic character of fracturing is determined in the analytical part (Niini and Ärmänen 2000). The structural quality of the rock is classified in the synthetic part. The classes vary from solid to loose rock. After that, the project site, including descriptions of, e.g. range and roughness of the fractures, is described in detail. (Niini and Ärmänen 2000).

Table 4. Engineering geological rock classification for Finnish purposes

1. Analytical part

Classification basis	Rock type								Fracturing			
Index property	1. Weathering 2. Degree of organization of rock parts 3. Grain size 4. Main minerals								1. Fracture type 2. Density of fractures 3. Quality of fractures			

2. Synthetic part

Structural consistency	Solid rock									Loose rock			Fragmented rock				
Structure type	massive			schistous			composition			Loose rock			Weathered	I	II	III	IV	V
Quality of rock	1	2	3	1	2	3	1	2	3	1	2	3	rock					

3. Descriptive part

Detailed description of the project site

Under structure type there are five classes and under those classes rock quality is evaluated in three classes: 1) sparse fracturing, 2) little fracturing and 3) abundant fracturing only in one direction. If there is abundant fracturing in more than one direction, the rock belongs to the fragmented rock class. Inside this class there are five classes: I) only one or two open fractures divide the rock mass into two parts, II) abundant fractures, but no fracture fillings, III) densely fractured and few filled fractures, IV) densely

fractured and clay fracture fillings, and V) rock has fractured to little pieces and contains a lot of fault gouge material. (Niini and Ärmänen 2000).

3. THE GEOLOGICAL BACKGROUND OF THE HELSINKI AREA

3.1. Tectonic background of the Helsinki area

The bedrock of Helsinki was created in a collision between an Archean continent and Svecofennian terrains. This collision 1.9-1.8 Ga ago was very complex and included many phases of deformation. Helsinki is situated in the southern part of the Svecofennian domain. The Svecofennian orogeny was progressive, so that the events started first in the northern part of the domain and continued to the south (Pajunen et al. 2008). The periodical summary of these processes can be seen in (Table 5) (Pajunen et al. 2008).

The tectonic history of the Svecofennian orogeny can be divided to six major tectonic phases (1-6) according to Pajunen et al. (2007, 2008) (Table 5) and later post-Svecofennian events (7-10) according to Pajunen et al. (2001, 2007) (Table 5):

Table 5. Tectonic events of the Svecofennian domain according to Pajunen et al. (2001, 2007, 2008)

Event	Main effect to the Helsinki area	Ago (Ga)	Phase
1	Primary sediment structures and volcanic series	-1.9	
2	Deformation of the first sedimentation structures and volcanic series	1.9 to 1.89	
3	Compressional stress in N-S- direction, local extension, which lead to volcanism, also sedimentation	1.88-1.87	Svecofennian orogeny
4	Deformation of the previous structures in N-S direction	-1.87	
5	Evolution of the new Archean-Svecofennian continent, sedimentation, and generation of Southern Finland Granitoid Zone	1.87-1.84	
6	Deformation of the N-trending deformation zones, ending of the Svecofennian orogeny	to 1.8	
7	Penetration of rapakivi granites and associated diabase dykes	1.65	
8	Reactivation of the faults	-0.450	Post-orogeny processes
9	Post-glacial events		

The tectonic events cover the history of the local bedrock from the first sedimentation phase via the island arc collision to the cooling of the newly formed continental crust (Pajunen et al. 2008). The events after Svecofennian orogeny include the emplacement of the rapakivi granites and associated rocks, the reactivation of faults, and later the post-glacial uplifting (Pajunen et al. 2007).

In the first phase, the island arc collides to the Archean continent, in phase two the island arc collapses, and in phase three a continuous collision with some local extension takes place. The new Proterozoic continental crust formed during phases 1–3, continental collision took place in phases 4–6 (Pajunen et al. 2008). These major geotectonic events can be divided more accurately into smaller deformation facies D_a-D_i (Pajunen, et al., 2008). D_a to D_d represent deformation facies of island arc generation, and collision with the Archean continent (Pajunen et al. 2008). The deformation facies D_e to D_i represent the deformation faces which deformed the new Svecofennian crust and older Archean crust (Huotari and Wennerström 2017, Pajunen et al. 2008). The crust cooled after deformation and continued to deform in a brittle way (Pajunen et al. 2008).

3.1.1. Svecofennian orogeny

Before collision of the Svecofennian terrains and the Archean continent, primary sedimentation and volcanism was occurring in a marine environment: sedimentation happened at the bottom of the sea and later in shallower water, forming limestone, iron-formations, sulphide ores and other volcanic products (Pajunen et al. 2007). Earliest such products have been deformed into gneissic and migmatic rocks (Pajunen et al. 2007). In some areas there are relict of primary structures, for example flame-like old fold structures (Pajunen et al. 2001).

The collision started in the north from where it began to spread to the south. The collision was oblique against the NW-trending shore line of the Archean continent (Pajunen et al. 2008). This led to the thickening of the crust and N-S directional shortening 1.9–1.89 Ga ago (Pajunen et al. 2008). These events created large scale isoclinal folds and subduction volcanism (Pajunen et al. 2007). Even though it is possible to distinguish these folds from some outcrops, further geological interpretation is difficult to do because of overprinting by later deformation events (Pajunen et al. 2001).

After initial collision the island arc started to collapse circa 1.88–1.87 Ga ago. This started in the northern parts of the Svecofennian domains first and then spread to the south (Pajunen et al. 2001). Overall, the crust was in compressional stress in N-S direction, while locally crust in the southern Svecofennian domain was in extension (Huotari and Wennerström 2017, Pajunen et al. 2008). Island arc collapse caused the crustal extension (Pajunen et al. 2008). Extension also caused increased heat flow, and this led to low-grade metamorphism and volcanism in an intra-arc environment 1.88–1.87 Ga ago (Pajunen et al. 2008). On the surface, extension lead to dome and basin structures and shedding (Pajunen et al. 2007). The metamorphism generated biotite schistosity throughout the rocks and in many places earlier structural elements vanished (Pajunen, et al. 2007).

After the collapse of the island arc follows the collision of the newly formed crust to the Archean continent (Pajunen et al. 2008). The preceding extension event was local and, when it ended in the south, the northern domains were already under compressional stress (Pajunen et al. 2008). The compression was in N-S direction, which lead to folding with fold axes in E-W-direction (Pajunen, et al. 2008). The compression direction changed to

NE-SW-direction about 1.87–1.86 Ga ago (Pajunen et al. 2007). This new compression direction caused earlier folds to be folded again so that dome and basin structures were created (Pajunen et al. 2007). After this shortening event, the Archean and Proterozoic domains could be considered as one continent (Pajunen et al. 2008).

The compression continued to influence the newly formed continent 1.86–1.80 Ga (Pajunen et al. 2008). The transtension direction changed from the NE-direction via E (1.85 Ga ago) to SE (1.85–1.84 Ga ago) and after that E-SE (1.84–1.80 Ga ago) (Pajunen et al. 2007, 2008). During that time period the stress field of the continent flipped several times, which happened due to compression and temperature difference of the rock bodies (Pajunen et al. 2007). Overall the marks of the transpression phase are very different in different areas, because the local kinematics changed from tension to collision (Pajunen et al. 2007). The areas affected with tensile stress, were generated boudinage structures, oblique faulting, and melting of the crust, whereas areas with compression were generated folds and reverse faults. Flipping of the transpression direction lead to the formation of the Southern Finland Granitoid Zone (SFGZ) (Pajunen et al. 2008)

The stress field rotated to ESE-E direction and the crust cooled more in (Pajunen et al. 2008). The cooling is seen in the structural evolution of for example the Vuosaari-Korso shear/fault zone, where the shear structures changed to semi-ductile structures (Pajunen et al. 2008). At late stage of the Svecofennian orogeny the deformation was demerged in smaller sections and as the crust was cooling, the deformation state changed from ductile to brittle (Pajunen et al. 2007).

3.1.2. Post-Svecofennian processes

The biggest event after the end of the Svecofennian orogeny was the emplacement of the Rapakivi granites ~1.65 Ga ago, 150 Ma after the last events of the Svecofennian orogeny (Pajunen et al. 2007). They were emplaced in about a depth of 5–7 km when the bedrock was still tectonically active (Pajunen et al. 2007). The emplacement was related to a right-handed movement (Pajunen et al. 2007). The rapakivi magmas utilized large tectonic suture zones, for example Porkkala-Mäntsälä shear zone in the case of the Bodom and Obnäs plutons (Mertanen et al. 2008). The bedrock was reactivated also 450 Ma ago

because of the Caledonian orogeny (Wennerström et al. 2006). These movements happened along the old shear zones (Pajunen et al. 2007).

After rapakivi magmatism and Caledonian movements the bedrock has continued to deform. There are minor earthquakes (Wennerström et al. 2006) and brittle structures are still developing (Pajunen et al. 2007).

3.2 Faulting in the Helsinki area

In previous examinations of the fault systems in Helsinki data, which was collected from different outcrops around the Helsinki area and from the tunnels, was used. The fault rocks have been studied microscopically and geophysical maps were exploited. (Pajunen et al. 2001, Wennerström et al. 2006, Elminen et al. 2008).

Faults in Helsinki can be divided based on plasticity into three classes: ductile shrearing and faults, transitional faults, and brittle faults (Pajunen et al. 2001). Within these classes, the faults can be divided based on direction and dipping, for example, according to Elminen et al. (2008) (Table 6). There is also a separate class of reactivated faults: reactivated ductile faults in brittle phase (Table 6) (Elminen et al. 2008).

According to Pajunen et al. (2001), the fault zones in Helsinki area can be classified into four basic groups based on their plasticity of deformation, and more accurately into eight groups based on the different stress fields in uniform PT-circumstances. These eight groups are:

Ia Ductile mylonite gneisses

Ib Biotite schistosity zones

IIa Ductile shear structures, NEE-SWW

IIb Ductile shear structures, E-W

IIc Ductile shear structures, N-S

IIIa Transitional, sharp cutting shear zones, NE-SW

IIIb Ultramylonite junction SE-NW

IVa Brittle fault zones, steep

In more accurate study of fault zones of Wennerström et al. (2006) and Elminen, et al. (2008) are classified zones almost same way:

1. Ductile ENE-SWS and E-W

2. Ductile-semi brittle NE-SW

3. Brittle NW-SE

4. Reactivation of ductile to semi-brittle NE-SW

5. Brittle N-S

6. Brittle E-W

7. Brittle low-angle faults

Ages of the faults differ, and ductile faults have developed already during Svecofennian, whereas the youngest brittle faults have developed after emplacement of the rapakivi granites (Table 6) (Pajunen et al. 2007). The fault rocks vary from mylonite to breccia (Table 2). Most fragile fault zones are in brittle faults, but even ductile faults in E-direction are fragmented (Pajunen et al. 2007).

The ductile faults have been generated during the Svecofennian orogeny (Elminen et al. 2008). They follow or only slightly crosscut the regional schistosity (Pajunen et al. 2007). The directions of the ductile faults are NE, ENE and E (Elminen et al. 2008). They were generated during transpression phase of the crust: faults were generated are because of transtension (Pajunen et al. 2007). The fault rock type is meso- to ultramylonitic, and their dips are 62–90 degrees to the south and south side up shear (Elminen et al. 2008). Widths of the mylonitic zones are 0.5 to 5 meters (Elminen et al. 2008). The ductile faults were first generated in horizontal direction between surface rocks and intrusive rocks after the magmatism waned (Pajunen et al. 2007).

Transitional faults were generated during the late phases of the Svecofennian orogeny. They crosscut earlier structures of the Svecofennian (Wennerström et al. 2006). The longest faults, Porkkala-Mäntsälä and Vuosaari-Korso, in the Helsinki area belong to the this group (Elminen et al. 2008). They are 5–25 km long and they extend to the depth of 2–3 km (Elminen, et al. 2008). The dips of the faults are 70–90 degrees (Elminen et al. 2008). The direction of the Porkkala-Mäntsälä fault is NE-SW and the direction of the Vuosaari-Korso fault is N-S (Pajunen et al. 2007). The movement has happened in zones, because the bedrock cooled differently in different areas (Pajunen et al. 2007). The fault rock types are ultramylonite or breccia, and also pseudotachylites are found from N-S directional faults (Pajunen et al. 2007). The width of the faults varies from one centimeter

to several meters (Pajunen et al. 2007). There are fractures in same directions near the fault zones these also include slickensides (Pajunen et al. 2007).

At the same time, while the rapakivi granites were emplaced into the bedrock, older faults were reactivated (Elminen et al. 2008). The rapakivi phase reactivated faults in NE direction including major Porkkala-Mäntsälä and Vuosaari-Korso fault zones (Elminen et al. 2008). The younger brittle structures cut older ductile structures, which makes faults more fragile (Wennerström et al. 2006).

The brittle faults in the Helsinki area can be divided based on the time of formation and dip (steep or low angle), and in more detail, based on direction (Pajunen et al. 2007). During the rapakivi phase steep brittle faults were generated and afterwards low–angle brittle faults formed (Pajunen et al. 2007).

Steep brittle faults crosscut both Svecofennian structures and rapakivi granites (Pajunen et al. 2001). Whereas the transitional faults reach the depths of 2–3 km, brittle faults are shallower (Pajunen et al. 2001). Faults create a network in the Helsinki area, the direction of which is WNW-ESE to NNW-SSE so that the difference in directions is circa 30 degrees (Elminen et al. 2008). The dip is 75–90 degrees and dip direction are either NE or SW (Elminen et al. 2008). Fault valleys are 1–5 km long, which are oriented to NW-SE (Elminen et al. 2008) and if the fault rocks are exposed, they include breccia and fault breccia (Pajunen et al. 2001). Fractures with similar directions also exist in the area, especially slickensides in the road cuts (Wennerströn et al. 2008). Slip directions measured from the fault planes divided to the steep and subhorizontal (Elminen et al. 2008). The steep slipping faults are normal faults, whereas the subhorizontal lineations indicate sinistral shearing (Elminen et al. 2008).

Youngest faults are formed after the rapakivi phase. They are low-angle ($\leq 45^{\circ}$) brittle faults (Elminen et al. 2008) and dip directions angles can be divided into four major directions: 10, 100, 190, and 280 degrees (Pajunen et al. 2007). The widths of the faults are 5–15 cm and the fault rocks are breccia or gouge with occasional slickensides (Elminen et al. 2008). These faults were generated as a result of thrust movements near the surface (Elminen et al. 2008, Pajunen et al. 2007).

Table 6. Summary of the fault types based on Pajunen et al. 2001, Elminen et al. 2008, Pajunen et al. 2007 and Wennerström et al. 2006.

	Ductile faults		Transitional faults	Reactivation	Brittle faults, steep			Brittle faults, low angle
	I		II	III	IV			V
	a	b	a	a	a	b	c	a
Fault rock type	Mylonite, mylonite gneiss	Mylonite, mylonite gneiss	Mylonite to ultramylonite	Breccia	Breccias and fault breccias	Breccia, joints filled with quartz and carbonate	Fault breccia but also related slickensides with chloritic filling	Fault breccias
Direction of main headings	ENE-SWS	E-W	NE-SW, but also NNE-SSW and N-S. Sometimes classified separately (Pajunen et al. 2007).	NE-SE	WNW-ESE and NNW-SSE	N-S	E-W	N, S, E and W
Dip, dip direction and shear	Dip is steep. Reverse shear	Dip is steep. Oblique. reverse shear	Dip is steep, oblique reverse sinistral shear	Dip is steep, strike-slip dextral shear	Steep, normal sinistral oblique shear	Steep, strike-slip sinistral shear	Steep, strike-slip dextral and sinistral shear	Low angle 45 degrees and also under, reverse shear
Age	Svecofennian	Svecofennian	Late Svecofennian	Connected with placing of rapakivi granites	Connected with placing of rapakivi granites	After placing rapakivi granites	After placing rapakivi granites	After placing rapakivi granites
Width (based on the tunnel data)	Hard to distinguish from brittle structures and reactivation	< 2m	1-2 m	1-2 m	2-3 m	1-2 m	Most 1-3 m, but also some > 11m	1-2 m
Kinematics	Thrusting coming from the south	Thrusting coming from the south	Thrusting from east to north-east	Extension in N-S direction in possible transtensional system	Extension in N-S direction in possible transtensional system	NNE-SSW directional extension	Unknown	Different origin
Length	< 10 km	1-2 km	Major zones 100 km and minor zones 5-25 km. Both Vuossari-Korso and Porkkala-Mäntsälä faults belong to this group	See paragraph II	1-5 km	5-15 km	< 10 km	Difficult to measure

3.3. Fracturing in the Helsinki area

3.3.1. Parameters of the fracture investigation

Fracturing in Helsinki has been studied in various previous studies, for example Pajunen, et al. (2001) and Wennerström et al. (2008). The studies have focused on the outcrops and road cuts, but there are also tunnel observations (Wennerström et al. 2008). Investigated characteristics are based on Q-system of Barton et al. (1974), with slight modifications (Wennerström et al. 2008). An observation form for fracture investigation has also been developed (Pajunen et al. 2002a) and was also used in this study.

Previous fracture studies have focused on investigating the relationship of fractures and other tectonic features (Elminen et al. 2008). The investigated features are dip and direction, fracture trace length, fracture spacing, fracture zone, fracture set number, fracture wall outline, fracture wall roughness, and fracture type (Pajunen et al. 2002).

The direction of fracture was defined so that fractures, whose direction difference is ± 15 degrees and dip difference is ± 20 degrees, belong to the same fracture group (Wennerström et al. 2008). The dip 0 degrees means horizontal fracture and 90 degrees means vertical fractures (Pajunen et al. 2001). The dip of the fractures was classified in three categories: gentle (0–20 degrees), mildly steep (20–50 degrees), and steep (> 50 degrees). The fractures with gentle dip (< 30 degrees) can be problematic in construction and because of that are important to be noticed (Pajunen et al. 2001).

Using this approach, it was noticed that in a single outcrop the maximum quantity of fracture directions was four, and possible other fracture directions mean localized tension zone (Pajunen et al. 2001). The fracture direction is the mean value of the parallel fracture (Pajunen et al. 2001).

Fractures were classified in three different classes: dense, open, or filled (Pajunen et al. 2001). The aperture was measured from the widest part of the fracture (Pajunen et al. 2001). The length of the fracture was measured even if fracture continued beyond the measuring area (Pajunen et al. 2001). Wennerström et al. (2008) classified length of the fractures in three groups: short (mean length < 5m), moderately long (5–10 m), and long (>10 m). The fracture density was measured perpendicular to the fracture direction

(Wennerström et al. 2008, Pajunen et al. 2001). Joint wall roughness was classified in three classes: class one means a smooth surface, class two means fractures mildly rough, and class three means a rough surface (Pajunen, et al., 2001). The measuring was made on average surfaces (Pajunen et al. 2001). All slickensides belong to the roughness group one and Wennerström, et al. (2008) studied slickenside fractures separately due to their possible connection to the faults and shear zones. Possible alternations between the fracture surface and fracture fillings have been also detected and they are classified based on hardness and consistency of the filling (Pajunen et al. 2001). The most solid fracture fillings are hard silicate minerals (for example quartz and epidote) and soft fillings are carbonates and clay minerals (Pajunen et al. 2001). Clay minerals are divided further into non-swelling and swelling clays (Pajunen et al. 2001). It is also possible that fracture filling has migrated outside of the system (for example fine sand) or the filling has been completely weathered (Pajunen et al. 2001).

2.3.2. *Results of previous fracture studies*

In the research of Pajunen et al. (2001), five main dip direction classes were detected in the Helsinki area, which are, respectively 40–70, 90–110, 130–160, 220–250 and 310–340 degrees. These dip directions are common in elsewhere in Finland as well (Pajunen, et al. 2001). The rest of the dip directions were classified as local tectonic features (Pajunen et al. 2001). In the research of Wennerström et al. (2008), the main directions of the fractures were under six headings: E, NE, NNE, N, NW and WNW.

The dip of the fractures is usually steep, but fractures with a gentle dip are also found in noticeable amounts (Wennerström et al. 2006). It is also important to note that fractures with steep dip are mostly seen on outcrops (Wennerström et al. 2006). The observed fractures were mainly dense, but also opened fractures were found (Pajunen, et al., 2001). Only few filled fractures were found (Pajunen, et al. 2001). Fractures were usually 1–5 metres long, but over 10-meter-long fractures were also found (Pajunen et al. 2001). Fracture density was usually loose: > 1m and 1–0.4 m. In only a handful of fracture populations, the fracture density was under 0.1 m (Pajunen et al. 2001).

The steeply dipping NE fracture direction is the most common in fractures of six main fracture directions of Wennerström et al. (2008), but both NE and moderately dipping NW directions occur systematically in the Helsinki area. In roadcuts, the fractures with

NE and NNE directions are found from different outcrops. In roadcuts more gently dipping fractures may also be observed, whereas N directional steep fractures are seen on outcrops (Wennerström et al. 2008). There is usually one fracture direction, which is parallel with the main foliation in the Helsinki area (Pajunen et al. 2001). This is commonly the NE-direction, whereas the NNE fractures cut the main foliation (Wennerström et al. 2008). In the case of NNE-directional fractures, shearing can be seen and steep NNE-directional fractures are focused near Vuosaari-Korso shear zone (Wennerström et al. 2008). In local diabase veins fractures with same direction are found (Wennerström et al. 2008). If the Helsinki area is divided to smaller areas based on tectonic and metamorphic history, in the area where Kumpula is located, steep, short N-trending fractures can be found (Wennerström et al. 2008).

4. METHODS AND DATA

4.1. Drill hole

The drill core was salvaged from drill hole during drilling. It was collected to the about 80 wooden boxes, each containing around five meters of drill core. The drill core was not logged before, so the project started with core logging. The core logging started with photographing the core and drawing directional lines (downwards right = blue, downwards left = left) to the core (Figure 6). The core was not oriented during drilling, so the directional lines were drawn by fitting the core pieces together and estimating the continuity by naked eye.

Figure 6. Drill core box number 11 and 12 after drawing accessory lines and before logging, on the left dry core and on the right wet core.

The depth of the fracture, fracture fillings, roughness of the fracture surface and estimated angles of the fractures were recorded during logging. Also, clearly slickenside fractures were marked.

The depth of the fracture was measured based on the markings of the drillers. The fracture fillings were distinguished based on the colour of the filling and the roughness of the fracture surface was classified in three classes. Surface of the fracture means here the surface between the fracture walls, not the contact line between the fracture and the drill core. The class 3 means rough surface, class 2 medium rough, and class 1 smooth surface. The α-angle of the fracture was estimated in four classes 0–40, and 45–90 degrees instead of calculating α-angle from each fracture during logging. The 0 angle is perpendicular to the drilling direction. The 40-degree-angle class included all angles between almost 0 to 45 degrees, and the 45-degree angle class included all angles between 45 and almost 90 degrees, and parallel to the drilling direction were classified within the 90-degree-angle class. This classification helped to identify specific fractures from the dense fracture zones, in which, for example one parallel fracture was cutting perpendicular fractures. Simultaneously with logging the RQD values were calculated between every 27 meters.

4.1.1. Data processing with Wellcad

A lot of geophysical data was collected from the drill hole during drilling, including acoustic and optical images. Such imaging data was processed in Wellcad software of Advanced Logic Technology (ALT), which is widely used in examinations of drill hole data.

Optical image data
Optical imaging was carried out with ALT instrument called QL40-OBI 40. The user guide of the instrument (ALT/ Mount Sopris) describes that it is camera designed for imaging boreholes. There are three components in the sensor: digital camera, light-bulbs, and conical mirror. Picture orientation is based on a three-component magnetometer and acceleration transducer inside the camera sensor. The accuracy of the picture is 720 pixels per circle and 0.5 mm in vertical axes. Factors that affect the quality of the image are shooting velocity, borehole conditions in vertical axes, and borehole walls, and water depend on the horizontal axes. (ALT/ Mount Sopris a).

Acoustic image data

Acoustic imaging was carried out with ALT instrument called ABI40. It is a borehole camera and a recording instrument. The image is oriented similarly to the optical image and is similarly very sensitive to magnetic failures.

The acoustic imaging method uses ultrasound pulse. It is measuring amplitude and delay of the signal after it has hit the fracture surface (backward signal). Sampling frequency is 288 points per cycle so that the probe rotates ten cycles per second. The given resolution is affected by sampling frequency, exposure speed, and conditions in the bore hole. The conditions in the bore hole are mainly affected by the quality of water – if it flows, the gas bubbles in the water can stop the signal. (ALT/ Mount Sopris b)

Processing acoustic and optical drill hole data

Data from the drill hole has been raw processed by GRM company. The data was presented in logs: one log contained the optical image, and the other log contained the acoustic image of the drill hole (Figure 7). The optical image begins at the depth of 1.9 m and acoustic image from the depth of 31.0 m and they both continue to the bottom of the drill hole.
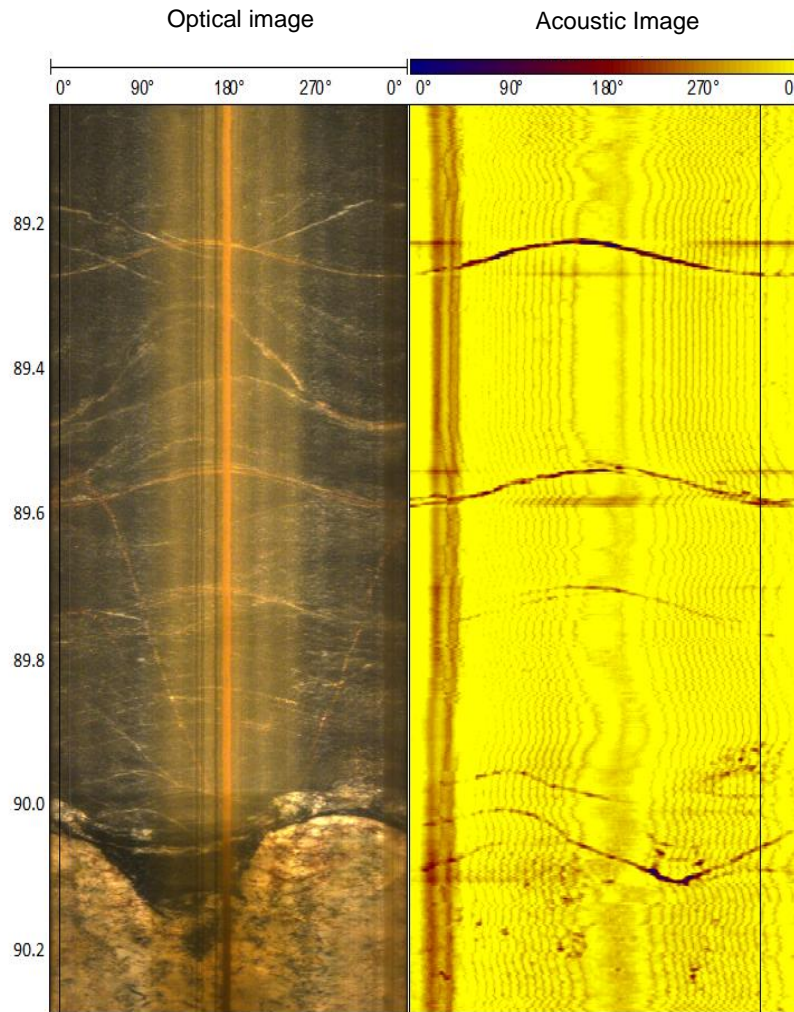
Figure 7. Example images of optical and acoustic logs from the drill hole from the depth of 89.0-90.2 meters.

The drill hole was not oriented, which meant that measuring β- and α-angles from each fracture and adjusting them to real dip direction and dip would have been very difficult by hand. Therefore, the acoustic and optical images were used for this purpose. A new structural log called "structural column was created on top of the optical image log. The optical and acoustic image were compared to each other do that it was possible to draw the identified fractures on the structural column. The software calculated the dip and azimuth of the fractures with a presumption that the drill hole was drilled perpendicularly to the ground and so that 0 direction is north.

After drawing the fractures, the data was compared to the core logging data. The fractures were classified in Wellcad in different fracture classes, which appear on the log in different colours (Figure 8). Fracture classes based on the logging data are: 1) slickensides, 2 minor fractures (filled and unfilled), 0) crushed zones and fractures. Class

3 was added during Wellcad processing phase after it was noticed that the acoustic image contained fractures, which were not visible in the drill core. Class 2 was later divided in Excel to filled and unfilled fractures based on logging data.

Depth [m]	Azimuth	Dip	Aperture	Type
89.25	331.3	25.6	0.000	2
89.56	346.9	25.6	0.000	2
89.74	331.9	34.2	0.000	2
89.99	277.0	38.0	0.000	2
90.04	271.6	35.0	0.000	2
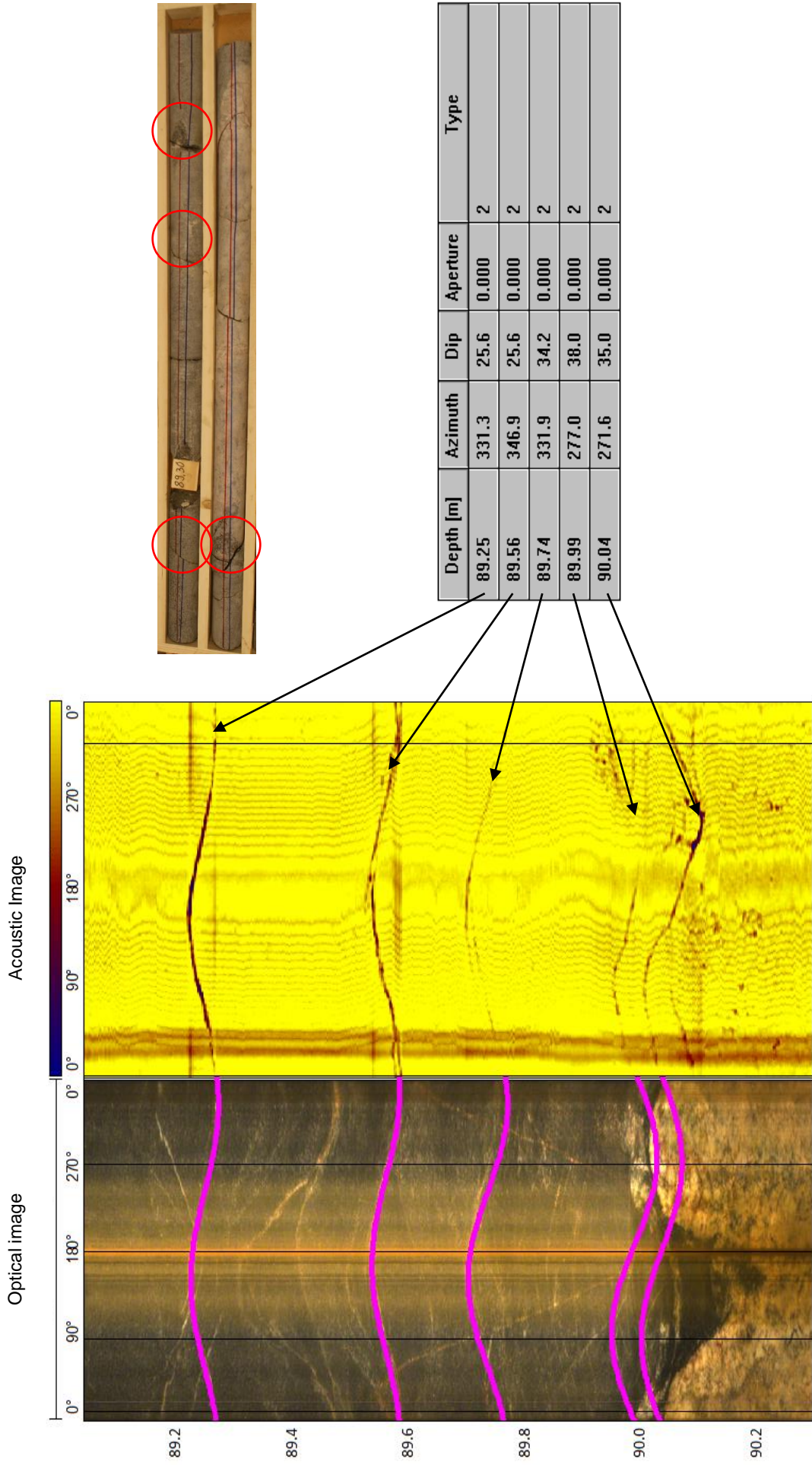
Figure 8. Classification of fractures in Wellcad and image of the drill core, where the tabulated and imaged fractures are indicated with a red circle.

4.1.2. Data corrections

The α and β-angles were calculated for the defined fractures in Wellcad based on the logging data from the drill core and acoustic and optical images from the drill hole. The angles were corrected to the right environment in Excel. The drill hole plunge direction was 45 degrees and plunge 70 degrees so that the drilling direction fluctuated slightly between the starting point and the ending point. The drilling direction had been registered during drilling every 5 meters, so to each fracture the drilling direction was measured not father than 2.5 meters.

The company GRM has processed the image from the drill hole so that the upper edge of the drill hole is on the edge of the image (0 degrees). This direction is 45 degrees. The correct azimuth of the fractures has been calculated based on the β-angle and drilling direction of the drill hole in the following way, when the Wellcad based azimuth is under 315 degrees:

$$Correct\ dip\ direction =$$
$$Wellcad\ based\ azimuth\ (\beta) + drilling\ direction\ of\ the\ drihole,$$

[1]

And following way if the Wellcad based azimuth is 315–360 degrees:

$$Correct\ dip\ direction =$$
$$Wellcad\ based\ azimuth\ (\beta) + drilling\ direction\ of\ the\ drillhole - 360° \qquad [2]$$

The dips of the fractures were corrected based on the α-angle (calculated in Wellcad), the real dip direction of the fracture plane (from equation 1), and drilling direction of the drill hole. The calculation of the dip was more complex, because the effect of dip direction must be considered in the equation. Fractures are planes, which approach drill hole from different directions and create different angles between drill hole. Between the drill hole and the ground there are two angles: to the drilling direction this angle is approximately 70 degrees, whereas on the opposite side it is 110 degrees like seen in idealized Figure 9.

After the calculation of dip directions of fractures, data was divided into two groups. One is fractures with dip directions of 315–360 degrees and 0–135 degrees and the other is fractures with dip directions of 135–315 degrees. The first class is fractures, which are dipping roughly in the drilling direction (45±90 degrees) and the second class includes

fractures, which are dipping away of the plunge direction of the drill hole (225± 90 degrees).

The fracture surface, imaginary ground surface and drill hole create a triangle, where it is possible to calculate the angles R_1 and R_2 seen in the Figure 9. between the drill hole and the fracture plane. When that angle is known, it is possible to calculate the real dip from the triangle, which has been created by fracture plane, (real) ground surface and drill hole like in Figure 9. The equations of the dip corrections are given below.
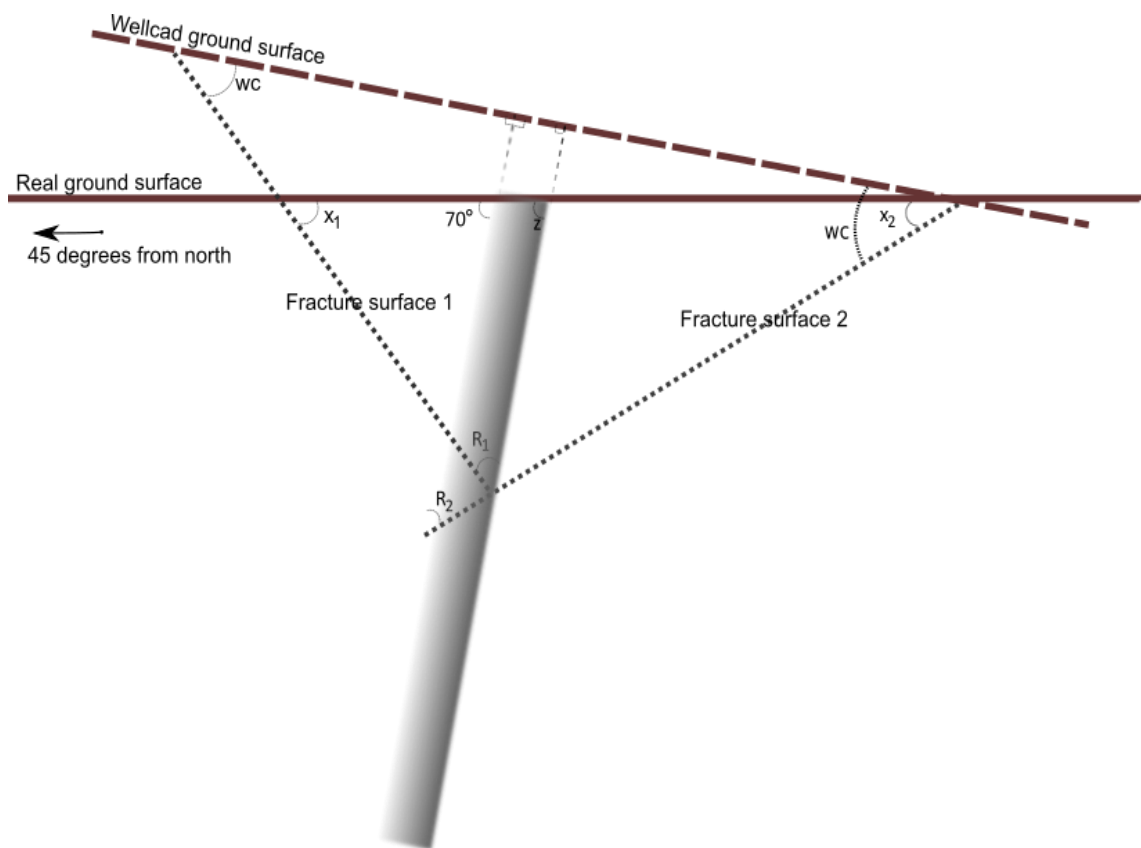
Figure 9. Image of the drill hole in real situation vs. Wellcad basic situation. The drill hole plunge is 70 degrees. When operating in Wellcad, it is assumed that the drillhole is situating 90 degrees from the ground. Wc= dip of the fracture calculated in Wellcad-based assumption, R₁= angle between fracture surface and the drill hole, when the calibrated azimuth is 135–315 degrees, R2=angle between fracture surface and the drill hole, when the calibrated azimuth is 0–135 degrees or 315–360 degrees, z= angle between drill hole and the ground, x= the real dip of the fracture.

$$\begin{cases} 180° - (90° + wc) = R_1 \\ 180° - (z + R_1) = x_1 \end{cases}$$

[2]

$$\underline{90° + wc - z = x_1, \ when \ 0° \le wc \le 70°}$$

[3]

$$\begin{cases} 180° - (90° + wc) = R_2 \\ 180° - \big((180° - z) + R_2\big) = x_2 \end{cases} \qquad [4]$$

$$\underline{-90° + wc + z = x_2, \ when \ wc \geq 20°} \qquad [5]$$

$$\underline{180° - x_1 = x_{1p},}$$
$$when \ wc > 70 \ and \ calibrated \ dip \ direction \ is \ 135 - 315 \qquad [6]$$

$$\underline{90° - (wc + z) = x_{2p},}$$
$$when \ wc < 20 \ and \ calibrated \ dip \ direction \ is \ between \ 315 - 360 \ or \ 0 - 135 \qquad [7]$$

4.1.3 XRD-measurements

The compositions of the fracture fillings were investigated with the X-Ray Powder Diffraction method (XRD). A total of 11 different filling samples from 11 different fractures from different depths were collected. The samples were taken simultaneously with the core logging by scratching the fracture filling material to a plastic bag with a tungsten carbide pencil. The samples were chosen on the basis of the thickness of the filling. The amount of fracture filling sample needed for the analysis was about a size of a pinhead. From the 11 samples, most distinct ones were chosen for the analysis.

The X-ray diffraction method was chosen in order to get general view of the kind of fillings there are in the fractures. XRD is a rapid method especially for detecting clay minerals.

The analysis was carried out with XRD instrument PANalytical X'Pert[3]Powder in University of Helsinki. The machine uses CuKα radiation so that the scanning range is 2–76$^{°}$ 2θ. The samples were ground in a little mortar. A little bit of acetone was added to make fracture filling powder more liquiform for putting the sample on a glass plate. International Centre for Diffraction Data (ICDD) were used to interpret the results.

4.2. Field mapping

Brittle structures observed in the drill core and hole were compared to the surrounding brittle structures in outcrops around the Kumpula hill. The field work was carried out in the area in summer 2016 and complemented in fall 2016 and fall 2017. There are different outcrops on the top of the hill, next to it and on its sides. The outcrops were divided into

ten subareas. They are bound by vegetation, roads, or height above sea level. Outcrop observation form of Pajunen et al. (2002) was used in the mapping. For the purposes of this study strike, dip and dip direction, the length of the fracture, roughness of the fracture surface, waviness of the fracture (approximately Jr-value), aperture, and fracture filling were measured or described. In addition, the number of fracture sets (Jn-factor) and the fracture density of the same fracture set were measured. Minor faults and rock type of the outcrop were also identified, if possible.

4.2.1 Field mapping observations

First two field mapping areas were located in the southern part of the Kumpula hill and they are large outcrops (Figure 10). First one is discontinuous, heavily weathered and covered in lichen. There were small grooves, which were growing grass. The second outcrop was the same one on which the drill hole was drilled. The second outcrop had similar issues with the first one, but the southern part of the outcrop was suitable for making measurements from the fractures. Third outcrop (Figure 10) was quite a small outcrop between two apartment houses and, because it was above the surrounding ground level, it was possible to make measurements from both the walls of the outcrop and from the top of the outcrop.

Fourth outcrop (Figure 10) was situated outside of the Kumpula hill on its western side. It resembles the first outcrop with scour marks, lichen, and a small groove with grass. On its northern part, however, there were a couple of clear long fractures.

Fifth area was a vertical outcrop. There were a couple of very continuous fractures, which crosscutt the schistosity of the rock. Sixth outcrop was a small one and was covered with grass on top of it. There were fresh recent ruptures and fewer actual fractures.

Seventh outcrop was small and round-shaped eastern part of the hill, with only one clear fracture.

Rest of the mapping areas are roadcuts along Kustaa Vaasa road and Hermannin rantatie road, which are divided into three mapping areas, due to length and discontinuity of the outcrop. The northern part of the roadcut has long fractures, with uniform angles. The

middle part has only a couple of dipping fractures and more horizontal fractures. The last part of the road cutting along Hermannin rantatie road has also dipping fractures of a uniform angle, but fewer horizontal fractures than the middle part.
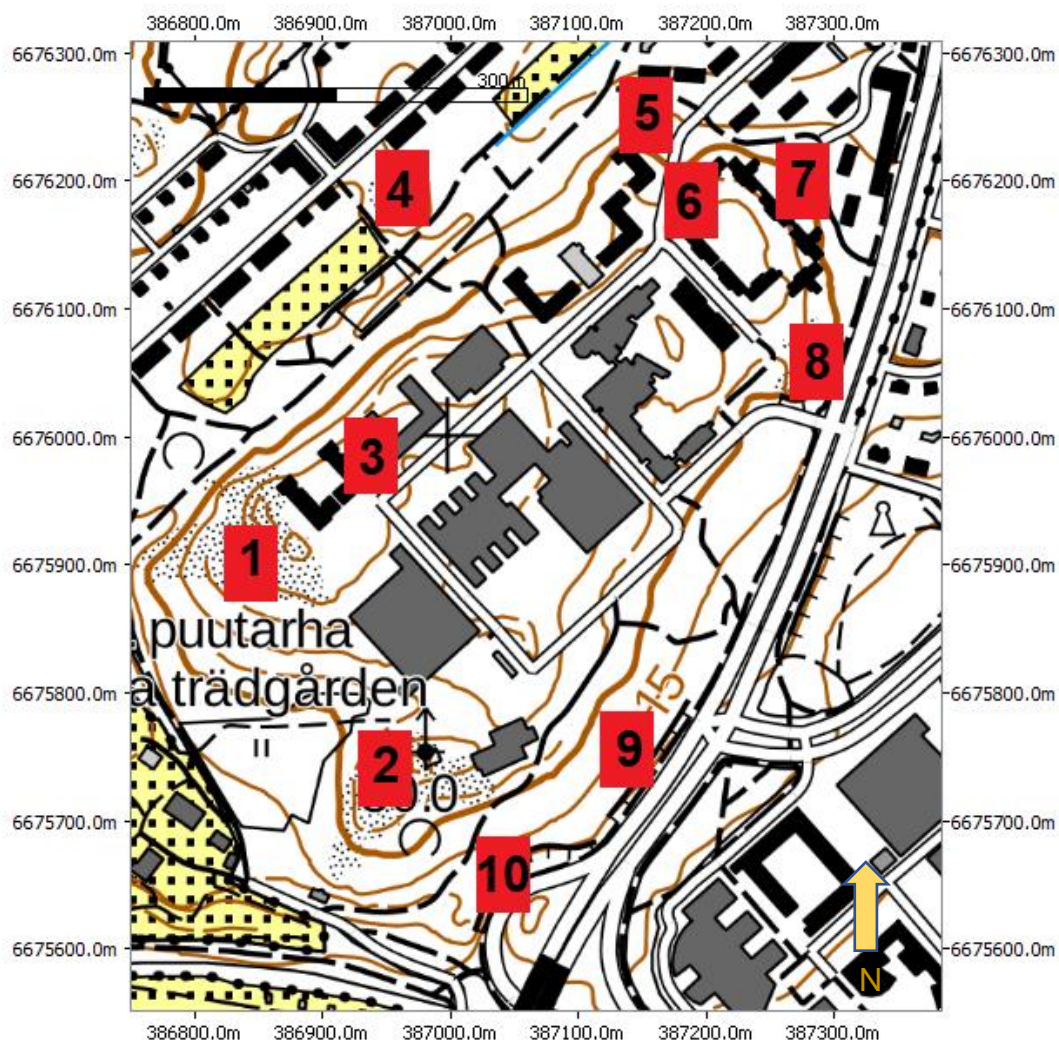
Figure 10. The map of the Kumpula hill and its surroundings, with numbers of the studied outcrops marked.

4.3. 3D-modelling

The gathered orientation data from the drill hole and outcrops on the hill were examined in 3-dimensions. The modelling was carried out with University of Helsinki software by Midland Valley called Move (version 2013.1). It is a modelling software, which is used for structural modelling.

The model was constructed from brittle fracture data from the drill hole and data from the mapped outcrop fractures. The elevation model from the Finnish National Land Survey

(elevation model 10 m) from the area and the general map of the Kumpula area (Figure 11 a. and b) were also added. The software was used in two ways: it is used to statistically examine the fracture orientations and making graphical interpretations.
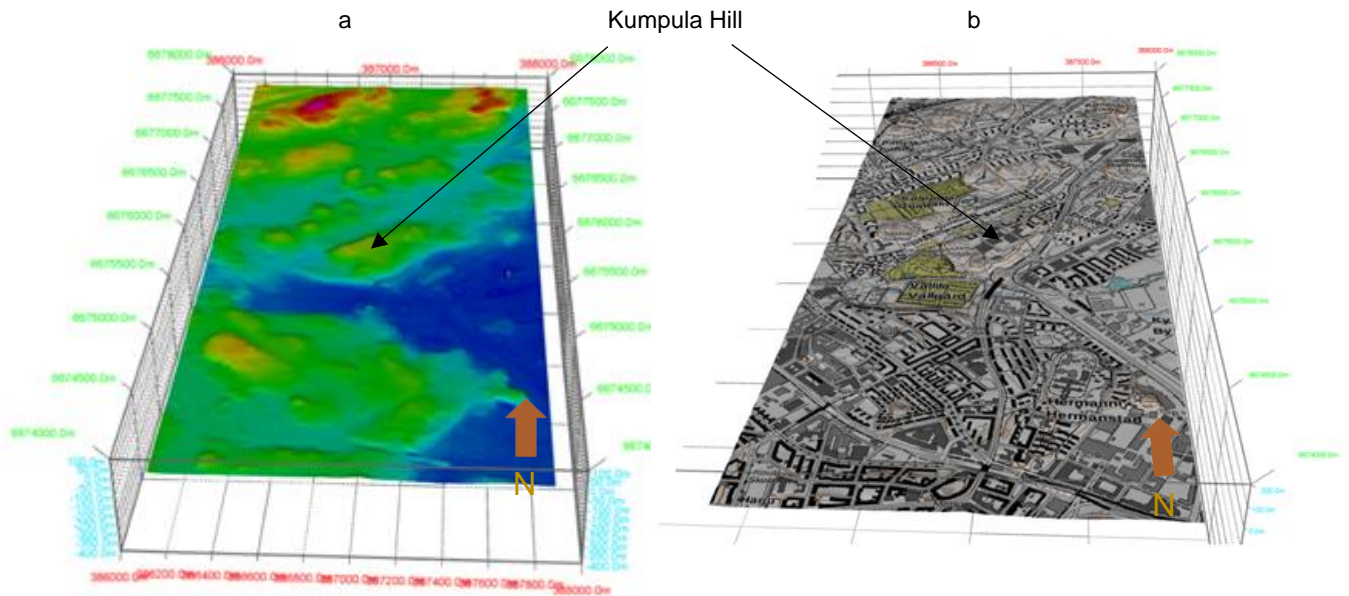
Figure 11. a. The 10 m elevation model of the Kumpula hill and nearby area and b. the general raster 1:1 M map of the same area. Both maps are N-S directional.

The drill hole data was input to the Move in a text-file with an AsciiWell data - format. It included the coordinate data, depth, dip and dip direction data of the fractures and the drill hole itself (Figure 12). Also, fracture type was added to the inspection.
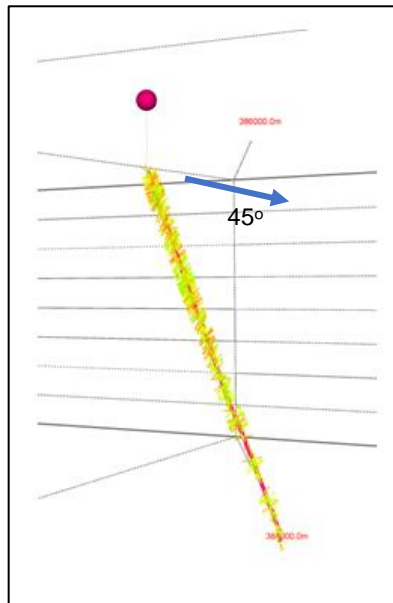
Figure 12. Drill hole with fractures after inputting them to the software. Picture is taken from the south. The drilling direction is marked with the blue arrow.

The outcrop data was added to the inspection in a text-file as an Ascii data -format. It included the coordinate data of individual fractures. The fracture data with dip and dip direction was input in one group and data with only strike information was input in another group. The feature data from the drill hole fractures and outcrop fractures are excluded from the model and are inspected differently. Some fracture places were adjusted individually due to fractures not being in their correct places.

After the data was adjusted, it was classified further. The drill hole data was split to the different groups based on type, dip, and depth. Two crushed zones were discriminated from the other structures. The statistical diagrams from directions (dip, dip directions and strike) were illustrated in the program. The fractures, which have the same strike as the crushed zone are discriminated from the main type group to investigate visually the connection with the crushed zones. Outcrop fractures were divided based on location (northern hill fractures versus southern hill fractures) and dip direction of the different groups.

5. RESULTS

5.1 Kumpula Campus drillhole

5.1.1. Logging and well data analysis

The first impression of the drillhole was obtained during the geological logging phase, (see section 4.1). Among fracture detection, the preliminary RQD value was calculated for the six boxes of the core (approximately to 27 m). The average value was 94 %.

In the geological logging, the fracture surface roughness was evaluated. The roughness was estimated using a three-level scale: 1 for smooth, 2 for moderately smooth and 3 for rough surfaces. Roughness classes were compared to the strike directions of all fractures, filled fractures and unfilled fractures. The comparison was not made with slickenside fractures, because they all belong to the class 1 while crushed zones and fractures belong to the class 3. The 'tight' fracture class was added to the fracture classification after the Wellcad processing phase since the fracture surface of this type was inaccessible in core logging. Variation was found in strike directions between different roughness classes. The main strike direction in every class was NW-SE, but in the moderately smooth and rough fractures secondary strike directions are also present.

In addition, variation was recorded between the roughness classes of filled fractures. The main strike direction was NW-SE in the class 1 and 2, but in the class 3 it was NNE-SSW. In class 1 there was less deviation between strikes of the fractures, but in class 2 there was more variation in the NE-direction. The roughness class 3 of the filled fractures was more scattered. The NE-direction was the dominating direction, but there were lots of rough surfaced fractures also in the E-W and NE-SW directions.

Unfilled fractures exhibit also variation roughness. The roughness class 1 was very narrow with a NW strike, but in the class 2 the strike direction separated to the NNW-SSW and E-W strikes. The class 3 was similar with class 1, but the main strike direction differed from class 1 by five degrees.

In the next phase the logging data was correlated with the wireline logging images of the drill hole using Wellcad software. Acoustic and optical images are available of the drill

hole, which were used in the analysis. With the help of the image data the logged fractures in the core were correlated to the imaged fractures. This way the correct dip and dip direction of the fractures could be determined. It was possible to recognize approximately 85 % of the logged fractures from the optical and acoustic images and add a new fracture group, tight fractures, based on the acoustic image. These were fractures that were not open in the drill core but were seen clearly in the acoustic image. Other fracture groups defined during the logging phase were slickensides, fractures without filling (unfilled fractures), filled fractures and crushed zones and fractures. The classification to the fracture groups were made according to the tectonic character (slickensides), filling (minor fractures versus filled minor fractures) and fragmentation (crushed zones and fractures) (Table 7.).

Table 7. Fracture types of the drill hole and percentage fraction

Fracture type	Number of fractures	Percentage fraction
Crushed zones/fractures	20	2.85
Filled fractures	350	49.93
Unfilled fractures	169	24.11
Tight fractures	80	11.41
Slickensides	80	11.41

RQD, Jn and Jr values were calculated based on logging data and Wellcad analysis. These more accurate RQD, joint roughness (Jr) and number of joint sets (Jn) values were calculated with as homogenous depth intervals as possible. The deviation follows mainly the rock type or texture difference boundaries. The drill hole was divided to 72 depth intervals. The Jr value were established based on the logging data and acoustic image of the drill hole. It was evaluated to all other fractures except the ones, which were only visible in the acoustic image, and fractures from the first 30 meters, because no acoustic images were available for them. The drill hole is dry to this depth.

The RQD value varies from 100 to 65 percent (Table 8). Exception was made in the crushed zones, whose RQD values were evaluated as zero. In 22 depth intervals the RQD value was 100 %. Most of the 100 percent depth intervals were between 180–300 meters, but there were four 100 percent depth intervals also between 43.18 to 75.72 meters. The most broken depth intervals (RQD less than 70 percent) were at 7.97 to 8.81 and 208.4 to

208.76 meters. Other depth intervals have the RQD value over 80 percent and 90 percent. The mean RQD value was 93.73 %.

The Jr value was an average value of the roughness of each fracture on that depth interval. The minimum Jr value was 0.5 and maximum was 4 (Table 8). The fourth fracture class was excluded from the inspection and fractures were evaluated as 0.5, 1, 1.5, 2 and 3. Slickensided fractures were divided between classes 0.5 and 1.5.

Average Jr value was 1.65. In 16/72 depth intervals the Jr value was over 2. Jr value was 3 only in the crushed zones. Value was between 1-2 in 38 depth intervals out of 72 and Jr value was 1 in seven depth intervals. One of the depth intervals did not have fractures, to which a Jr value could be determined.

Fractures were grouped into sets of 0–30, 30–60, 60–90, 90–120, 120–150, 150–180, 180–210, 210–240, 240–270, 270–300, 300–330, and 330–360. In that way the average Jn value was 7.7. Overall the Jn value differed from 1 to 20. The Jn value was 6 (2 main fractures and random direction) in 17 depth intervals out of 72. Jn value was 9 (3 main fracture directions) in 7 depth intervals and 12 (3 main fracture directions and random direction) in 8 depth intervals. The Jn value was 15 in 14 depth intervals. In crushed zones the Jn value was 20. Fewer than two main fracture and random directions (Jn value under 6) was in 26 depth intervals, of which 15 depth intervals have value 3 (one main fracture direction and random direction).

Table 8. RQD, number of joint sets (Jn), joint roughness (Jr) and fracture density values for determined depth intervals of drill hole. The minimum trace length is 0.36 m and maximum is 24.11 m. Mean trace length is 5.14 m. The full data of the analysis is represented in Appendix IV.
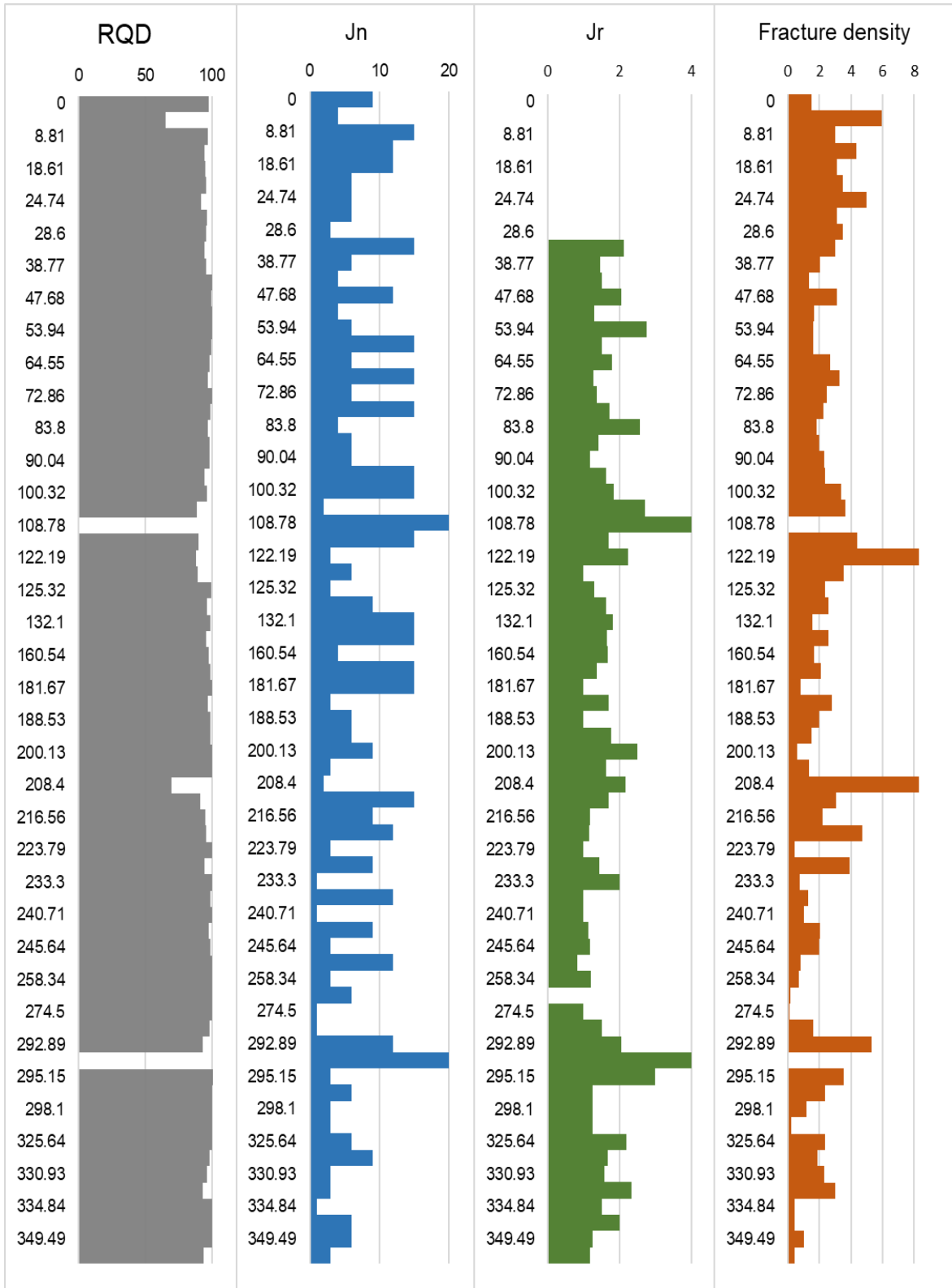
5.1.2. Fracture fillings

From each open fracture in the drill core any fracture fillings were noted. Based on colour and texture it was possible to detect 6–8 different fracture fillings. The most common type of fracture filling has a green colour. This green colour also varies from dark to light green, where the lighter green fracture filling is stickier than the darker green. White/grey and red fracture fillings were also observed. The red filling was stickier in some fractures, but in other fractures it was impossible to rub out and the character of the filling was different. All possible fracture fillings are seen from top to bottom of the drill core and in some fractures, there are two fillings on top of each other.

The fracture fillings samples were sampled of several depths, because it was hard to compare only by colour if the sample of that type of filling was taken already. The total amount of samples taken from the drill core was 11 and 5 of them were selected for XRD-analysis. If the texture and colour were uniform, the fillings were assumed to be the same filling.

The analysed samples of fracture fillings represented five different fractures from five different depths and dip directions (Table 9). One of the fractures was slickenside and one was an almost horizontal fracture. Dip direction and dip of the fracture was not able to be determined due to the shape of the fracture in the optical image of drill hole in Wellcad.

The colour of the samples varies from red to grey and green. The grey sample contain sulfide mineral (pyrite) and the red sample contains hematite. The last three sample were greenish. All samples contain clay minerals and most of the samples contains feldspars except the fourth sample, which was from a slickenside fracture, comprising only clay minerals and mica. Albite was found from the samples 2 and 5, whereas anorthite was found from the samples 3 and 4. From the samples 1 and 2 were also found two other feldspars: microcline from the first sample and sanidine from the second sample.

First sample from the depth of 48.02 m and last sample from the depth of 213.52 metres has granite/granite-gneiss as a surrounding rock type. Both fillings contain clinochlore. The colour of the fillings differs from grey to the green.

First two samples were the only ones containing amphiboles (tremolite). Clay mineral vermiculite was found from sample 2, 4 and 5. Quartz was found only in the first sample and manganese oxide (todorokite) only from the last sample.

The dip direction of the samples differs, but in samples 1, 2 and 4 the dip was almost the same. The fifth sample had an almost horizontal fracture. The sample 3 fracture penetrates the drill hole only momentarily so it's dip direction and dip should be almost the same as with the drill hole itself.

Table 9. Fracture filling results in XRD. Rock types after Penttilä (in prep.201X).

Sample n:o	Depth	Rock-type	Dip direction	Dip	Fillings	Note
1	48.02	granite	70.97	40.51	Clinochlore quartz pyrite anorthite microcline tremolite	
2	56.68	horblende-gneiss	239.57	43.85	hematite albite sanidine vermiculite tremolite	
3	72.15	migmatite	along dillhole	along drillhole	clinochrysotile kaolinite montmorillonite saponite anorthite	Real dip direction and dip was impossible to determinate, because of the shape of the fracture in drill hole image
4	130.59	amphibolite	329.30	47.13	antigorite vermiculite phlogopite	Slickenside fracture
5	213.52	granitegneiss	14.44	3.68	clinochlore vermiculite albite todorokite	

5.1.3. Fracture orientations

The corrected fracture data was examined in 3D-modelling software (Move version 2013.1 of the Midland Valley). This way it was easier to get an impression, for example, of the main direction data of the fractures and fracture groups and compare the data to the outcrop fracture data (see chapter 5.2.). The connection between fracture direction (strike and dip direction) and depth intervals, different fracture groups, dip and depth, dip and different fracture groups and dip versus dip direction were examined.

Strike and dip direction

The main dip direction was 45–50 degrees from north. Most of the fracture dip directions were between 35–60 degrees and so the mean dip direction was 77.4 degrees (Figure 13 a). The second main dip direction area was roughly to the south. There was also a remarkable amount of fractures, whose dip direction was to the SE and SW.

The main strike direction was approximately in the NW-SE axel (Figure 13 b). Most of the fracture strike direction was divided between 300–330 degrees. There was a lot of variation among other fracture strike directions, but no distinct other second main strike directions emerged.
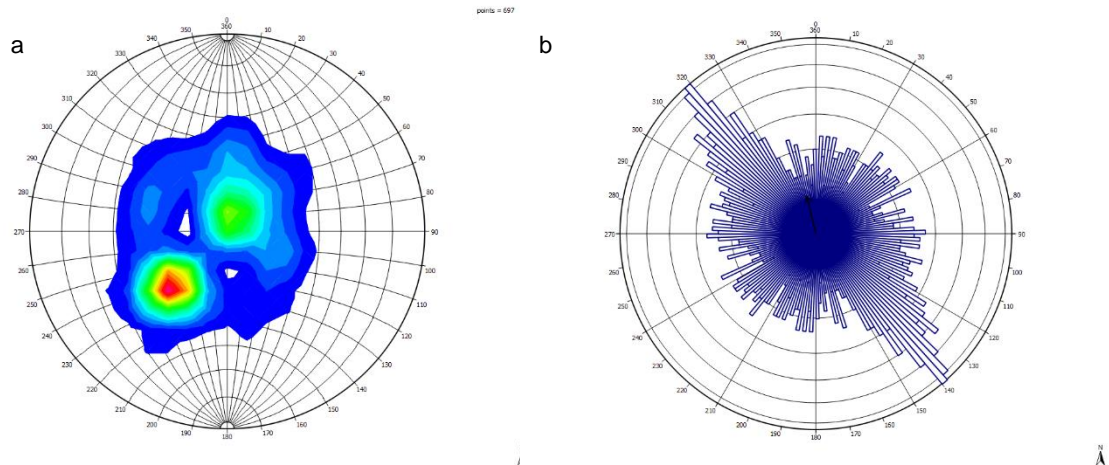
Figure 13. a) Wulff's equal angle lower hemisphere stereographic projection of poles of the dip directions and dips from all the fractures of the drill hole. Mean dip/dip direction was 39.9/77.4. b) Bidirectional rose diagram of the strike direction from the same fracture set. Mean strike is 347.35. Number of points used is 701.

Drill hole fractures were grouped into depth intervals of 50 meters starting from 0. An exception was made for only the last 20 metres (350–370.2 m). Between these depth intervals the possible strike variation was examined (Figure 14).

To the depth of 200 metres the main strike of the fractures was NW-SE, but in the interval of 200–250 metres besides NW-SE a second main strike direction NNW-SES is also present. The main direction wanders towards north in the last depth intervals so that in the 250-300 metres it was NNW-SES and in the last two it was approximately N-S. In the 250–300 metres there was also the second main strike direction to the E-W, which was associated with the crushed zone in the depth of approximately 294.4–295.14 meters.
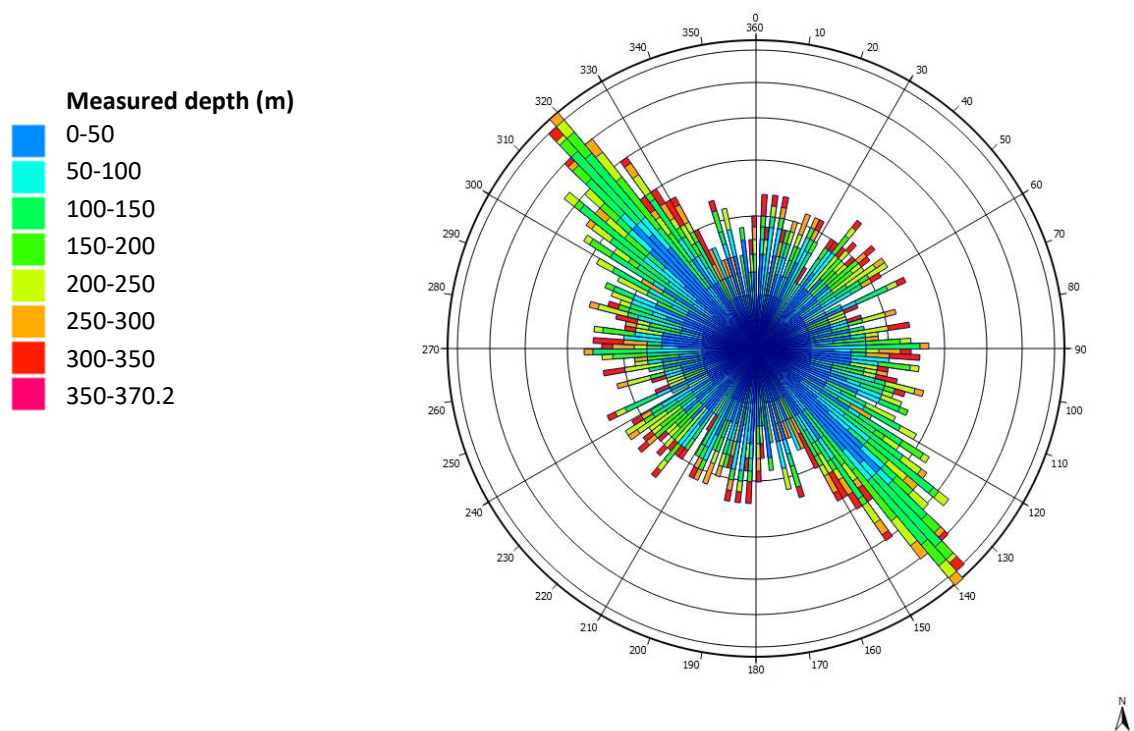
Figure 14. Rose diagram of the strike of the drill core fractures versus different depth intervals.

The dip directions and strikes of the different fracture groups were studied. There was some deviation in dip direction between different fracture groups, which were seen clearly in rose diagrams of different fracture groups (Table 10).
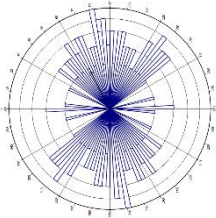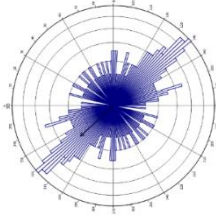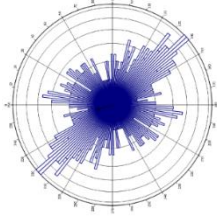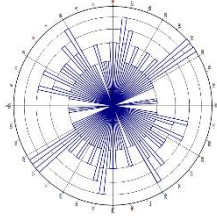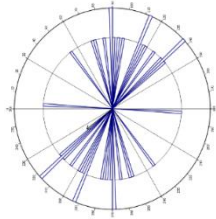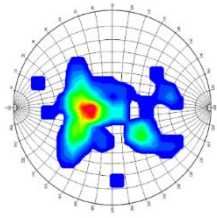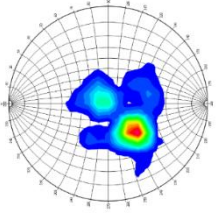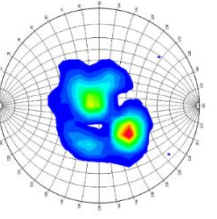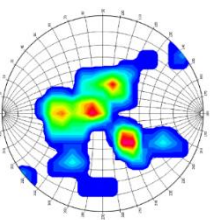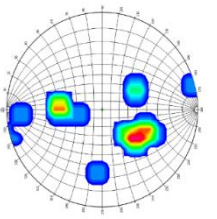
The main dip direction of the slickensides was 45–50 degrees and the second main dip direction was around 150–190 degrees. Correspondingly the main strike direction was approximately in the E-W direction, but the main strike direction does not stand out clearly, the main strike area was between NE-SE/SW-NW.

Tight fractures were a small group (80/701). The main dip direction was 50–55 degrees and the second main dip direction was 185–195 degrees and its strike was in the SE-NW direction.

Filled and unfilled fractures have mainly the same main dip direction and strike direction. The main dip direction was around 45 degrees and the second main direction was roughly the same. The main strike was roughly in the NW-SE axel in both fracture groups. The biggest difference was in mean dip directions, which was about 73 for the filled fracture and about 47 for the minor fracture. This means that dip directions of filled fractures were dispersed more than unfilled minor fractures.

The 'crushed zones and fractures' - class comprise two crushed zones and fractures that were crushed more than usual. It was hard to make a generalization, because the group was unorthodox and small (20 fractures) compared to the other fracture groups. There were some suggestions that the main strike direction was ESE-WNW and main dip direction was around 50 degrees. The main strike of the first crushed zone (108.78–109.21 metres) was NW-SE and the second crushed zone (294.4–295.14 metres) was as mentioned earlier E-W. The start and end points were relatively vague for the first crushed zone, so the dip and dip directions were difficult to determinate accurately, but for the second crushed zone the ending and starting points were clearly distinguishable so the dip/dip direction of the start point was 46.4/181.12 and for the end point it was 47.07/188.23 degrees.

Table 10. Strike and dip and dip direction of the fracture groups

	Slickensides (N=80)	Unfilled fractures (N=169)	Filled fractures (N=350)	Tight fractures (N=80)	Crushed zones (N=20)
Strike					
Mean strike	62.92	317.28	343.22	83.13	322.42
Dip and dip direction					
Mean dip/dip direction	39.98/152.92	40.05/047.28	38.80/073.22	41.11/173.13	53.01/52.42

The number of fractures from each depth interval (Table 11) and main dip direction of all fractures and fracture classes was examined (Table 12). The main dip direction of the fractures fluctuates between depth intervals. The main dip direction based on all fractures was 45–55 degrees in the first 250 metres, but in the depth of 250 meters the main dip direction changed to the direction of 180–185 degrees. Two new main dip directions in 225–230, and 275–280 degrees appeared in the last 70 meters depth.

The main dip direction varied at different depth intervals inside of the fracture group. In slickensides for the different depth intervals the main dip direction was changing so that it was close to 45-55 degrees or 150-190 degrees. For tight fractures, the main dip direction changes between depth intervals so that just 100–150 and 150–200 metres intervals, it was around, in general, 45–55 degrees. The main dip directions were close to each other at every depth interval except in between 150–200 and 250–300 metres in minor fractures (filled and unfilled), so that in the depth interval 150–200 metres it was around 230 degrees in the filled fractures and in the unfilled fractures it was around 50. The main dip direction for the depth interval of 250–300 metres was around 180 degrees in the filled fractures and in the unfilled fractures around 55 degrees.

Table 11. Depth intervals, number of fractures and percentage amount of fractures in every interval

Depth interval	Number of fractures	Percentage fraction
0-50	139	19.83 %
50-100	111	15.83 %
100-150	151	21.54 %
150-200	99	14.12 %
200-250	96	13.69 %
250-300	55	7.85 %
300-350	37	5.28 %
350-370.20	13	1.85 %

Table 12. Main dip directions of different depth intervals

Depth interval (m)	Main dip direction (in degrees from north)					total number of fractures
	All	**Slickensides**	**Unfilled**	**Filled**	**Tight**	
0–50	45–50	185–190	45–50	35–50	20–25 125–130 150–155 185–190	139
50–100	45–50	45–55 [1] 145–155 [1]	40–45 50–55 325–330	45–50	185–190 [1]	111
100–150	45–50	35–40 [1] 45–50 [1]	45–50	45–50	45–55	151
150–200	50–55	135–140 175–180 210–215	50–55	230–235	50–55 280–285	99
200–250	50–55	170–175	60–65	50–55	[2]	96
250–300	180–185	[2]	55–60	180–185	50–60 135–145 175–185	55
300–370	225–230 275–280	[3]	260–270 275–280	225–230 270–280	[3]	50

1) under 10 % of fractures at that depth

2) under 10 % fractures, all at different direction

3) no fractures

Dip of the fractures

The dip of the fracture is divided into five classes: horizontal fractures (dip under 10 degrees), gentle fractures (dip 10 to 30 degrees), moderate gentle fractures (dip 30 to 50 degrees), moderate steep fractures (dip 50 to 70 degrees) and steep fractures (dip over 70 degrees). The dip was compared with depth, fracture group and dip direction.

Dip angle from 0 to 90 degrees encountered with every depth interval, and every fracture groups. The most common fracture the dip was 40–50 degrees, and this dip appears in every depth interval as well as every fracture group (Figure 15).

The percentage amount of moderate horizontal fractures increased towards the bottom, whereas in horizontal fractures (0-10 degrees) the percentage amount was biggest in depth intervals of 150–200 metres.

The biggest percentage amount of steep fractures (dip over 70 degrees) was in the depth interval of 300–350, whereas the smallest amount of steep fractures was in the depth interval of 50–100 meters.

Moderate gentle fractures were the biggest dip group in every depth interval. The percentage amount of moderate gentle fractures was over 50 percent in depth intervals of 50–100, 100–150, and 150–200 meters.

The amount moderate steep fractures were on average 20 % in depth intervals of 0–50, 50–100, 100–150, 200–250, and 250–300 meters. The percentage amount of steep fractures was under 20 % in depth intervals of 150–200 and 300–350 meters. In those intervals the percentage amount of gentle fractures was bigger.
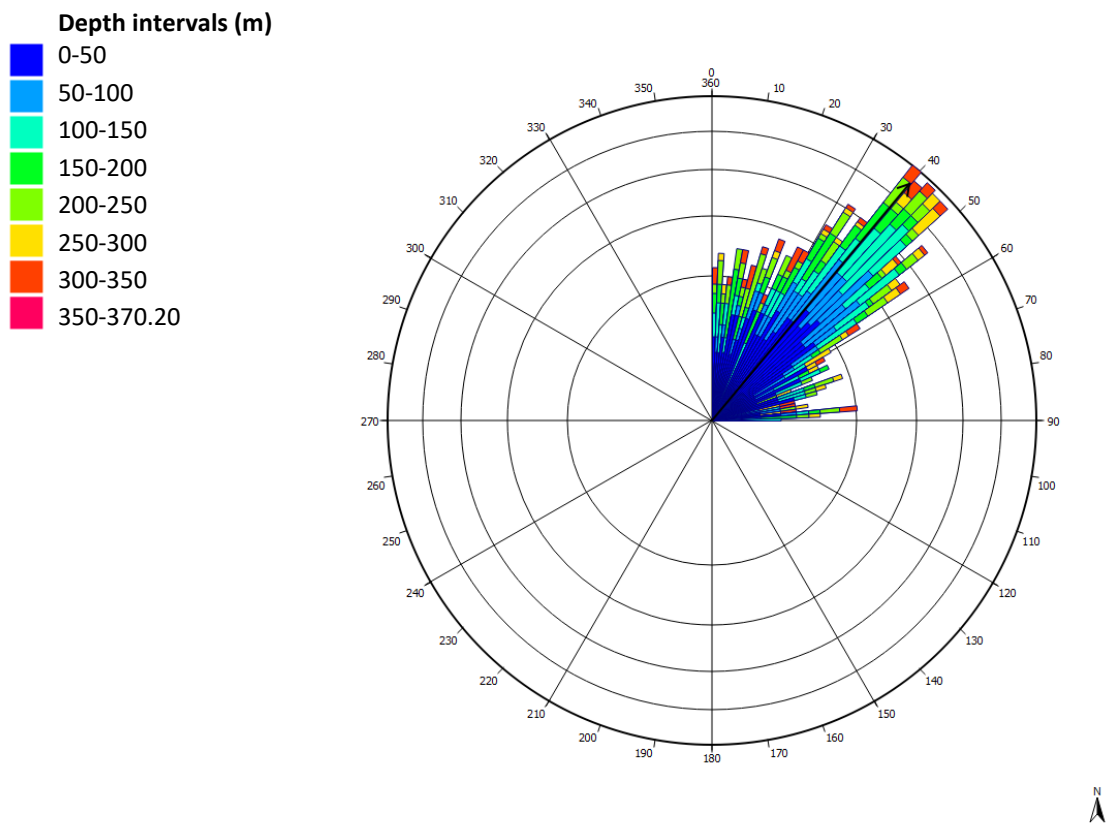
Figure 15. Rose diagram of dips of the all fractures of the drill core versus depth intervals.

The dip of 30–50 was the most common in all fracture groups also in every depth interval. (Figure 16). There were some exceptions in unfilled fractures, filled fractures and tight

fractures. The most common dip is 50–70 degrees with minor fractures in the depth interval of 200–250 metres, while in 250–300 metres it was 70–90 degrees and 350–370.20 metres it was 10–30 degrees. The most common dip was 10–30 degrees with filled fractures in depth intervals of 250–300 and 350–370.20 metres.
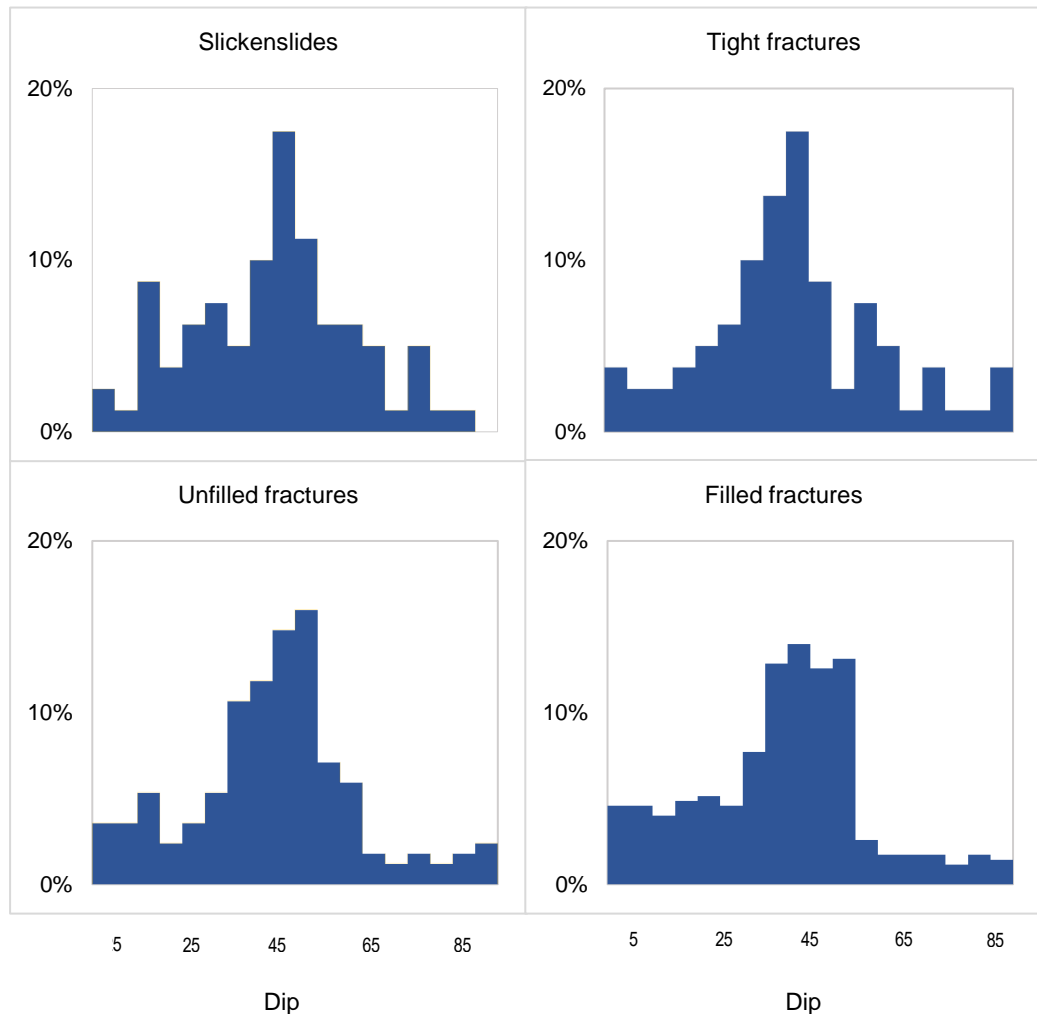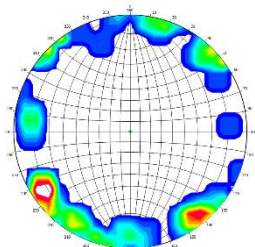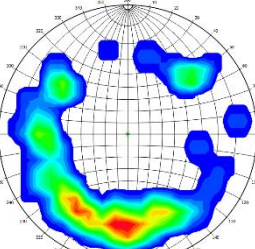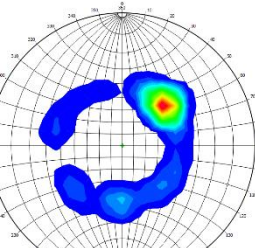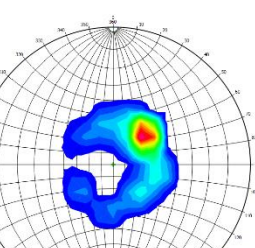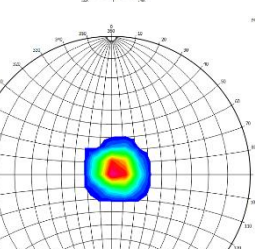
Figure 16. Different fracture groups versus dip.

Dip directions and dips were compared to each other (Table 13). Horizontal, moderately gentle, and moderately steep fractures have one clear dip direction, and steep and gentle fractures also have one dip direction, but more variation as well. The main dip direction of moderately gentle and moderately steep fractures was the same as the main dip direction of all fractures.

Table 13. The connection between dip and dip directions. Density contours showing dip directions not poles.

Dip (in degrees)	Main dip direction (in degrees)/ mean dip direction	Stereographic projection
under 10	235-240 203.47	
10-30	180-190 203.79	
30-50	45-50 59.13	
50-70	45-50 57.66	
over 70	30-35 60.68	

5.2 Kumpula hill outcrop fracture features

5.2.1. Properties of fractures

Bedrock of outcrops were studied around the Kumpula hill to see how the fractures in outcrops correlate with the drill hole data. There were 10 outcrops around the Kumpula hill, out of which 6 of 10 were natural rock exposures and 4 out of 10 were road cuttings. The rock exposures were heavily lichened and so there were only around 50 fractures, where it was possible to make some observations.

The characteristics observed were strike, dip and dip direction, the length of the fracture, roughness of the fracture surface, waviness of the fracture (approximately Jr-value), aperture, and fracture filling (Table 14). Apart from these, the number of fracture sets (Jn-factor) and the fracture density of the same fracture set were determined. Some of the listed features were impossible to measure from some fractures, mostly because lichen or other vegetation. Fractures were placed in fracture groups using strike angle. The groups were 0–30, 30–60, 60–90, 90–120, 120–150, 150–180, 180–210, 210–240, 240–270, 270–300, 300–330, and 330–360 degrees. Usually there were two main fracture directions on the outcrop, which were cutting two or three individual fracture directions. Usually not only individual directions are the same with the main strike, but their strike differs only some degrees from other main direction. Then again there was just one main fracture set direction in the road cutting sites.

Lengths of the fractures were measured where possible so that length represent the minimum length for some fractures. The measured length of the fracture was usually under 5 metres. There were few fractures, whose length was 5–10 metres including two slickensides, and only one fracture, which could be measured to be over 10 metres long. From the road cuttings it was impossible to measure length, so the height of the fracture was evaluated. There were two fractures in outcrop 10, which ended connected to each other. Other fractures in the same outcrop split the rock wall. The height of these fractures was over 4 meters.

The aperture was measured from the widest place between fracture walls and generally it was wider on the outcrops than road cuttings. There were a couple of fractures where

there was no other half and for some of the fractures the aperture was approximately 10 cm. The mean aperture among all the fractures was 3.2 cm.

Fracture fillings were recorded for only a handful of fractures (9 out of 53). Based on colour and texture on the outcrop 3, fillings were identified as the same in the drill core. Fillings in this outcrop were multicolour: mixed red and green. Fracture fillings were also found from the road cutting 8, where the fillings were also red-green and red.

Roughness of the surface was measured from fractures, where the dip and dip direction were possible to be measured. The roughness estimation was the same three class system than with the drill core logging from Pajunen et al. (2002a), where 1 meant smooth surface, 2 moderately smooth and 3 a rough surface. The mean roughness was approximately 1.5 based on 35 fractures out of 53. Two fractures were situated so high that it was impossible to reach the surface of the fracture.

The waviness of the fracture was estimated also in a three-class system, where 1 meant that difference between end points of the measured fractures were under 1 cm, 2 meant that the fracture was curved over 1 centimetre and 3 meant that the fracture was gradual (Pajunen et al. 2002a). Most of the fracture were planar, especially in the road cuttings, and only 2 measured fractures belong to the group 3. The mean waviness value was 1.6 among all measured fractures.

Fracture density was difficult to calculate for some outcrops, because of the lichen, which covered some of the fractures. In total, the fracture density was calculated for eight fracture sets in 6 outcrops. The density was usually very low (below 1 fracture/1 metre) except in one place in outcrop 10, where fracture density to the strike direction NNW was 1.09. Overall there were no places, where fracture density was very high.

The strike direction differed relatively lot among fractures and there was no major difference between the main strike direction and other directions. The main direction was approximately E–W, but there was another main direction to the N–S and NW–SE directions.

There were 9 outcrops, in which it was possible to measure dip and dip direction. There was variation of quality between fracture surfaces where dip and dip direction were measured. Total amount of fractures with dip and dip direction was 37 out of 53. The dip was moderately steep (50–70) or steep (over 70 degrees) in most fractures. Beside horizontal fractures in road cuttings, which were left outside of the analysis (outcrops 8, 9 and 10) there were four measured fractures, where the dip was moderately gentle. The mean dip was 65.84 degrees. There were slickensides, whose dip was approximately 90 degrees, but both were lacking the other wall of the fracture, thus from these fractures dip directions was determined to go towards the missing wall. The main dip direction was NE and SES and the mean dip direction was 173.18 degrees (Figure 17).
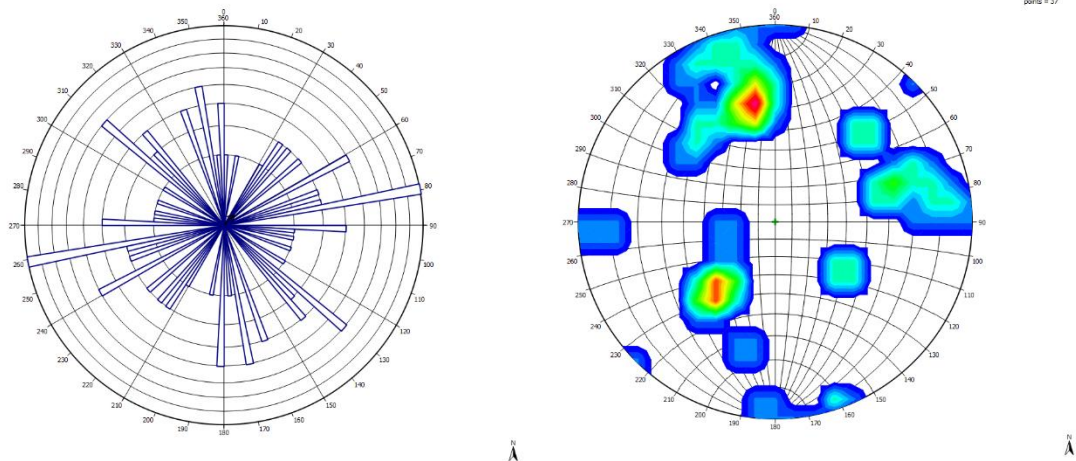
Figure 17. a) Bidirectional rose diagram of strike direction of outcrop fractures. Total number of fractures is 53. Mean strike direction is 46.67 degrees. b) Wulff's equal area lower hemisphere stereographic projection of outcrop fractures. Total number of fractures is 37 and mean dip/dip direction is 65.84/173.18.

Table 14. Main features of the outcrop fractures

Outcrop	Type [3]	Number of fracture sets	Joint surface	Main direction of the fracture set	Fracture length (longest fracture/mean length)	Fracture density (number of fractures/length of line)	Slickensides	Dip direction/dip example	Individual fracture direction(s)
1	A	2		NW-SE	5/5.0	7/15	x	045/55	N-S
				NE-SW	7/2.0	7/13			
2	A	2	1.75	W-E	8/5	4/16		170/70	NEE-SWW
			1.66	NE-SW				310/50	NWW-ESE
3	A	2	1.00	N-S	4/2.8		x	260/60	E-W
			1.00	WNW-ESE	4/2.6??			170/60	NNW-SES
4	A	2	1.67	NE-E to SW-W	2/2	5/6			NNE-SSW
			2.00	NNW-SES	11/5.7	3/8		260/60	NW-SE
5	A	1[1]	1.00	NNE-SSW				300/45	
6	A	1	1.50	NNW-SES		4/9		260/80	NE-SW
7	A	1[1]	1.00	NE-SW	1.0/1.0				
8	B	1[2]	1.50	E-W		4/10		180/60	
9	B	1[1[2]	1.00	E-W					
10	B	1[2]	1.00	NW-SE	12/11			040/55	NWW-ESE
									N-S

[1] Only one fracture observations
[2] Only measurd fracture height, not length
[3] Type A = rock exposure, B = road cut

5.3. 3D-modelling

Modelling was done in Midland Valley's 3D-software called Move (version 2013.1). The handled data was the elevation model from the National Survey of Finland, the general map from Helsinki (relation 1:100 000), the drill core fracture data and outcrop fractures data. The drill core data was input to the program in a text-file and it originally included the coordinates, dip, dip direction and fracture type. The software calculated strike based on the dip direction. The original idea was to put the fracture features to the software also, but there was no logical tool for that.

The measured outcrop data includes the coordinate data, strike, dip and dip direction data of the fractures. Fractures with dip and dip direction data and only strike data were put to the software in different files. The coordinates of the fractures were measured with a gps-device, but still some of the fractures were not located at the correct place so they were adjusted individually based on the map.

The classification of the fractures continued in the program and so it was possible to process all direction diagrams in the software (section 5.1.3). Two crushed zones in the drill hole were separated from fractures in the crushed fracture group. The full analysis of the strike directions was made to the outcrop fractures and compared to the northern and southern side hill data together. Also, an important step was to compare drill hole data and outcrop data to each other.

Any major faults were not detected on the outcrops. Little faults were discovered based on the veins from the outcrop 3 and 6, but the observed movement was under 15 centimetres, so they were not marked into the model. The crushed zones in the drill hole were only major structures, which were detected according to the available data. The crushed zones were examined visually so that they were extended to the surface at the same dip direction and dip angle as they are in the drill hole (Figure 18). The shallower crushed zone appears to continue at the exact same angle as the valley of Vallila and the other has the same angle as the fractures of the outcrop 8 (Figure 19). Crushed zones continued in same dip direction and dip both 400 metres to every direction from the drill hole. They collide underground in location where the edge of the Kumpula hill is very gentle and covered with soil. The drill hole fractures were examined to see how they were

related to the crushed zones (Figure 20). The strike direction of the crushed zone one is approximately 320 degrees and the second is approximately 90 degrees.

Figure 18. The Kumpula hill from east side. On the left is marked the crushed zone from the depth of 109.0 and on the right is crushed zone from the depth of 296.0. Both are extended from original observation point (from the drill hole) 450 meters in every direction so that they cut with the surface of the ground. The pink point is the place of the drill hole.
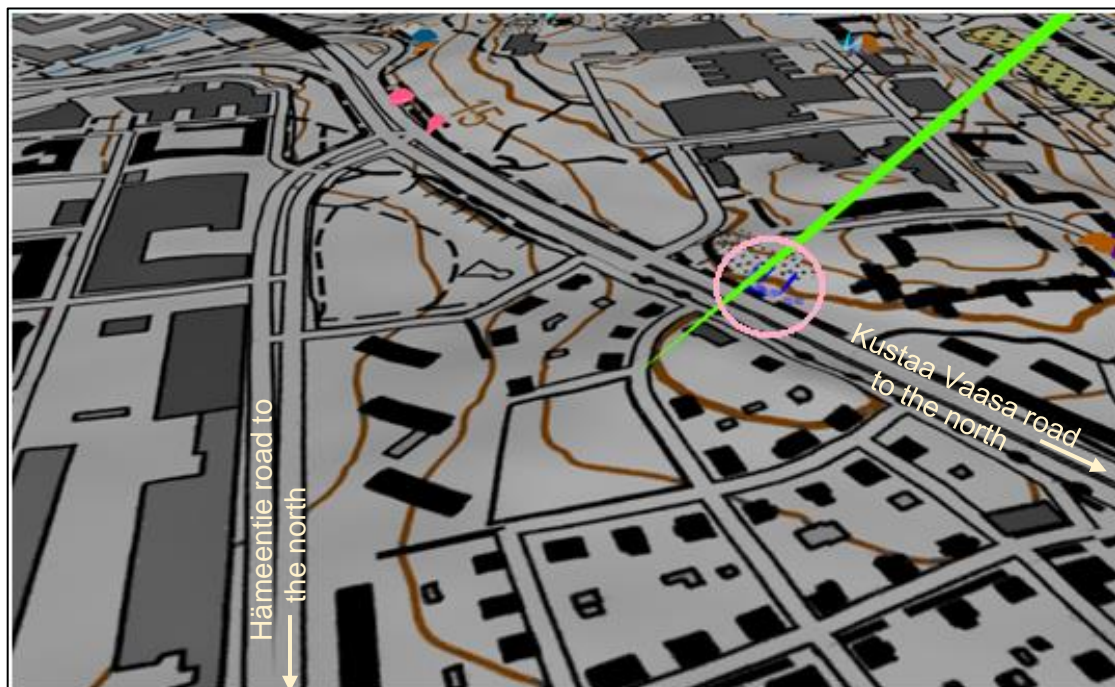
Figure 19. The green surface is the extended crushed zone from the drill hole and the blue planes (circled with pale pink) are fractures on the road cutting (outcrop 8).
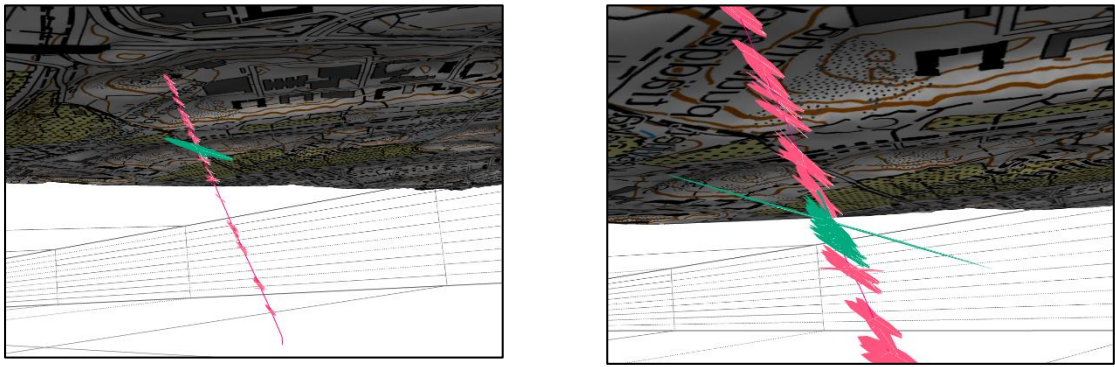
Figure 20. The green surface is the crushed zone and the pink surfaces are filled fractures with same strike (± 15 degrees). Filled fractures with strike of 300-330 degrees are found from top to bottom in the drill hole, but they are also found to be very dense near the crushed zone (fractures marked in green).

The strike direction on north side and south side of the Kumpula hill was compared with each other (Figure 21). On the south side of the hill, there was more variation between the strike of the fractures, but the the main strike direction was E–W (Figure 22a). There were fewer measurable fractures on the north side of the hill and less distribution between strike direction, so the main strike directions were N–S, and E–W (Figure 22b).
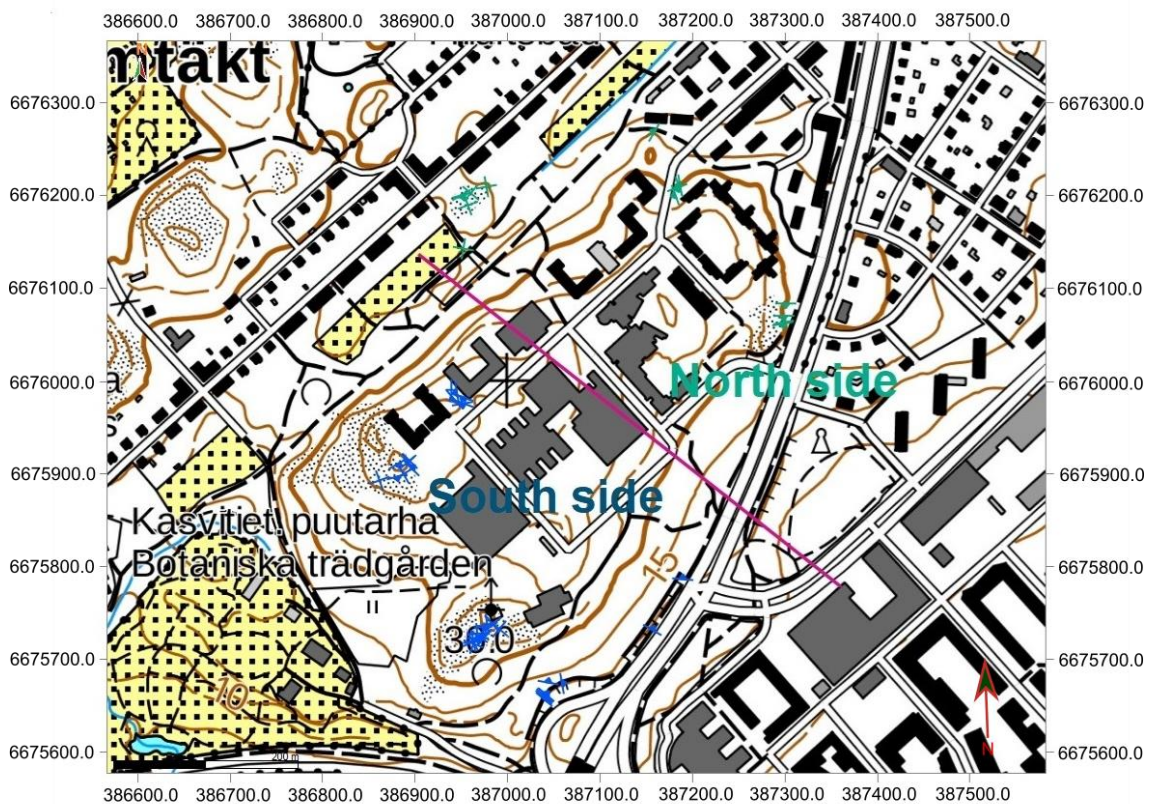
Figure 21. The 2D-map from the Kumpula area divided to the northern and southern sides.
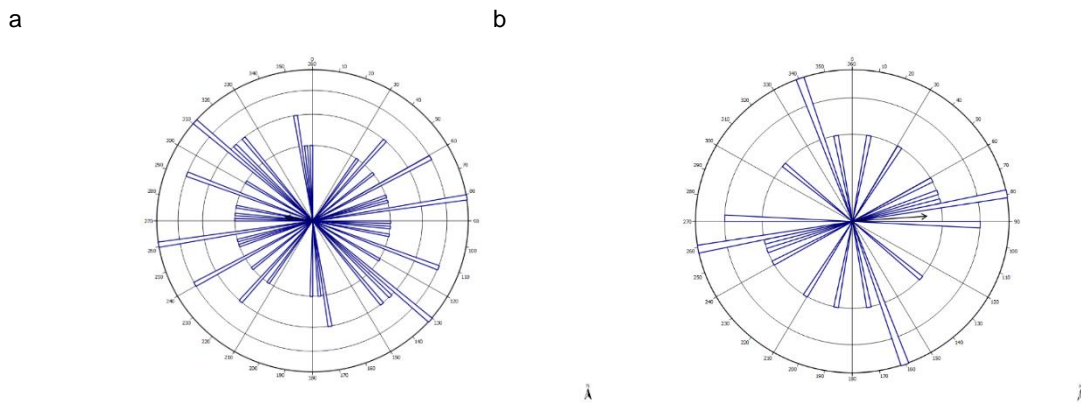
Figure 22. a. Strike directions from the south side of the hill and b. Strike directions from the north side of the hill.

6. DISCUSSION

6.1. Error sources

Major error sources can be found for example in calculating and defining the orientation of the drillhole and outcrop fractures. There were many phases, as the drill hole data was handled (logging, Wellcad prosessing phase, calculating corrections to the orientation data and classification fractures), and in every phase there is the possibility of making errors when calculating and defining fractures. There were fewer processing phases with outcrop data and the detection of important fractures but was more difficult in the field.

The strike, dip and dip direction of the drill hole fractures were defined mainly based on acoustic and optical images of the drill hole. The drill hole image was oriented the way that 0 degrees was the high side of the hole (Tiensuu and Kivinen 2016). Fractures orientations were found out with the interactive tool of the Wellcad software. These were plotted to the structural log to imitate the trace of the fracture on the optical image and acoustical image. The fracture was seen on the acoustic image and optical image as a sinusoidal wave and most of the fractures were easy to draw this way. A problem was caused by fractures whose shape did not imitate the curve of the sinusoidal waves and consequently the sinusoidal wave of the log was adjusted as close as possible to the real situation. This fracture dip and dip direction data might not be fully correct.

The drilling direction of the drill hole was 45 degrees from north and drilling dip was 70 degrees, but Wellcad gives values to the fractures so that the drill hole would be

perpendicular to the ground. The correction to the Wellcad values were made based on the equations (in p. 38–39), which considered the drilling direction at each depth (for the dip direction) and the real dip direction of the fractures and drilling dip of the drill hole at each depth (for the dip). Correction to the dip and dip direction of the fractures were calculated for each fracture. The dip and dip direction of the drill hole were measured every five meters during drilling. The dip and dip direction corrections of the fractures were made based on five meter stations so, when the fracture is just in between two stations the correction possibly did not apply.

The places of the fractures on the outcrops were measured with a GPS-device, but it was discovered that some of the fractures were not in the correct place when they were input to the 3D-model. The places were then corrected based on the map on top of the elevation model and pictures of the outcrops.

The most difficult thing was the outcrops themselves. They were covered with lichen, scour marks and other vegetation and therefore many of the fracture features were almost impossible to measure with certainty. For example, some the fracture surfaces were weathered and lichened so much that the real dip and dip direction could be some degrees bigger or smaller and even small differences could affect the fracture classification. Some marks, which were thought to be weathering or scour marks filled with lichen, turned out to be fractures. This type of marks was very common on the outcrop 4.

The total number of fractures was calculated to be over 800 in the logging phase. There were individual parts in the drill hole images, where only one or two fractures were detected but there were also longer parts, where no more than 2 fractures were detected. The combining of the logging data to image data in the drill hole was made mostly based on the acoustic image and if the acoustic image was unclear possible fractures could not be detected (Figure 23). There were some fractures for which the acoustic image was unclear, even though there should have been fracture(s) according to the logging data. Also, there is a shadow zone in the same direction as the drill core has been drilled according to Terzaghi (1965), which means that fracture quantity in that direction could be bigger.
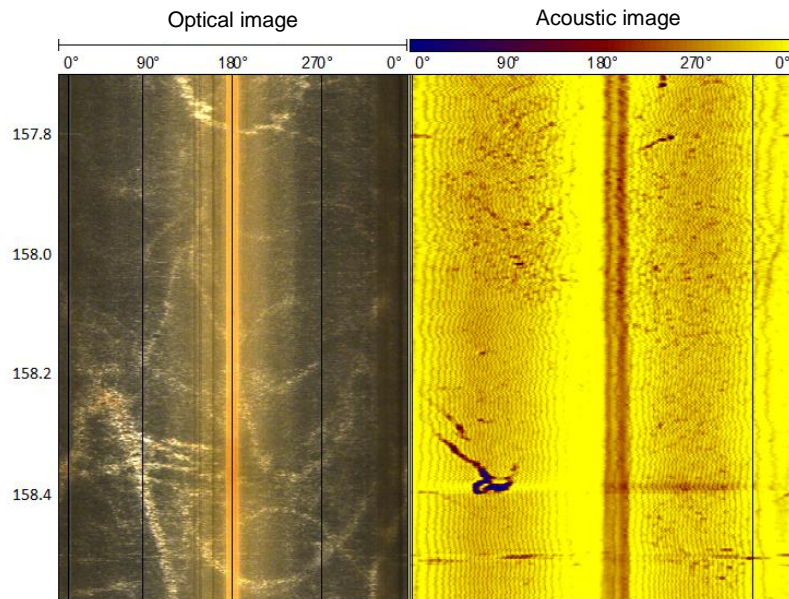
Figure 23. An example unclear acoustic image and dark, fine grained rock type, where it is impossible to detect fractures, which were logged from the drill core. Some marks are seen on the acoustic image, but not enough to be able to draw a curve. According to logging data there should be one slickenside at this depth.

Tight fractures were a fracture group, which was added to the inspection in the Wellcad phase. They include fractures, which are difficult to detect in the drill core, but are seen clearly in the acoustic and sometimes even optical images (Figure 24). Tight fractures all have the sinusoidal curve on the acoustic image, which means that they are probably natural fractures instead of drilling induced fractures (Tingay et all. 2008). Category could include fractures, which are slickensides, filled or unfilled fractures, but based only on the image it is difficult to accurately classify them. They were added to the inspection because they could affect the weakness of the rock when building on it.
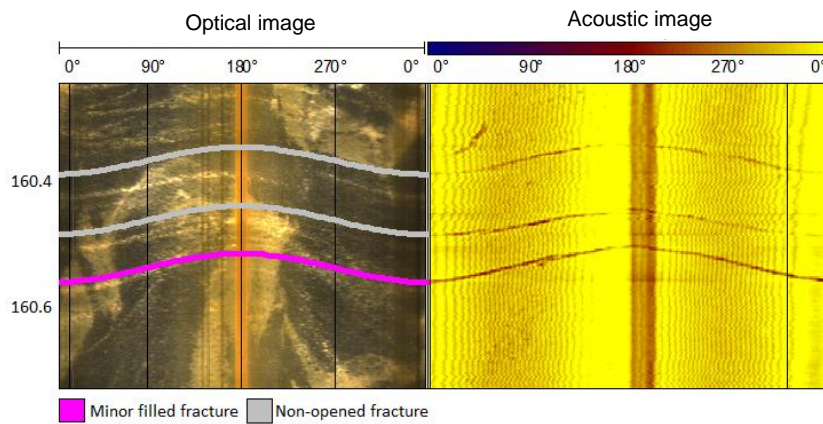
Figure 24. Wellcad-image from the drillhole (depth on the left). Fractures are marked top of the optical image, where the pink colour means a minor filled fracture and grey colour non-opened fracture. On the acoustic image can be seen similar marks.

6.2. Rock Quality

The amount of fractures, from which the dip and dip directions could be determined, narrowed to approximately 700 including two crushed zones. Based on RQD values, the rock is relatively unbroken (RQD 94 %), but those fractures, which are detected in the logging, but not from the acoustic image of the drill hole could diminish the RQD value a little, if they are natural fractures.

Instead of calculating the actual Q'-value, it was decided that it was more reasonable to calculate only the Jn value, estimate the Jr value and evaluate fracture fillings of the drill core with descriptive method. The whole Q-value has been calculated also for drill holes for example in Olkiluoto linked with nuclear waste disposal studies (including Aalto et al. 2011), but in the Q-method handbook of Norwegian Geotechnical Institute (2013) it has been pointed out that for drill holes the value Ja could be sometimes difficult to estimate because water during drilling, which can wash out clay minerals. The Jn value was calculated to the whole drill hole whereas the Jr value was made only for the parts, where acoustic images were available (approximately from 31 to 370 meters).

The Jr value was calculated to estimate friction in the fracture (Norwegian geotechnical institute 2013). It is difficult to measure safely the Jr value from the drill holes, because the fracture contact with surrounding rock is evaluated in decimetre to meter scale and in the drill hole there were seen to be under 10 cm of that contact (Norwegian geotechnical

institute 2013). The trace of the fracture on the acoustic image with logging data were used to evaluate the Jr-value of the fracture in this study. The acoustic image was used for this purpose, because the acoustic image has a clear mark from the fracture. This mark is also used widely in the literature to recognize fractures (for example Williams and Johnson 2004). Most of the fracture surfaces in the acoustic images were planar and only a handful were graded. There was only little variation between depth intervals of the drill core. The average value was 1.65 so that the value varied between 2.58 to 1 except in the crushed zones. This means that overall the fractures are mostly planar, little bit undulating with some rough fractures. If planar fractures have clay fillings, the friction between fracture walls is very low and this could diminish the Q'-value even though the RQD, Jn and Jr values are very good (NGI 2013).

The Jn value varied between depth intervals. There are under three joint sets for over 50 % percent of depth intervals, in meters that is 193.4. However, there are still 14 depth intervals, where there are four or more joint sets, which mean that the rock is heavily fractured. This is 120.05 meters from the approximately 370 meters long drill hole. Even though the Jn value is high, the RQD is close to 100 percent or even 100 in these depth intervals. If the depth interval is long (for example over 6 meters) and there is for example only four fractures, which were far away from each other and degree of their strike differ just a little over 30 degrees, they are calculated to the different fracture sets. The RQD value could be under 70 percent even though there are only two joint sets in the drill hole. This means that those fractures are very close to each other (the space between two fractures is under 10 cm) and these kinds of zones could be important to recognize, when building. This is an example for the limitations of especially the RQD parameter and why it is necessary to the evaluate rock quality with different parameters (Barton et al. 1974, Azimian 2014). One parameter to evaluate possible shearing is the relationship between Jn and Jr. If this Jn/Jr value is over 6 the possible collapse is likely for example during tunnel blasting (Barton and Grimstad 2014).

Rock quality of the outcrops was harder to evaluate, but the planarity of the fractures and number of fracture sets and fracture density was calculated in most outcrops. Things that make calculating the Q'-value difficult especially in northern countries is that surface outcrops could be more jointed than rock under that surface. Also, the most competent outcrops are revealed when the most fragmented parts could be covered with soil or the

surface of the outcrop is scoured by ice (NGI 2008). On the other hand, Kumpula hill is also an established urban area and some of the outcrops are buried under buildings and some conclusion of the rock quality of the hill could be made based on that large buildings are situated there already.

Overall based on the outcrops that were available for mapping on the Kumpula hill, the rock quality values in the drill hole are consistent with outcrop fractures. There is relatively low amount of fractures even in the road cuttings. The road cutting wall is almost continuous along Kustaa Vaasa road except one part, which is under soil, where there are walking paths to the top of the hill. This part of the rock quality of the hill could be worse than other parts, where there are coherent outcrops available. As mentioned in NGI (2008) the quality of the rock is hard to evaluate based on the outcrops, because outcrops that are available for mapping are the ones, which are the most coherent ones and the more worse quality parts are under soil. In the 3D-modelling phase those crushed zones discovered from the drill hole were examined, and it was noticed that if they are continued along the same dip and dip direction as they were in the drill hole, they collided into each other under that part of the Kumpula hill.

Most of the fractures are planar or just undulating in the meter scale (Jr value of 0.5 to 2), but without knowledge of the fracture filling, the friction was impossible to evaluate (NGI 2008). The characteristic feature on the outcrop 2 is that the fractures are long, and they curved in the meter scale, but on the other outcrops, fractures are short and planar (under five meters). The fracture fillings were not able to be detected from most of the fractures, so there is no information if this affects the Ja value. The filling was smeary in fractures, where the fracture fillings were found, but there was only under a 1 mm layer of it.

Usually two main fracture sets were found on the outcrops and a differing number of individual fractures. This means an average Jn value of 6. One fracture set was found on the road cuttings as well as horizontal fractures, and this means a Jn value 2-4. Depth intervals in the drill hole, which have Jn value 6 or under amounted to 61 %. The rest of the drill hole was more fragmented. A very fragmented part in the outcrops are only in the last road cutting place (outcrop 10), where the fracture density was over 1 fracture in one meter. The really crushed zone, which are noticed in the drill hole, were not noticed from outcrops.

6.3. Fracture classification in drill hole

Brittle structures in drill hole were classified according to drill core observations and further observations were made based on the images of the drill hole. There are multiple ways to classify fracture data in drill holes (Aalto et al. 2011, AREVA Resources Canada Inc. 2010, Gillespie et al. 2011). In this project, the classification was done in four steps 1) natural vs. unnatural fractures 2) filling or no filling 3) slickenside feature 4) other features. Between those classes some variation in strike and dip direction was found. The minor and filled fractures are roughly oriented the same way, whereas the slickenside fractures differ from other fracture group based on orientation and filling. This classification is only a starting point for closer looking. One further examination point would be lineation investigation from every slickenside possible to get information of the moving directions. Also, this would relate to filling examination to examine different fillings and make possible some timing. The filled fractures could be also classified further based on different fracture fillings.

6.4 Orientation between drill hole and outcrop: strike, dip, and dip direction

The drill hole was drilled in Kumpula hill to the NE-direction. Kumpula hill is situated so that it is approximately 670 meters long in NE-SW direction and 350 meters wide in the SE-NW direction. The drill hole is in the southern part of the hill in the outcrop 2.

The main strike of the drill hole fractures is on the NW-SE axis so that the mean strike is 347.35 degrees. The dip direction of fractures were mainly around 40 degrees. Another main dip direction is to the south. The second main direction is the same as the drill hole on the outcrop fractures. Striking direction approximately to the east is emphasized on the outcrops. The strike direction to NW-SE is emphasized especially on the southern side of the hill, where the drill hole is also situated. The strike directions of fractures on the northern side differ slightly from the southern side. The E-strike is seen on both, but on the northern side of the hill the other main strike is to the NWN (approximately 340 degrees from north). Consequently, it would be interesting to compare drill hole data from the northern side of the Kumpula as well to see would those strike observations on the northern side continued in deeper as well.

The dip directions of the outcrop were divided on two directions: NE and SES. The dip direction NE is seen in the drill hole fractures as well, but the SES is not the main or the second main dip direction of the drill hole fractures. Dip direction approximately to the south were seen on both sides of the hill and different types of outcrops, whereas the fractures with dip direction to the E are more common on the road cuttings and one slickenside on the outcrop 1.

The drilling dip of the drill hole was approximately 70 degrees. This means that fractures, whose dip was the same could be unrepresented in the drillhole, whereas this was a common dip on the outcrop fractures. The drillhole sample fractures, whose dip is between 40-50 degrees, whereas these fractures are rarer on the outcrop. This way the dip comparison is difficult.

There are some investigations about the fracture orientation and relationship to the tectonic features and history of the Helsinki area. In the paper of Wennerström et al. (2008) the research area was Helsinki, Vantaa and Espoo area and they investigated fracture properties from ice-polished outcrops, road cuttings and quarries. Considering 2211 joint sets, they discover six-major fracture strikes, which were E, NE, NNE, N, NW, and WNW. The main strike of the Kumpula Campus drill hole fracture was NW-SE and the main strike direction for Kumpula hill outcrop fractures was E-W, so these observations are consistent with the studies of Wennerström et al. (2008). They also divide their research area into smaller parts and investigate characteristic parts of fracturing in different areas. In the Kumpula area, the jointing is parallel with main foliation, which is heading towards NE. The foliation direction of the area is same as the most common dip direction of the drill hole fractures and it is found from the outcrop fractures (see Figures 13 and 17). The N trending fractures are steep, and fractures are usually short, but fractures in E and NW could be long (Wennerström et al. 2008). Long fractures to the E or NW were not detected from the research area. Instead the longest fractures on the research area were to the N-S direction.

In the project of Pajunen et al. (2001) the research area was Helsinki, Espoo, and Vantaa area. In this area they found five main dip directions of the fractures: 40– 70, 90–110, 130–160, 220–250, and 310–340 degrees. Overall, from the drill hole the fracture dip directions of 40–70, 130–160 and 220–250 were among the main directions, and 40–70

and 130–160 from the outcrops. Based on research of Pajunen et al. (2001) they discover that the Kumpula area fracture density is around >0.5 to 1, which is consistent with results of this research (Figure 25). The most brittle zones near the Kumpula was on the eastern side and southern side of the hill (Figure 25), so that the direction of the southern structure is approximately on the WNW-ESE axis and the eastern structure is on the N-S axis (Figure 25). The NW-SE direction is the main direction in drill hole fractures and it also appears on the outcrops as well, but there are only few fractures in N-S axis in the drill hole and in the ourcrops. Still, together with the discovery that shallower crushed zone has approximately the same direction as the Vallila valley, this is an interesting finding.
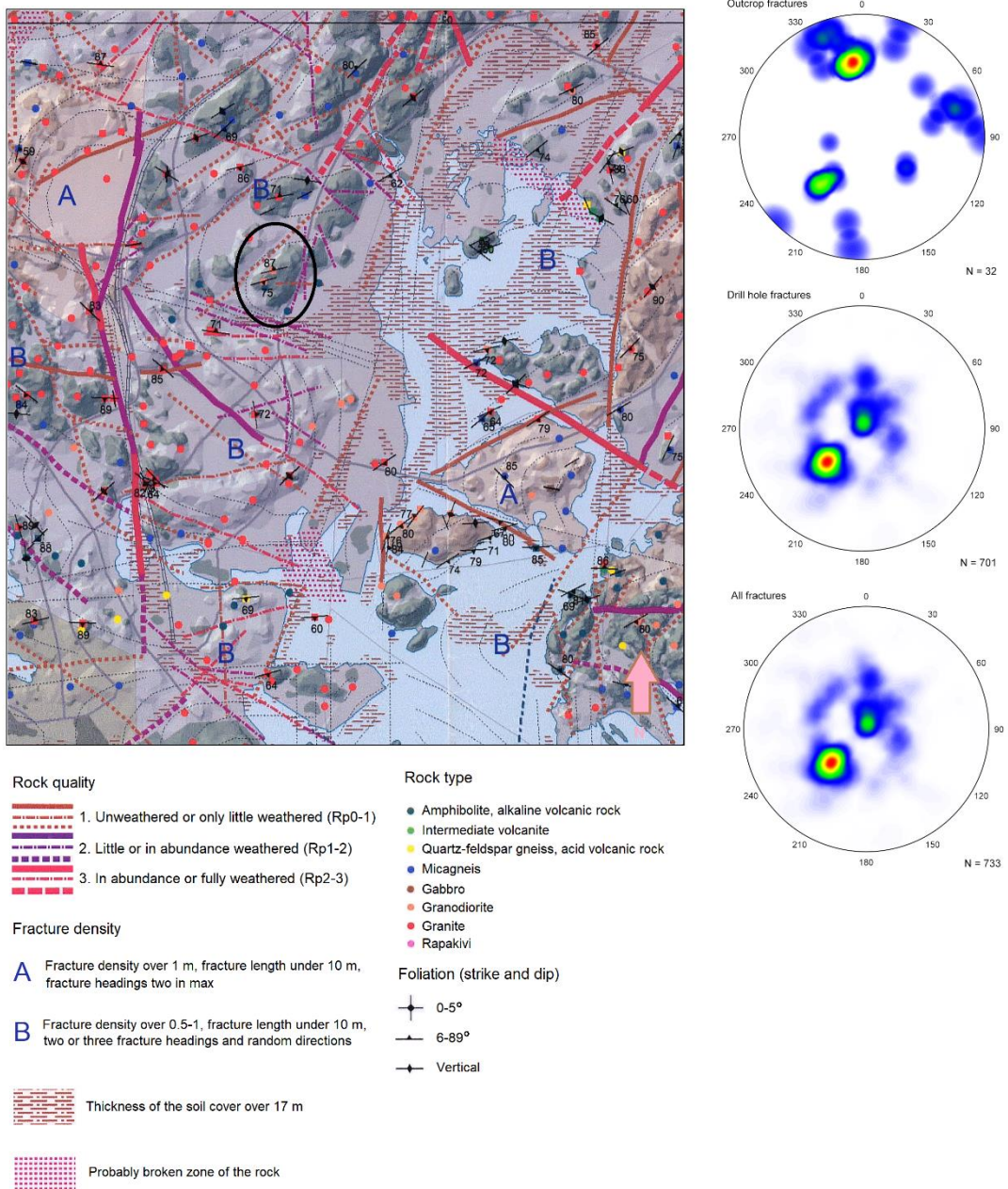
Figure 25. Modified 1:50 000 constructability map of Kumpula area after Pajunen et al. 2002. The Kumpula hill is marked on black circle to the map. The original legends of the map are in finnish, so beneath the map the main points have been translated in shorter versions. The map represented the most brittle zones of the bedrock around the Kumpula area. On the left are represented the equal angle lower hemisphere stereographic projection of poles of the dip directions from outcrops (N=32) (on top), drill hole (N=701) (in the middle) and from all fractures (N=733) at the bottom.

Fractures in the NW-SE axis and E-W axis have been connected to the tectonic phases of the crust evolution by Wennerström et al. (2008). They found out that, for example, NW-striking fractures were connected to the regional pattern of the strain more than the local. NW and WNW striking fractures had the same direction as the diabase dykes originating in the Mid-Proterozoic Rapakivi granite phase. The NE striking fractures are parallel with

the main foliation, but those fractures are not the main fracture groups in the Kumpula drill hole or even on the outcrops. In fact, there are only 76 fractures in the drill hole there, whose strike is to the NE (around 45 degrees), which is also the same as the drilling direction of the drill hole.

The main strike and dip direction changes between fracture groups of the drill hole. The filled, and unfilled fractures are the most abundant fracture classes (74 percent in drill hole fractures). Their main strike and dip direction are the same as previous studies of Pajunen et al. (2001), Wennerström et al. (2008). The slickensides differ from filled and unfilled fractures so that the other main dip direction is towards the SES and strike is towards E, but they follow the directions discovered by Pajunen et. al (2001) and Wennerström et al. (2008).

The dip direction to the south in the drill hole is the main direction at depth of 250–300 m and it is the dip direction of the second crushed zone in the depth of approximately 295 meters. The big fault zones situated to the NW and SE directions from Kumpula hill are related to the faults, which relate to Vuosaari-Korso shear fault zone. The main strike direction of the drill hole fractures is at right angle from the major fault zones and the main strike direction of outcrop fractures is a 45 degrees angle from major faults. There are also known crushed zones in Helsinki, which mainly define the shape of the cape of Helsinki (Vänskä and Raudasmaa 2005). There are three main directions of crushed zone in the Helsinki cape, which are NW-SE, E-W and NE-SW and these headings follow the main directions of the movements during geological history and are related to the major fault zones of the Helsinki (Vänskä and Raudasmaa 2005). The strike of the crushed zones of the drill hole are consistent with those headings: one crushed zone is to the NW-SE direction and the another is to the E-W direction. Also, if crushed zones are continued to the surface at the same dip direction and dip angle as they are in the drill hole, the shallower crushed zone appear to continue with the exact same angle as the valley of Vallila while the rest seems to have the exact the same angle as the fractures at the outcrop 8. Also, as mentioned above, if crushed zones are continued in the same dip direction and dip both 400 metres at every direction from the drill hole they collide underground at the exact location where there is no rock wall along the Kustaa Vaasa road.

6.5. Depth versus strike, dip direction and dip

The fractures strike, dip direction and dip were also compared in depth to see if there is some variation. This is done in different geological environments for example by Nie et al. (2013) to recognize fractures and faults related to the earthquakes and correlate fracture from different depths to changing stress state of the area. Also, Seeburger and Zoback (1982) have studied how the fractures correlate with depth and is there variation in orientation between depth intervals.

The drill hole was divided to 50 metre long parts and these parts were compared to each other. The main strike is the same in every depth interval except in the depth interval with the second crushed zone and here the strike differs from the common strike. In the bottom part the strike is the same than at the shallower depth intervals, but the dip direction changes 180 degrees to the SW. It is unsure if this change only local, or have deeper fractures different dip direction, or is this change related the fracture location in the northern part of the hill.

Steep fractures were located mostly in the bottom, whereas horizontal fractures were most common in the depth interval of 150–200 metres. There was variation whether there was only one clear strike direction or whether the strike direction cannot be distinguished clearly in different depth intervals. This varied between depth intervals, but overall the fracture dip versus depth intervals do not have much variation.

6.6. Fracture fillings

Fracture fillings were investigated with the XRD-method from the drill core. It was possible to recognize six to eight different fracture fillings in the drill core, and five of them were selected to the analysis. They were selected from different depths, fracture types and the colour of the filling.

Based on the XRD-analysis, the fillings differ between each other. They all contain clay minerals, while filling in the slickenside fracture contained only them. Near Kumpula the expansive fault gauge material has caused collapses in the water tunnels (Wegelius and Holopainen 1997). One collapse has been the result of penetration of major crushed zone. The fracturing was very dense in the crushed zones and fracture filling layer of clay

minerals was at maximum 1 cm (Wegelius and Holopainen 1997). The clay minerals included expansive clay minerals. The other collapse happened also due to a smectite clay mineral and lamprophyre vein (Wegelius and Holopainen 1997). Based on the lithological map of the area and location of that lamprophyre vein those collapses have happened near the Kumpula Campus drillhole. The thickness of the fracture filling was small in the drill hole (1 mm at maximum).

The fracture filling was investigated in this research only to some degree and now it is known that there are at least five different filling materials. The next step would be to study in detail how often each fracture filling appears in the drill hole and how are they related to the crushed zones and is there some filling, which could cause collapses. Most of the fractures in the drill core contain fillings so there could be more than five fracture fillings. Some of the fracture filling were on top of each other and this could give some hints of the time relationship of the fractures. One of the five fillings were from the slickenside fracture, but it would be interesting to study how the fracture filling material between slickenside fractures differ. Also, it would be interesting to investigate more the fracture filling relationship to the direction of the fracture (strike, dip and dip direction).

It is also possible that those five fracture filling materials are not interpreted correctly, because it is done just based on the X-ray powder diffraction method and the full understanding of fracture filling demands more measuring methods to determine accurately the composition of the fillings. These are ideas that could be handled in a future thesis related to the Kumpula Campus drill hole.

7. CONCLUSIONS

The thesis present studies brittle structures in the Kumpula Campus drill hole. The drill hole data was compared with outcrop data gathered from the Kumpula hill area. The drill hole data was excellent: a complete drill core and together with video and acoustic image logs from the drill hole. Only downsize was that drill core was not oriented. The quality of the data from the nearby outcrops was variable. Data was processed with several methods and the results were presented in a 3D-model of the area. There were four major research tasks, namely, classification of fractures of the drill hole, rock quality,

orientation of fractures and fracture fillings. These results from the drill hole were compared with the surrounding area and previous studies.

There were about 700 discontinuous structures in the drill core and the classification of these fractures based on drill core was first step of the study and give base to the whole research. The fractures were classified in four classes and the most fragmented parts of the core in the one class. The classification happened based on filling and tectonic features.

The drill core fracture data was investigated based on different fracture classes, depth, strike, dip and dip direction. There was seen clearly that slickenside fractures differ from other fractures based on filling and orientation and this study could be further extended by measuring lineation from the surfaces and taking more samples from the fillings. It would also be interesting to classify the filled fracture group as further by orientation, fillings and foliation.

Based on RQD the rock quality was excellent (94%) in the drill core. Jn and Jr value differ little bit between depth intervals. Due to lacking Ja value, the Q'-value could not be calculated, and this is something that could be done in future. Biggest problems were two crushed zones at the depths of approximately 110 meters and 295 meters, and some other minor dens fractured zones without core loss. This follows the overall impression about nearby outcrops, which have quite few fractures and no major faults. Even though the Ja value was not calculated, the fracture fillings were investigated on XRD-method. Fracture fillings was investigated only by XRD from five different spots. According to XRD-analysis they are all different fillings, but more closer investigations from the fracture fillings from themselves would be an interesting research topic.

Orientation (strike, dip and dip direction) was compared between fracture classes, depth intervals, and dip for the drill hole fractures. The main dip direction heading was approximately to the NE, so that mean dip direction was very close to the main heading 77.4 degrees. This main dip direction also emerged in the fractures of outcrops, but in the outcrops, there were also other main dip direction, which were not so common in the drill hole. The mean strike was 347.5 degrees from north, which is approximately the same direction as the brittle zone of the Vallila valley. In addition, it was found out that the

strike of the fractures wandered northward to the depth of the drill hole. In the outcrops, was noted that the strike of the fractures differs from the south and north side of the hill, and it could be interesting to study more, for example, will this be seen deeper. Overall these main dip direction findings are consistent with previous results made from the whole Helsinki area and this mean that they are not only the result of local tension but are part of larger stress field. Altogether this study gives a starting point for future projects both as a structural geology or engineering geological or geochemical point of view.

8. ACKNOWLEDGEMENTS

9. REFERENCES

Aalto, P. et al. 2011. Drilling and Associated Drillhole Measurements of the Pilot Hole ONK-PH14, Eurajoki: Posiva Oy. 3–178.

AREVA Resources Canada Inc. 2010. Geotechnical Core Logging Manual. AREVA Resources Canada Inc. 3–65.

Azmian, A., 2015. A New Method for Improving the RQD Determination of Rock Core in Borehole. Springer, Wien, 1–8.

Barton, N., Lien, R. and Lunde, J., 1974. Engineering Classification of Rock Masses for the Design of Tunnel Support. Journal of the International Society for Rock Mechanics, Vol 6, 189-236.

Barton, N. and Grimstad, E., 2014. Tunnel and cavern support selection in Norway, based on rock mass classification with the Q-system. Visited at the page 16.5.2018. https://www.researchgate.net/publication/321874893_Tunnel_and_cavern_support_selection_in_Norway_based_on_rock_mass_classification_with_the_Q-system

Davy, P., Darcel, C., Bour, O., Munier, R., and de Dreuzy, J.R. 2006. A note on angular correction applied to fracture intensity profiles along drill core, Journal of Geophysical Research, Vol 111, 1–7.

Deere, D. U. and Deere D. W. 1988. The Rock Quality Designation (RQD) Index in Practice. In: L. Kirkaldie, Rock Classification Systems for Engineering Purposes. American Society for Testing and Materials, Philadelphia, 91–101.

Dershowitz, W. S. and Einstein, H. H. 1988. Characterizing Rock Joint Geometry with Joint System Models, Vol 21, 21–51.

Elminen, T., Airo, M.-L., Niemelä, R., Pajunen, M., Vaarma, M., Wasenius, P., and Wennerström, M. 2008. Fault Structures in the Helsinki area, Southern Finland. In: Pajunen, M., Tectonic Evolution of the Svecofennian crust in Southern Finland - a basis for chracterizing bedrock technical properties. Geological Survey of Finland, 185–213.

Fossen, H. 2010. Fracture and Brittle Deformation. In: Fossen, H., Structural Geology. Cambridge University Press, New York, 120–149.

Fossen, H., Schultz, R. A., Shipton, Z. K. and Mair, K. 2007. Deformation bands in sandstone: a review. Journal of the Geological Society, Vol 164, 755–769.

Fox, A., Forchhammer, K., Pettersson, A., La Pointe, P., Lim, D.-H. 2012. Geological Discrete Fracture Network Model for Olkiluoto Site, Eurajoki, Finland, Version 2.0., Posiva Oy, 5–346.

Gillespie, M. R., Barnes, R. P. and Milodowski, A. E., 2011. British Geological Survey scheme for classifying discontinuities and fillings. British Geological Survey, Keyworth, Nottingham, 1–56.

Grimstad, E. and Barton, N., 1993. Updating of the Q-system for NMT. Norwegian Geotechnical Institute, Norway, 1–21.

Higgins, M. W., 1971. Cataclastic Rocks. United States Goverment Printing Office, Washington, 1–97.

Huotari, T. and Wennerström, M., 2017. Integroitujen geofysikaalisten ja kallioperägeologisten tutkimusmenetelmien kehittäminen yhdyskuntarakentamisen tarpeisiin, Geologian tutkimuskeskus, 7–147.

Korhonen, K.-H., Gardemaister, R., Jääskeläinen, H., Niini, H., and Vähäsarja, P. 1974 Rakennusalan kallioluokitus, VTT, Geotekniikan laboratorio, tiedonanto 12, 78 p.

Kukkonen, I.T., Koivisto, E. and Whipp, D. 2016. Helsinki University Kumpula campus drillhole project. In: Kukkonen et al. (Eds.), Lithosphere 2016 – Ninth Symposium on the Structure, Composition and Evolution of the Lithosphere in Finland. Programme and Extended Abstracts, Espoo, Finland, November 9–11, 2016. Institute of Seismology, University of Helsinki, Report S-65, 166 p.

Laitala, M., 1991. Helsingin kartta-alueen kalliopera, Espoo: Geological Survey of Finland, 7–47.

Marjoribanks, R., 2002. Structural Logging of Drill Core. The Australian Institute of Geoscientists, 1–75.

Mertanen, S., Airo, M.-L., Elminen, T., Niemelä, R., Pajunen M., Wasenius, P., and Wennerström, M. 2008. Paleomagnetic Evidence for Mesoproterozoic-Paleozoic Reactivation of the Paleoproterozoic Crust in Southern Finland. In: M. Pajunen, Tectonic Evolution of the Svecofennian crust in southern Finland - a basis for characterizing bedrock technical properties. Geological Survey of Finland, Special Paper 47, 215–252.

Mount Sopris Instruments/ ALT Advenced Logic Technology a. User Guide QL40 – Acoustic Borehole Imager. 1–45.

Mount Sopris Instruments/ ALT Advenced Logic Technology b. User Guide QL40 OBI and OBI40 Optical Borehole Imager, 1–36.

National Land Survey of Finland. 2016. Elevation model 10 m.

National Land Survey of Finland. 2016. General map of Finland, 1: 1 000 000.

National Land Survey of Finland.2018. General map raster 1:100 000.

NGI. 2013. Using the Q-system - Rock Mass Classification and Support Design.: Norwegian Geotechnical Institute, Oslo, 6–56.

Nie, X., Zou, C., Pan, L., Huang, Z., and Liu D. 2013. Fracture analysis and determination of in-situ stress direction from resistivity and acoustic image logs and core data in the Wenchuan Earthquake Fault Scientific Drilling Borehole-2 (50–1370 m). Tectonophysics, Vol 593, pp. 161-171.

Niini, H. and Ärmänen, E., 2000. Kalliorakennusgeologia. Otamedia Oy, Espoo, 3–149.

Niinimäki, R., 2004. Core Drilling of Pilot Hole OL-PH1 at Olkiluoto in Eurajoki 2003-2004, Posiva Oy, 1–95.

Pajunen, M., Airo, M.-L., Elminen, T., Mänttäri, I., Niemelä, R., Vaarma, M., Wasenius, P., and Wennerström, M. 2008. Tectonic evolution of Svecofennian crust in Southern Finland. In: Pajunen, M., Tectonic Evolution of the Svecofennian crust in Southern Finland - a basis for characterizing bedrock technical properties. Geological Survey of Finland, Special paper 47, 15–160.

Pajunen, M., Airo, M.-L., Elminen, T. and Wennerström, M., 2001. Kallioperän rakennettavuusmalli taajamiin - parametrisointi ja mallinnus, Geologian tutkimuskeskus, 3–60.

Pajunen, M., Airo, M-L., Elminen, T., Niemelä, R., Salmelainen, J., Vaarma, M., Wasenius, P., Wennerström, M. 2002a. Kallioperänrakennettavuusmalli taajamiin. Menetelmäkehitys ja ohjeistus. Raportti I. 95 s. Geologian tutkimuskeskus, arkistoraportti, K 21.42/2002/5.

Pajuenen, M., Airo, M-L., Elminen, T., Niemelä, R., Salmelainen, J., Vaarma, M., Wasenius, P., Wennerström, M. 2002b. Kallioperän rakennettavuuskartta 1:50 000 – Espoo, Helsinki, Vantaa.

Pajunen, M., Wennerström, M., Ikävalko, O., Elminen, T., Arkimaa, H., Wasenius, P., and Ajlani, M. 2007. Länsimetron kallioperän rikkonaisuusarviointi Matinkylän ja Ruoholahden välillä OSA I: Kallioperän geologinen kehitys sekä kallioperän hierto- ja siirrosvyöhykkeiden kuvaus ja luokittelu, Espoo: Geologian tutkimuskeskus, 1–46.

Palmström, A., 1995. Chapter 3: Collection of Geo-Data – Limitations and Uncertainties.. In: Palmström, A., RMi – a rock mass characterization system for rock engineering purposes. PhD. Thesis, Oslo University, 1–15.

Räisänen, M., 2018. Geochemical Study of The Kumpula Campus Drill Core and Outcrops: Applying a Portable XRF device for Whole Rock Analysis. University of Helsinki, 3–76.

Seeburger, D. A. and Zoback, M. D., 1982. The Distribution of Natural Fractures and Joints at Depth in Crystalline Rock. Journal Of Geophysical Research, Vol 87, 5517–5534.

Singhal, B. and Gupta, R., 1999. Fractures and Discontinuities. In: Applied Hydrogeology of Fractured Rocks. Springer, Dordrecht, 13–35.

Terzaghi, R., 1965. Sources Of Error In Joint Surveys. Geotechnique,15, 287–304.

Tingay, M., Reinecker, J. and Müller, B., 2008. Borehole breakout and drilling-induced fracture analysis from image logs, World Stress Map Project, 1–8.

Twiss, R. J. and Moores, E. M., 2001. Fractures and Joints. In: Twiss, R.J. and Moores, E.M., Structural Geology. W.H. Freeman and Company, New York, 37–50.

Wallin, B. and Peterman, Z., 1999. Calcite fracture fillings as indicators of paleohydrology at Laxemar at the Äspö Hard Rock Laboratory, southern Sweden. Applied Geochemistry, Vol 14, 953–962.

Wegelius, A. and Holopainen, P., 1997. Paisuvat kalliosavet, Helsinki: Helsingin Kaupunki - Kiinteistövirasto - Geotekninen Osasto, Tiedote 75, 1–102.

Wennerström, M. Airo, M.-L., Elminen T., Grönholm, S., Pajunen, M., Vaarma, M. and Wasenius, P. 2006. Helsingin seudun taajamakartoitus. Geologian tutkimuskeskus Espoo 1–90.

Wennerström, M., Airo, M.-L., Elminen, T., Niemelä, R., Pajunen, M., Vaarma, M. and Wasenius, P. 2008. Orientation and Properties of Jointing in Helsinki area, Southern Finland. In: Pajunen, M., Tectonic evolution of the Svecofennian crust in southern Finland – a basis for characterizing bedrock technical properties.: Geological Survey of Finland, Espoo, 253–282.

Williams, J. H. and Johnson, C. D., 2004. Acoustic and optical borehole-wall imaging for fractured-rock aquifer studies. Journal of Applied Geophysics, Vol 55, 151– 159.

Vänskä, P. and Raudasmaa, P., 2005. Helsingin keskustan kallioruhjeet. Helsingin kaupinki, Kiinteistövirasto, Helsinki, 5–54.

APPENDIX I: The depth stations of the drill hole.

Drilling depth	Dip	Azimuth	Coordinates (ETRS-TM35-FIN)		
m	deg	deg	X	Y	Z[1
0	-70.0088	45	386985.0	6675734	26.000
5	-69.9935	44.7449	386986.2	6675735	21.302
10	-69.8741	45.03364	386987.4	6675736	16.605
15	-69.7932	45.23645	386988.6	6675738	11.912
20	-69.7615	45.60771	386989.9	6675739	7.220
25	-69.7653	45.94855	386991.1	6675740	2.528
30	-69.7275	46.10258	386992.4	6675741	-2.163
35	-69.7591	46.70218	386993.6	6675742	-6.853
40	-69.8057	47.44234	386994.9	6675744	-11.545
45	-69.8171	47.67209	386996.1	6675745	-16.238
50	-69.8346	47.95072	386997.4	6675746	-20.931
55	-69.905	48.23097	386998.7	6675747	-25.626
60	-69.9108	48.32256	387000.0	6675748	-30.322
65	-69.932	48.39669	387001.3	6675749	-35.018
70	-69.946	48.35442	387002.6	6675751	-39.714
75	-69.9739	48.46042	387003.8	6675752	-44.412
80	-70.0055	48.63343	387005.1	6675753	-49.110
85	-70.0068	48.72125	387006.4	6675754	-53.808
90	-70.0189	48.87244	387007.7	6675755	-58.507
95	-70.046	49.1439	387009.0	6675756	-63.207
100	-70.1038	49.15378	387010.3	6675757	-67.907
105	-70.1351	49.22545	387011.6	6675758	-72.609
110	-70.1649	49.62499	387012.8	6675760	-77.312
115	-70.2013	49.69772	387014.1	6675761	-82.016
120	-70.1649	49.50002	387015.4	6675762	-86.720
125	-70.0773	49.50672	387016.7	6675763	-91.422
130	-69.9177	49.00208	387018	6675764	-96.121
135	-69.9195	49.35565	387019.3	6675765	-100.816
140	-69.9035	49.59124	387020.6	6675766	-105.512
145	-69.8863	49.7591	387021.9	6675767	-110.208
150	-69.8424	49.96338	387023.2	6675768	-114.902
155	-69.8425	50.18367	387024.6	6675769	-119.596
160	-69.8813	50.32386	387025.9	6675771	-124.290
165	-69.8631	50.38422	387027.2	6675772	-128.985
170	-69.8707	50.38165	387028.5	6675773	-133.679
175	-69.8853	50.55299	387029.9	6675774	-138.374
180	-69.8885	50.66134	387031.2	6675775	-143.069
185	-69.9017	50.72615	387032.5	6675776	-147.764
190	-69.8847	50.8174	387033.9	6675777	-152.460
195	-69.881	50.91095	387035.2	6675778	-157.155
200	-69.9106	50.92885	387036.5	6675779	-161.850
205	-69.8995	50.94331	387037.9	6675780	-166.546

210	-69.9245	51.00717	387039.2	6675781	-171.241
215	-69.9336	51.15803	387040.5	6675783	-175.938
220	-69.9229	51.2993	387041.9	6675784	-180.634
225	-69.9472	51.4072	387043.2	6675785	-185.331
230	-69.9175	51.76101	387044.5	6675786	-190.027
235	-69.8506	52.02504	387045.9	6675787	-194.722
240	-69.8051	52.18759	387047.3	6675788	-199.415
245	-69.6969	52.7335	387048.6	6675789	-204.106
250	-69.7026	53.07642	387050	6675790	-208.796
255	-69.7177	53.47019	387051.4	6675791	-213.486
260	-69.6479	53.63903	387052.8	6675792	-218.174
265	-69.5987	53.922	387054.2	6675793	-222.862
270	-69.5284	53.96319	387055.6	6675794	-227.547
275	-69.5185	54.17954	387057	6675795	-232.231
280	-69.4961	54.27443	387058.5	6675796	-236.915
285	-69.4234	54.28597	387059.9	6675797	-241.597
290	-69.4226	54.44191	387061.3	6675798	-246.278
295	-69.3617	54.5489	387062.7	6675799	-250.958
300	-69.4135	54.52606	387064.2	6675800	-255.638
305	-69.3662	54.75062	387065.6	6675801	-260.318
310	-69.3291	54.67565	387067	6675802	-264.996
315	-69.3293	54.79621	387068.5	6675803	-269.674
320	-69.3058	54.85187	387069.9	6675804	-274.352
325	-69.3064	54.93372	387071.4	6675805	-279.030
330	-69.3409	55.05318	387072.8	6675806	-283.708
335	-69.3201	55.32263	387074.3	6675807	-288.386
340	-69.2992	55.46954	387075.7	6675808	-293.063
345	-69.3198	55.6811	387077.2	6675809	-297.741
350	-69.3263	55.84445	387078.6	6675810	-302.419
355	-69.3006	55.9423	387080.1	6675811	-307.096
360	-69.3049	56.08678	387081.6	6675812	-311.774
365	-69.2873	56.13245	387083	6675813	-316.451

(1 Total vertical depth

APPENDIX II. The complete drill hole fracture data

Depth	X	Y	Azimuth	Dip	Main types	Filling	Roughness
2.48	386985.598	6675734.601	252.76	49.259	Unfilled fractures		1
2.77	386985.671	6675734.673	353.625	50.967	Unfilled fractures		3
4.58	386986.109	6675735.113	19.675	66.677	Tight fractures		
4.65	386986.126	6675735.13	22.055	60.037	Tight fractures		
4.73	386986.145	6675735.15	28.025	50.117	Filled fractures	1	2
4.86	386986.177	6675735.181	238.175	20.023	Unfilled fractures		1
5.88	386986.424	6675735.429	26.835	40.817	Filled fractures	1	1
7.27	386986.760	6675735.767	43.555	47.477	Filled fractures	1	1
7.67	386986.874	6675735.865	33.694	37.866	Tight fractures		
7.73	386986.889	6675735.88	188.314	37.864	slickenside	3	1
7.85	386986.918	6675735.909	182.944	35.824	slickenside	3	1
7.97	386986.947	6675735.938	193.694	21.224	Tight fractures		
8.06	386986.969	6675735.96	203.844	34.724	slickenside	2	1
8.16	386986.994	6675735.984	45.034	40.936	Unfilled fractures		1
8.20	386987.004	6675735.994	45.034	41.926	Unfilled fractures		1
8.26	386987.018	6675736.009	200.254	24.294	slickenside	2	1
8.81	386987.153	6675736.143	43.844	37.866	Filled fractures	1	2
9.57	386987.338	6675736.327	345.334	35.766	Filled fractures	2	2
9.79	386987.392	6675736.381	14.584	42.906	Filled fractures	2	2
10.48	386987.561	6675736.549	35.484	30.326	Unfilled fractures		1
11.25	386987.749	6675736.736	9.814	41.926	Unfilled fractures		1
11.42	386987.790	6675736.777	39.664	47.596	Unfilled fractures		2
11.64	386987.844	6675736.831	18.764	44.826	Unfilled fractures		1
11.91	386987.910	6675736.896	348.914	84.446	Filled fractures	2	1
12.96	386988.191	6675737.144	47.026	50.317	Filled fractures	1	2
13.23	386988.257	6675737.21	44.636	48.577	Unfilled fractures		1
13.41	386988.302	6675737.253	209.416	24.793	Tight fractures		
13.58	386988.344	6675737.295	203.446	14.783	Unfilled fractures		1
13.77	386988.390	6675737.341	140.756	4.493	Tight fractures		
13.84	386988.408	6675737.358	182.546	16.293	Unfilled fractures		2
14.05	386988.459	6675737.409	187.326	28.033	Tight fractures		
14.25	386988.509	6675737.457	44.936	2.467	slickenside	3	1
14.34	386988.531	6675737.479	19.566	48.577	Unfilled fractures		2
14.37	386988.538	6675737.486	5.236	59.557	Unfilled fractures		2
14.88	386988.664	6675737.61	180.756	8.163	Tight fractures		
15.16	386988.733	6675737.678	180.756	28.033	Unfilled fractures		2
15.28	386988.762	6675737.707	41.656	35.847	Unfilled fractures		3
15.59	386988.839	6675737.782	38.076	30.407	Unfilled fractures		1
16.39	386989.036	6675737.976	135.386	0.603	Unfilled fractures		3
16.44	386989.048	6675737.989	126.426	60.237	Tight fractures		
16.71	386989.114	6675738.054	46.136	6.707	Unfilled fractures		2
16.86	386989.151	6675738.091	9.716	0.407	slickenside	3	1
16.93	386989.168	6675738.108	47.026	41.017	Filled fractures	1	1

16.95	386989.173	6675738.112	42.246	44.907	Tight fractures		
17.11	386989.213	6675738.151	130.016	61.557	slickenside	3	1
17.32	386989.264	6675738.202	183.746	11.593	Unfilled fractures		2
17.49	386989.306	6675738.243	42.246	42.987	Filled fractures	7	1
17.54	386989.348	6675738.231	290.978	11.562	Tight fractures		
18.28	386989.531	6675738.41	323.218	48.608	Crushed zones	18.28	3
18.44	386989.571	6675738.448	45.608	60.268	Unfilled fractures		1
18.61	386989.613	6675738.489	22.918	80.348	Tight fractures		
18.93	386989.692	6675738.567	76.058	41.048	Unfilled fractures		2
19.03	386989.717	6675738.591	82.618	72.238	Tight fractures		
19.39	386989.806	6675738.678	345.908	47.708	Unfilled fractures		1
20.06	386989.973	6675738.839	145.308	31.322	Tight fractures		
20.22	386990.012	6675738.878	33.668	60.268	Unfilled fractures		3
20.52	386990.087	6675738.95	88.598	74.698	slickenside	3	1
21.33	386990.287	6675739.146	168.598	52.802	Tight fractures		
21.68	386990.374	6675739.23	73.068	44.938	Unfilled fractures		2
21.77	386990.396	6675739.252	114.858	64.068	Tight fractures		
21.85	386990.416	6675739.271	100.538	73.908	Tight fractures		
22.42	386990.558	6675739.409	56.948	43.018	Filled fractures	7	1
22.73	386990.663	6675739.463	108.039	46.805	Filled fractures	7	3
22.76	386990.670	6675739.471	58.489	46.805	Filled fractures	7	3
23.02	386990.735	6675739.533	343.859	55.985	slickenside	3	1
23.38	386990.825	6675739.62	105.649	71.795	Unfilled fractures		1
23.50	386990.854	6675739.649	289.229	85.455	Unfilled fractures		2
23.59	386990.877	6675739.67	26.849	69.475	Unfilled fractures		2
24.19	386991.026	6675739.814	83.559	62.225	Unfilled fractures		1
24.58	386991.123	6675739.908	48.939	51.195	Unfilled fractures		3
24.74	386991.163	6675739.947	93.709	67.435	Crushed zones		3
24.75	386991.166	6675739.949	173.409	82.025	Crushed zones		3
25.31	386991.305	6675740.084	186.249	18.425	slickenside	3	1
25.43	386991.335	6675740.112	66.849	49.485	Unfilled fractures		2
25.78	386991.422	6675740.197	139.079	45.895	Filled fractures	7	1
25.84	386991.437	6675740.211	36.399	52.035	Filled fractures	7	1
25.87	386991.445	6675740.218	40.579	53.655	Unfilled fractures		3
26.32	386991.557	6675740.326	43.559	32.645	slickenside	3	1
26.35	386991.564	6675740.334	43.559	47.705	Unfilled fractures		3
26.44	386991.587	6675740.355	168.939	12.385	slickenside	3	1
26.92	386991.706	6675740.471	69.829	64.655	Filled fractures	7	1
27.56	386991.910	6675740.58	133.263	64.102	slickenside	3	1
27.88	386991.990	6675740.656	76.553	56.772	Filled fractures	7	1
28.13	386992.053	6675740.716	129.093	43.052	Filled fractures	7	1
28.50	386992.146	6675740.804	126.103	45.912	Filled fractures	7	1
28.60	386992.171	6675740.828	147.003	44.888	slickenside	3	1
28.84	386992.231	6675740.886	112.973	52.892	Filled fractures	1	1
29.05	386992.284	6675740.936	49.093	51.232	Unfilled fractures		2
29.62	386992.427	6675741.072	66.403	39.052	Unfilled fractures		3

29.85	386992.484	6675741.127	154.763	24.728	Filled fractures	1	1
30.24	386992.582	6675741.22	146.403	26.398	slickenside	3	1
30.31	386992.600	6675741.237	167.893	24.148	slickenside	3	1
30.41	386992.625	6675741.26	104.613	51.232	Unfilled fractures		1
30.75	386992.710	6675741.342	46.703	31.582	Unfilled fractures		1
31.21	386992.825	6675741.451	77.743	40.072	Unfilled fractures		1
32.91	386993.327	6675741.746	175.062	20.459	Unfilled fractures		1
33.18	386993.396	6675741.809	61.632	54.461	Unfilled fractures		2
33.22	386993.406	6675741.819	117.742	57.471	Tight fractures		
33.34	386993.436	6675741.847	46.702	52.861	slickenside	3	1
33.41	386993.454	6675741.864	64.612	54.461	Filled fractures	1	3
33.78	386993.548	6675741.951	132.072	45.881	Filled fractures	1	2
33.83	386993.560	6675741.962	152.972	7.23	Unfilled fractures		
33.88	386993.573	6675741.974	197.152	10.72	Filled fractures	1	3
33.93	386993.586	6675741.986	170.282	38.689	Unfilled fractures		3
33.95	386993.591	6675741.991	309.692	75.789	Tight fractures		
34.21	386993.656	6675742.052	47.892	47.711	Unfilled fractures		1
34.26	386993.669	6675742.064	342.822	42.041	Crushed zones		3
34.64	386993.765	6675742.153	272.972	13.179	slickenside	3	1
34.71	386993.783	6675742.17	280.132	5.4	Filled fractures	1	3
34.84	386993.816	6675742.2	185.212	19.789	Filled fractures	1	3
34.94	386993.841	6675742.224	221.632	37.429	Filled fractures	1	3
35.36	386993.947	6675742.323	185.802	46.439	Crushed zones		3
35.63	386994.016	6675742.386	178.642	46.079	Crushed zones		3
36.28	386994.180	6675742.539	140.432	13.179	Filled fractures	1	2
36.47	386994.228	6675742.584	311.182	1.56	Unfilled fractures		1
37.77	386994.619	6675742.797	14.012	37.934	Unfilled fractures		1
38.77	386994.874	6675743.029	330.432	48.564	Unfilled fractures		1
38.95	386994.920	6675743.071	286.842	35.756	Tight fractures		
39.19	386994.981	6675743.127	132.812	65.764	Filled fractures	1	2
39.32	386995.014	6675743.158	138.782	39.336	Filled fractures	1	3
39.50	386995.060	6675743.199	43.862	37.934	Filled fractures	1	1
40.89	386995.414	6675743.523	154.902	21.156	Filled fractures	1	1
42.15	386995.735	6675743.817	49.832	41.994	Filled fractures	1	1
42.30	386995.773	6675743.852	55.202	39.994	Filled fractures	1	2
42.52	386995.865	6675743.848	46.482	38.963	Filled fractures	1	1
42.83	386995.944	6675743.92	45.882	45.823	Unfilled fractures		2
43.18	386996.034	6675744.001	47.672	27.023	Unfilled fractures		2
43.64	386996.151	6675744.107	191.552	43.017	slickenside	3	1
44.08	386996.264	6675744.209	155.132	17.047	Filled fractures	1	1
46.12	386996.785	6675744.682	186.182	39.347	Tight fractures		
46.53	386996.890	6675744.777	176.032	13.237	Unfilled fractures		2
46.81	386996.961	6675744.842	149.162	19.847	Tight fractures		
47.68	386997.212	6675744.961	187.051	48.345	slickenside	2	1
48.18	386997.340	6675745.076	253.921	40.505	Filled fractures	2	1
48.86	386997.514	6675745.232	172.131	18.495	Filled fractures	2	3

49.14	386997.586	6675745.296	30.641	28.135	Unfilled fractures		2
49.16	386997.591	6675745.301	38.701	7.755	Unfilled fractures		2
49.30	386997.627	6675745.333	27.651	47.635	Unfilled fractures		3
49.40	386997.652	6675745.356	24.671	38.945	Unfilled fractures		2
50.13	386997.839	6675745.524	338.101	42.945	Unfilled fractures		3
50.51	386997.937	6675745.611	191.831	49.515	Tight fractures		
50.77	386998.003	6675745.671	307.051	19.865	Unfilled fractures		3
50.92	386998.042	6675745.705	216.911	14.055	Unfilled fractures		1
51.47	386998.182	6675745.832	24.071	51.125	Filled fractures	2	2
52.05	386998.331	6675745.965	117.801	39.965	Filled fractures	2	1
52.70	386998.512	6675746.049	101.361	47.565	Filled fractures	1	1
52.99	386998.587	6675746.115	101.361	52.715	Filled fractures	2	1
53.94	386998.830	6675746.332	200.471	50.125	Filled fractures	2	2
55.53	386999.238	6675746.696	36.291	42.875	Unfilled fractures		3
56.07	386999.376	6675746.819	345.541	45.735	Unfilled fractures		3
56.29	386999.433	6675746.87	161.661	45.065	Filled fractures	2	3
56.39	386999.458	6675746.892	297.781	44.015	Unfilled fractures		2
56.59	386999.510	6675746.938	41.661	39.895	Filled fractures	2	2
56.64	386999.522	6675746.95	59.571	43.845	Filled fractures	2	2
56.82	386999.569	6675746.991	276.891	33.975	Filled fractures	2	3
57.04	386999.625	6675747.041	257.781	20.605	Unfilled fractures		2
57.54	386999.763	6675747.126	70.413	80.199	Unfilled fractures		2
57.79	386999.827	6675747.183	308.023	27.641	slickenside	2	1
59.39	387000.237	6675747.548	116.983	40.899	slickenside	2	1
61.03	387000.658	6675747.922	1.753	50.199	Unfilled fractures		1
61.32	387000.733	6675747.988	343.253	52.709	Unfilled fractures		2
62.22	387000.963	6675748.193	36.983	47.559	Filled fractures	3	1
63.94	387001.395	6675748.569	19.737	50.178	Filled fractures	3	1
64.26	387001.477	6675748.642	179.737	46.612	Tight fractures		
64.55	387001.552	6675748.708	186.907	43.592	Tight fractures		
64.83	387001.623	6675748.771	40.637	39.868	Unfilled fractures		1
66.01	387001.926	6675749.04	110.487	42.848	Unfilled fractures		1
66.53	387002.059	6675749.159	67.497	41.868	Filled fractures	4	3
66.54	387002.062	6675749.161	56.757	41.868	Filled fractures	4	3
66.99	387002.177	6675749.264	28.097	36.768	Filled fractures	4	1
67.37	387002.275	6675749.35	29.887	35.708	Filled fractures	4	2
67.41	387002.285	6675749.359	43.617	35.708	Unfilled fractures		3
67.56	387002.314	6675749.368	20.294	38.834	Filled fractures	4	1
67.94	387002.412	6675749.455	175.514	49.056	Filled fractures	4	1
68.07	387002.445	6675749.484	92.534	49.304	Filled fractures	6	1
68.15	387002.466	6675749.503	115.814	51.854	Filled fractures	6	1
68.22	387002.484	6675749.519	152.234	30.136	Filled fractures	6	1
68.47	387002.548	6675749.575	185.664	55.636	Tight fractures		
68.58	387002.576	6675749.6	48.354	42.834	slickenside	1	1
68.79	387002.630	6675749.648	287.164	44.486	Filled fractures	1	2
69.10	387002.709	6675749.719	69.254	43.804	Filled fractures	1	1

69.27	387002.753	6675749.757	44.774	51.014	Filled fractures	6	1
69.54	387002.822	6675749.819	49.544	31.364	Filled fractures	6	1
70.16	387002.981	6675749.96	47.164	41.854	Filled fractures	6	1
70.28	387003.012	6675749.987	75.224	37.794	Unfilled fractures		2
70.68	387003.114	6675750.078	154.624	49.626	Tight fractures		
71.64	387003.360	6675750.296	23.874	35.694	Filled fractures	1	2
71.91	387003.429	6675750.358	17.904	39.854	Filled fractures	1	3
72.41	387003.557	6675750.472	237.014	34.406	Tight fractures		
72.86	387003.686	6675750.505	15.03	38.806	Filled fractures	1	1
73.28	387003.794	6675750.6	317.71	50.986	Unfilled fractures		2
73.86	387003.943	6675750.732	106.37	42.806	Filled fractures	1	2
74.11	387004.007	6675750.788	358.91	43.776	Unfilled fractures		2
74.80	387004.184	6675750.945	5.47	30.226	Filled fractures	4	2
74.97	387004.227	6675750.983	195.92	29.694	Unfilled fractures		1
75.45	387004.351	6675751.092	42.49	33.526	Filled fractures	1	1
75.72	387004.420	6675751.153	46.07	47.496	Filled fractures	4	1
76.63	387004.653	6675751.359	148.16	62.384	Filled fractures	1	3
76.95	387004.735	6675751.432	359.5	49.276	Unfilled fractures		1
77.50	387004.901	6675751.497	95.203	50.105	Filled fractures	1	1
77.54	387004.911	6675751.506	309.533	19.356	Filled fractures	1	1
77.92	387005.008	6675751.592	185.353	32.436	Filled fractures	1	1
78.06	387005.044	6675751.623	157.883	24.426	slickenside	1	1
78.43	387005.139	6675751.707	137.593	2.79	Filled fractures	1	1
78.71	387005.211	6675751.77	121.763	12.025	Unfilled fractures		1
78.84	387005.245	6675751.8	328.033	37.735	Tight fractures		
79.13	387005.319	6675751.865	115.503	79.825	Filled fractures	4	1
79.63	387005.448	6675751.978	149.823	85.696	Unfilled fractures		3
80.46	387005.661	6675752.165	42.663	32.405	Unfilled fractures		3
80.68	387005.717	6675752.215	51.023	40.805	Unfilled fractures		2
80.72	387005.727	6675752.224	52.213	38.775	Unfilled fractures		2
81.42	387005.907	6675752.382	15.793	32.405	Unfilled fractures		3
83.34	387006.433	6675752.765	212.301	30.197	Tight fractures		
83.80	387006.551	6675752.869	29.621	47.463	Unfilled fractures		3
84.74	387006.793	6675753.08	326.931	58.653	Unfilled fractures		3
84.95	387006.847	6675753.127	55.881	59.343	Unfilled fractures		3
84.99	387006.857	6675753.136	54.091	46.563	Unfilled fractures		2
85.78	387007.060	6675753.314	305.441	21.997	Filled fractures	1	1
86.19	387007.166	6675753.407	45.731	53.413	Filled fractures	1	2
86.99	387007.371	6675753.587	49.911	46.563	Filled fractures	1	3
87.05	387007.387	6675753.6	129.911	46.563	Unfilled fractures		3
88.85	387007.902	6675753.902	127.682	47.451	Filled fractures	1	1
89.25	387008.005	6675753.992	20.212	45.621	Filled fractures	1	2
89.56	387008.085	6675754.061	35.742	45.621	Filled fractures	6	2
89.74	387008.131	6675754.102	20.812	54.201	Filled fractures	6	2
89.99	387008.195	6675754.158	325.882	57.931	Unfilled fractures		1
90.04	387008.208	6675754.169	320.512	54.971	Filled fractures	4	2

90.45	387008.314	6675754.261	38.122	50.941	Filled fractures	1	1
90.68	387008.373	6675754.312	202.902	32.869	Filled fractures	1	1
91.45	387008.572	6675754.485	48.872	27.951	Filled fractures	1	2
91.57	387008.603	6675754.512	39.322	48.351	Filled fractures	6	1
92.10	387008.739	6675754.63	52.452	38.761	Filled fractures	7	2
92.12	387008.744	6675754.635	67.382	34.551	Filled fractures	7	2
92.13	387008.747	6675754.637	38.122	38.761	Filled fractures	7	1
92.17	387008.757	6675754.646	51.262	39.781	slickenside	3	1
92.55	387008.857	6675754.63	77.804	46.524	Filled fractures	7	1
94.36	387009.324	6675755.034	219.294	17.276	Tight fractures		
94.46	387009.350	6675755.056	97.504	37.694	Filled fractures	1	1
94.52	387009.365	6675755.07	104.664	41.754	Filled fractures	1	1
95.14	387009.525	6675755.208	293.924	45.406	Filled fractures	1	3
95.17	387009.533	6675755.214	286.154	34.896	Tight fractures		
95.39	387009.589	6675755.263	60.484	44.654	Filled fractures	1	1
96.58	387009.896	6675755.529	261.084	28.286	Unfilled fractures		2
97.64	387010.131	6675755.7	47.964	50.006	Unfilled fractures		1
98.70	387010.404	6675755.936	154.224	26.774	slickenside	3	1
99.09	387010.504	6675756.023	234.824	29.344	Filled fractures	1	1
99.49	387010.607	6675756.112	359.604	51.696	Filled fractures	1	2
99.61	387010.638	6675756.138	30.644	57.126	Filled fractures	1	3
99.70	387010.661	6675756.158	47.964	62.506	Filled fractures	1	2
99.74	387010.671	6675756.167	48.554	57.846	Filled fractures	1	1
100.32	387010.821	6675756.296	179.904	30.764	Crushed zones		3
100.54	387010.877	6675756.345	49.754	44.596	Filled fractures	1	2
100.74	387010.929	6675756.389	110.344	2.156	Filled fractures	1	1
100.83	387010.952	6675756.409	323.184	52.516	Filled fractures	1	2
100.91	387010.973	6675756.427	356.024	43.646	slickenside	3	1
101.32	387011.078	6675756.518	334.224	0.096	Unfilled fractures		1
101.60	387011.150	6675756.581	142.584	84.484	Filled fractures	1	3
102.25	387011.318	6675756.725	87.964	54.116	Filled fractures	1	1
102.73	387011.495	6675756.689	356.095	63.695	Filled fractures	1	3
103.00	387011.565	6675756.749	31.315	70.525	slickenside	3	1
103.13	387011.599	6675756.777	145.345	11.095	Filled fractures	1	2
103.48	387011.689	6675756.855	348.925	55.615	slickenside	3	1
104.07	387011.841	6675756.985	332.215	39.665	Filled fractures	1	1
104.25	387011.887	6675757.025	17.885	6.365	slickenside	3	1
104.72	387012.009	6675757.129	118.185	16.435	Unfilled fractures		1
104.77	387012.022	6675757.14	297.585	51.345	Filled fractures	1	3
104.88	387012.050	6675757.164	60.565	30.065	Unfilled fractures		1
105.24	387012.143	6675757.243	299.975	40.245	Filled fractures	1	3
105.92	387012.318	6675757.394	125.045	47.335	Filled fractures	1	1
106.46	387012.457	6675757.513	34.295	64.285	Tight fractures		
106.70	387012.519	6675757.566	46.835	42.645	Crushed zones		3
106.75	387012.532	6675757.577	46.835	44.565	Crushed zones		3
106.91	387012.573	6675757.612	23.555	64.865	Crushed zones		3

107.13	387012.63	6675757.661	11.015	37.605	Filled fractures	1	1
108.19	387012.957	6675757.742	38.285	47.305	Filled fractures	1	3
108.26	387012.975	6675757.757	37.685	52.455	Filled fractures	6	3
108.40	387013.011	6675757.788	34.105	73.505	Filled fractures	6	3
108.41	387013.014	6675757.79	32.315	73.905	Filled fractures	6	3
108.46	387013.027	6675757.801	28.725	67.565	Filled fractures	6	3
108.52	387013.042	6675757.814	32.905	70.955	Unfilled fractures		3
108.78	387013.11	6675757.871	50.815	22.125	Crushed zones		
109.21	387013.221	6675757.966	234.695	2.945	Crushed zones		
109.37	387013.262	6675758.001	43.655	52.455	Filled fractures	6	1
109.55	387013.309	6675758.04	44.845	51.635	Filled fractures	6	1
110.03	387013.433	6675758.146	26.935	52.455	Crushed zones		3
110.03	387013.433	6675758.146	22.165	54.055	Crushed zones		3
110.11	387013.453	6675758.163	36.495	52.455	Crushed zones		3
110.14	387013.461	6675758.17	49.625	53.255	Crushed zones		3
110.23	387013.484	6675758.19	26.935	49.085	Crushed zones		3
110.26	387013.492	6675758.196	19.775	45.475	Filled fractures	6	2
110.28	387013.497	6675758.201	16.785	44.535	Filled fractures	6	2
110.34	387013.513	6675758.214	57.985	49.085	Filled fractures	6	2
110.38	387013.523	6675758.222	32.315	45.475	Filled fractures	6	3
110.46	387013.544	6675758.24	45.445	44.535	Filled fractures	6	3
110.48	387013.549	6675758.244	19.175	44.535	Filled fractures	6	3
110.81	387013.634	6675758.317	36.495	41.635	Filled fractures	6	3
111.39	387013.784	6675758.444	35.895	47.305	Unfilled fractures		2
112.01	387013.944	6675758.58	36.495	45.475	Unfilled fractures		1
112.38	387014.04	6675758.661	38.875	43.585	Filled fractures	6	1
112.44	387014.055	6675758.675	34.695	43.585	Filled fractures	6	1
112.60	387014.07	6675758.741	38.948	53.219	Filled fractures	6	3
112.61	387014.072	6675758.744	36.568	55.549	slickenside	3	1
112.71	387014.098	6675758.766	28.208	51.599	Crushed zones		3
112.93	387014.155	6675758.814	37.758	48.169	Filled fractures	6	2
112.94	387014.158	6675758.816	46.708	50.759	Filled fractures	6	2
113.52	387014.307	6675758.943	145.218	38.511	Tight fractures		1
113.78	387014.374	6675759.001	47.908	35.439	slickenside	3	1
114.06	387014.447	6675759.062	38.948	41.599	Filled fractures	6	2
114.34	387014.519	6675759.124	37.158	41.599	Filled fractures	6	1
114.39	387014.532	6675759.135	45.518	49.049	Filled fractures	6	1
114.51	387014.563	6675759.161	43.728	43.549	Filled fractures	6	2
114.57	387014.578	6675759.174	49.698	44.499	Filled fractures	4	1
114.68	387014.607	6675759.198	38.948	41.599	Filled fractures	6	1
115.00	387014.689	6675759.269	35.368	43.549	Unfilled fractures		1
115.23	387014.749	6675759.319	47.308	37.539	Filled fractures	1	1
115.54	387014.829	6675759.387	40.148	33.299	Filled fractures	1	3
115.58	387014.839	6675759.396	48.508	35.439	Filled fractures	1	2
115.90	387014.922	6675759.466	44.918	43.549	Tight fractures		
116.00	387014.948	6675759.488	38.948	44.499	slickenside	3	1

116.12	387014.979	6675759.515	28.208	45.439	Filled fractures	6	1
116.25	387015.012	6675759.543	46.118	47.269	Filled fractures	6	1
116.81	387015.157	6675759.666	39.548	42.579	Filled fractures	6	1
117.83	387015.468	6675760.019	49.5	37.575	Filled fractures	6	1
117.88	387015.481	6675760.03	10.99	4.2	Filled fractures	6	2
117.88	387015.481	6675760.03	228.31	89.945	Tight fractures		
118.54	387015.651	6675760.176	26.22	37.575	Filled fractures	6	1
119.49	387015.897	6675760.386	240.54	42.405	Tight fractures		
120.03	387016.037	6675760.505	46.51	37.575	Unfilled fractures		1
120.62	387016.189	6675760.635	266.22	26.835	Tight fractures		
120.74	387016.22	6675760.662	125.32	45.475	Filled fractures	6	2
121.50	387016.417	6675760.829	38.16	45.475	Unfilled fractures		2
121.64	387016.453	6675760.86	49.5	41.635	Tight fractures		
121.70	387016.469	6675760.874	208.31	5.8	Unfilled fractures		3
121.77	387016.487	6675760.889	46.51	54.055	slickenside	3	1
121.86	387016.51	6675760.909	50.69	41.635	Tight fractures		
121.93	387016.528	6675760.924	39.95	45.475	Filled fractures	1	1
122.08	387016.567	6675760.957	49.5	38.615	Tight fractures		
122.16	387016.587	6675760.975	46.51	39.635	Unfilled fractures		
122.19	387016.595	6675760.982	49.5	39.635	Unfilled fractures		1
122.32	387016.629	6675761.01	212.49	25.735	Unfilled fractures		1
122.44	387016.66	6675761.037	47.11	45.475	Filled fractures	1	2
122.46	387016.665	6675761.041	48.31	46.405	Unfilled fractures		3
122.54	387016.756	6675761.359	59.657	44.623	Unfilled fractures		3
122.57	387016.763	6675761.366	52.497	42.703	Unfilled fractures		3
122.58	387016.766	6675761.368	54.287	42.703	Tight fractures		
122.61	387016.774	6675761.375	47.717	66.593	Filled fractures	1	3
122.61	387016.774	6675761.375	240.547	6.647	Filled fractures	1	3
122.73	387016.805	6675761.401	49.507	36.623	Filled fractures	1	3
122.88	387016.844	6675761.435	50.107	33.423	Filled fractures	1	2
123.50	387017.004	6675761.573	57.567	8.613	Filled fractures	1	1
123.63	387017.038	6675761.602	218.467	11.037	Unfilled fractures		1
124.69	387017.313	6675761.839	303.837	51.977	Tight fractures		
124.77	387017.333	6675761.857	47.717	42.703	Filled fractures	1	1
124.99	387017.391	6675761.906	96.667	35.563	Filled fractures	1	1
125.22	387017.45	6675761.957	327.117	86.783	Tight fractures		
125.23	387017.453	6675761.96	49.507	37.663	Filled fractures	1	1
125.32	387017.476	6675761.98	178.467	2.857	Filled fractures	1	2
125.65	387017.562	6675762.053	14.877	25.633	Filled fractures	1	1
125.95	387017.639	6675762.12	16.667	29.013	Filled fractures	1	1
125.96	387017.642	6675762.123	196.077	77.627	slickenside	3	1
127.35	387018.002	6675762.433	32.787	40.733	Unfilled fractures		1
127.46	387018.031	6675762.458	135.477	1.877	Filled fractures	1	1
128.34	387018.347	6675762.806	44.222	42.862	Unfilled fractures		2
128.91	387018.495	6675762.934	137.362	19.268	Unfilled fractures		1
129.85	387018.74	6675763.145	179.752	40.318	Unfilled fractures		2

130.05	387018.792	6675763.19	183.332	36.918	Unfilled fractures		2
130.15	387018.818	6675763.212	53.782	31.392	Unfilled fractures		2
130.40	387018.882	6675763.268	41.842	48.452	Unfilled fractures		2
130.53	387018.916	6675763.298	44.822	58.742	Unfilled fractures		2
130.68	387018.955	6675763.331	154.672	46.778	slickenside	3	1
130.76	387018.976	6675763.349	149.302	47.128	slickenside	3	1
130.94	387019.023	6675763.39	146.912	43.808	slickenside	3	1
131.23	387019.098	6675763.455	177.362	30.578	slickenside	3	1
132.10	387019.324	6675763.65	54.972	46.652	Unfilled fractures		1
133.03	387019.731	6675763.691	193.236	26.59	Unfilled fractures		
134.34	387020.073	6675763.983	346.076	78.71	Unfilled fractures		3
134.75	387020.18	6675764.074	72.046	46.65	Unfilled fractures		1
134.91	387020.221	6675764.11	104.286	51.04	Filled fractures	1	3
135.31	387020.326	6675764.199	55.326	41.88	Tight fractures		
135.67	387020.42	6675764.28	118.606	41.88	Unfilled fractures		1
135.97	387020.498	6675764.347	359.806	89.19	Filled fractures	1	3
136.98	387020.762	6675764.572	231.146	74.21	Filled fractures	1	3
137.98	387021.16	6675764.693	50.781	37.837	Filled fractures	1	1
138.92	387021.406	6675764.902	227.501	66.133	Filled fractures	1	3
139.95	387021.676	6675765.131	51.381	59.447	Filled fractures	1	1
140.75	387021.886	6675765.309	45.411	54.317	Crushed zones		3
141.37	387022.048	6675765.447	93.771	51.057	Filled fractures	1	1
141.98	387022.208	6675765.582	84.221	45.737	Filled fractures	1	1
142.21	387022.268	6675765.634	81.231	39.897	Unfilled fractures		1
142.55	387022.515	6675765.634	345.879	85.864	Crushed zones		3
142.99	387022.63	6675765.731	101.099	51.074	Filled fractures	1	1
143.58	387022.786	6675765.862	193.039	0.696	Tight fractures		
145.01	387023.162	6675766.18	204.979	15.636	Tight fractures		
146.65	387023.594	6675766.544	49.759	31.424	Unfilled fractures		2
146.79	387023.63	6675766.575	236.029	8.256	Tight fractures		
147.47	387023.809	6675766.725	45.579	34.684	Unfilled fractures		1
147.55	387023.992	6675766.633	193.843	47.222	Tight fractures		
147.62	387024.011	6675766.649	55.333	31.468	Filled fractures	1	1
149.06	387024.391	6675766.967	309.963	87.612	Filled fractures	4	1
149.29	387024.452	6675767.018	186.683	9.952	Filled fractures	4	2
149.35	387024.468	6675767.031	44.593	28.128	Filled fractures	4	1
150.28	387024.714	6675767.237	47.573	40.968	Filled fractures	4	1
150.31	387024.722	6675767.244	49.363	24.728	Unfilled fractures		1
150.58	387024.793	6675767.303	312.653	32.692	Tight fractures		
150.89	387024.875	6675767.372	282.803	38.772	Tight fractures		
151.00	387024.904	6675767.396	285.783	33.912	Filled fractures	4	1
151.16	387024.946	6675767.432	48.773	22.448	Filled fractures	4	2
151.31	387024.986	6675767.465	51.153	23.588	Unfilled fractures		2
151.37	387025.002	6675767.478	298.923	30.032	Filled fractures	4	2
151.59	387025.06	6675767.527	111.753	12.188	Filled fractures	4	2
151.64	387025.073	6675767.538	318.623	31.468	Unfilled fractures		1

151.72	387025.094	6675767.556	294.143	36.502	Tight fractures		
151.89	387025.139	6675767.593	218.323	2.622	Filled fractures	4	1
152.09	387025.192	6675767.637	49.063	2.418	Filled fractures	4	2
152.35	387025.261	6675767.695	233.843	9.092	Filled fractures	4	2
152.66	387025.411	6675767.605	313.464	16.343	Filled fractures	4	2
152.68	387025.417	6675767.61	140.934	9.953	Filled fractures	4	3
153.22	387025.56	6675767.728	259.144	29.083	Filled fractures	1	3
155.37	387026.129	6675768.202	315.854	70.347	Filled fractures	1	3
155.89	387026.266	6675768.316	318.244	39.957	Unfilled fractures		1
156.04	387026.306	6675768.349	236.454	14.833	slickenside	3	1
156.04	387026.306	6675768.349	88.094	11.067	slickenside	3	1
156.51	387026.431	6675768.453	354.064	65.727	slickenside	3	1
156.59	387026.452	6675768.47	181.524	28.583	slickenside	3	1
156.92	387026.539	6675768.543	316.454	39.957	Filled fractures	1	3
156.96	387026.55	6675768.552	273.464	8.213	Filled fractures	1	2
157.50	387026.733	6675768.581	139.874	52.531	slickenside	3	1
160.17	387027.44	6675769.167	347.044	55.109	Filled fractures	1	2
160.37	387027.493	6675769.211	50.324	43.869	Tight fractures		
160.46	387027.517	6675769.231	50.324	44.819	Tight fractures		
160.54	387027.538	6675769.248	50.324	44.819	Filled fractures	1	1
161.94	387027.909	6675769.556	221.074	21.871	Filled fractures	1	1
162.34	387028.015	6675769.644	53.314	39.919	Unfilled fractures		1
162.64	387028.124	6675769.696	50.984	41.937	Unfilled fractures		1
163.10	387028.246	6675769.797	45.014	37.877	Tight fractures		
164.08	387028.505	6675770.012	62.924	46.707	Unfilled fractures		3
164.17	387028.529	6675770.032	52.774	37.877	Unfilled fractures		3
164.81	387028.699	6675770.173	72.474	37.877	Unfilled fractures		2
166.59	387029.171	6675770.563	147.104	56.533	Tight fractures		
167.71	387029.498	6675770.725	156.652	42.601	slickenside	3	1
168.87	387029.806	6675770.979	98.142	38.909	Filled fractures	1	2
168.99	387029.838	6675771.005	82.622	40.939	Unfilled fractures		3
169.92	387030.085	6675771.209	112.472	42.909	Unfilled fractures		1
170.08	387030.127	6675771.244	222.922	54.591	Unfilled fractures		3
170.46	387030.228	6675771.327	340.232	9.929	Unfilled fractures		2
170.74	387030.302	6675771.388	213.962	26.541	slickenside	3	1
170.94	387030.355	6675771.432	211.572	49.411	slickenside	3	1
171.52	387030.509	6675771.559	50.982	32.539	Unfilled fractures		1
171.94	387030.621	6675771.651	177.542	62.071	slickenside	3	1
172.39	387030.74	6675771.749	49.192	33.629	Unfilled fractures		2
172.47	387030.761	6675771.767	73.072	41.929	Unfilled fractures		2
172.93	387030.956	6675771.739	338.913	33.615	Unfilled fractures		1
172.94	387030.959	6675771.741	350.853	20.115	Unfilled fractures		2
173.43	387031.089	6675771.848	196.823	49.965	Tight fractures		
173.89	387031.211	6675771.949	135.333	40.285	slickenside	3	1
174.06	387031.257	6675771.986	203.983	42.375	slickenside	3	1
174.56	387031.389	6675772.095	129.063	5.545	Filled fractures	4	2

175.03	387031.514	6675772.197	43.983	32.525	Unfilled fractures		1
175.92	387031.751	6675772.392	213.543	33.555	Filled fractures	4	2
176.74	387031.969	6675772.57	205.773	4.585	Unfilled fractures		1
176.84	387031.995	6675772.592	226.073	1.685	Unfilled fractures		1
177.02	387032.043	6675772.632	221.893	38.195	slickenside	3	1
177.24	387032.102	6675772.68	51.743	42.895	Filled fractures	1	2
177.63	387032.245	6675772.679	43.501	50.221	Filled fractures	1	1
177.97	387032.336	6675772.753	50.061	39.911	Unfilled fractures		1
178.58	387032.498	6675772.885	293.651	33.159	Filled fractures	1	1
179.02	387032.615	6675772.981	261.411	41.629	Filled fractures	1	1
179.24	387032.673	6675773.029	240.511	36.199	Filled fractures	1	1
179.94	387032.86	6675773.182	46.481	39.911	Filled fractures	1	1
180.07	387032.894	6675773.21	140.511	87.879	Tight fractures		
180.97	387033.134	6675773.406	186.181	22.499	Filled fractures	1	1
181.02	387033.147	6675773.417	213.651	32.739	Filled fractures	1	2
181.67	387033.32	6675773.558	238.121	26.009	Filled fractures	1	1
182.40	387033.514	6675773.717	35.141	28.081	Unfilled fractures		1
185.21	387034.321	6675774.266	125.946	34.668	Filled fractures	1	1
185.69	387034.449	6675774.37	186.246	25.472	Tight fractures		
186.72	387034.723	6675774.594	176.096	39.432	slickenside	3	1
187.37	387034.896	6675774.735	41.766	49.348	Unfilled fractures		2
187.51	387035.023	6675774.705	174.397	14.105	slickenside	5	1
187.57	387035.039	6675774.718	176.787	10.845	Unfilled fractures		3
187.97	387035.146	6675774.805	170.817	9.135	Filled fractures	4	2
188.53	387035.296	6675774.926	283.657	33.155	Tight fractures		
188.82	387035.373	6675774.989	216.787	32.315	Unfilled fractures		1
188.86	387035.384	6675774.998	37.687	71.675	slickenside	3	1
189.28	387035.496	6675775.089	229.327	32.315	Unfilled fractures		1
191.19	387036.005	6675775.504	106.937	25.825	Filled fractures	4	1
191.38	387036.056	6675775.545	146.337	2.665	Filled fractures	4	2
191.59	387036.112	6675775.591	95.597	42.895	slickenside	4	1
194.16	387036.807	6675776.072	143.451	49.421	Filled fractures	1	3
194.45	387036.884	6675776.135	142.851	47.091	Filled fractures	1	1
194.90	387037.004	6675776.232	213.901	2.661	Filled fractures	1	1
195.10	387037.057	6675776.276	207.331	21.231	Filled fractures	1	1
196.67	387037.476	6675776.616	50.911	30.319	Unfilled fractures		1
197.84	387037.777	6675776.836	229.439	57.431	slickenside	3	1
197.99	387037.817	6675776.868	230.629	39.741	Filled fractures	1	2
199.13	387038.121	6675777.115	220.479	35.131	Filled fractures	1	3
199.17	387038.132	6675777.124	215.109	45.471	Filled fractures	1	1
199.23	387038.148	6675777.137	221.079	52.761	Filled fractures	1	3
199.60	387038.247	6675777.217	232.419	56.931	Filled fractures	1	3
199.88	387038.321	6675777.278	234.209	52.561	Filled fractures	1	2
200.13	387038.388	6675777.332	238.389	53.881	Filled fractures	1	3
201.90	387038.86	6675777.715	218.389	84.511	Filled fractures	1	3
202.08	387038.908	6675777.754	157.199	55.531	slickenside	3	1

205.37	387039.798	6675778.414	71.243	85.66	Unfilled fractures		2
207.41	387040.343	6675778.855	223.483	35.85	Filled fractures	1	2
208.11	387040.568	6675778.866	131.007	50.185	Unfilled fractures		1
208.24	387040.603	6675778.894	223.547	47.305	slickenside	3	1
208.40	387040.646	6675778.928	186.527	10.885	Filled fractures	1	3
208.65	387040.712	6675778.982	219.367	25.495	Filled fractures	1	2
208.71	387040.728	6675778.995	222.947	17.155	Filled fractures	1	2
208.76	387040.742	6675779.006	221.757	21.275	Filled fractures	1	2
211.06	387041.356	6675779.502	245.637	23.755	Filled fractures	1	2
211.44	387041.457	6675779.584	46.227	57.305	Unfilled fractures		3
211.95	387041.593	6675779.694	241.457	17.875	Filled fractures	1	2
212.37	387041.706	6675779.784	257.577	51.715	Filled fractures	1	3
212.42	387041.719	6675779.795	19.367	54.295	Filled fractures	6	1
212.88	387041.961	6675779.751	102.498	44.766	Filled fractures	6	3
212.96	387041.982	6675779.768	229.068	0.744	Filled fractures	6	1
213.04	387042.004	6675779.785	51.158	43.816	Filled fractures	6	1
213.11	387042.023	6675779.8	326.978	39.866	Unfilled fractures		2
213.21	387042.049	6675779.822	123.998	80.466	Filled fractures	6	1
213.32	387042.079	6675779.845	209.968	8.304	Filled fractures	6	2
213.36	387042.089	6675779.854	201.008	17.884	Filled fractures	6	1
213.44	387042.111	6675779.871	145.488	55.834	Filled fractures	6	1
213.52	387042.132	6675779.888	194.438	3.684	Filled fractures	6	1
213.59	387042.151	6675779.903	195.638	11.734	Filled fractures	6	2
213.73	387042.188	6675779.934	208.168	19.284	Filled fractures	6	1
213.78	387042.202	6675779.944	193.248	12.554	Filled fractures	6	1
213.95	387042.247	6675779.981	77.428	45.706	Filled fractures	6	2
214.13	387042.296	6675780.019	207.578	18.594	Filled fractures	6	1
215.72	387042.721	6675780.361	235.638	6.504	Filled fractures	6	3
215.92	387042.774	6675780.404	238.618	4.634	Filled fractures	6	2
216.12	387042.828	6675780.447	170.558	43.594	slickenside	3	1
216.32	387042.881	6675780.49	51.758	42.846	Filled fractures	1	2
216.56	387042.946	6675780.542	34.438	43.816	Filled fractures	1	2
217.24	387043.128	6675780.688	236.228	35.884	Filled fractures	1	3
218.98	387043.677	6675780.919	173.689	38.553	Filled fractures	1	2
219.33	387043.77	6675780.994	170.109	24.923	slickenside	3	1
219.36	387043.778	6675781	164.729	27.653	slickenside	3	1
219.42	387043.794	6675781.013	180.259	14.143	slickenside	3	1
219.47	387043.808	6675781.024	170.699	14.143	slickenside	3	1
219.52	387043.821	6675781.035	165.929	20.623	slickenside	3	1
220.20	387044.003	6675781.18	232.199	33.593	Unfilled fractures		2
220.51	387044.087	6675781.247	122.939	82.807	slickenside	3	1
220.51	387044.087	6675781.247	255.479	33.593	slickenside	3	1
220.69	387044.135	6675781.285	155.779	17.153	slickenside	3	1
220.73	387044.145	6675781.294	150.999	17.873	slickenside	3	1
221.33	387044.306	6675781.423	194.579	17.873	Filled fractures	1	2
221.37	387044.317	6675781.431	189.209	34.383	Filled fractures	1	2

221.52	387044.357	6675781.463	321.149	67.807	Filled fractures	1	1
221.81	387044.435	6675781.525	268.019	9.173	Filled fractures	1	1
221.84	387044.443	6675781.532	201.749	8.293	Unfilled fractures		1
221.96	387044.475	6675781.558	325.329	39.877	Filled fractures	1	1
222.12	387044.518	6675781.592	143.239	53.973	slickenside	3	1
222.30	387044.566	6675781.63	136.079	54.953	slickenside	3	1
222.45	387044.606	6675781.663	128.909	72.077	slickenside	3	1
222.49	387044.617	6675781.671	131.299	71.197	Tight fractures		
222.62	387044.851	6675781.464	50.217	50.163	Filled fractures	1	1
223.09	387044.978	6675781.565	55.587	68.293	Filled fractures	1	1
223.79	387045.166	6675781.714	37.077	87.763	Filled fractures	1	1
225.00	387045.491	6675781.972	86.927	6.553	Filled fractures	1	1
228.71	387046.893	6675782.542	312.661	38.227	Unfilled fractures		1
230.76	387047.448	6675782.977	130.571	75.673	Filled fractures	1	1
231.39	387047.618	6675783.111	144.301	41.657	slickenside	3	1
231.58	387047.669	6675783.151	134.751	39.883	Filled fractures	1	2
231.81	387047.732	6675783.2	190.861	39.447	slickenside	3	1
231.88	387047.751	6675783.215	207.581	39.747	slickenside	3	1
232.00	387047.783	6675783.241	97.731	28.053	Filled fractures	1	1
232.07	387047.802	6675783.255	159.821	17.867	Filled fractures	1	3
232.37	387047.883	6675783.319	177.131	41.397	Tight fractures		
232.59	387048.295	6675783.262	160.685	45.601	slickenside	3	1
232.91	387048.382	6675783.33	291.425	14.071	Filled fractures	1	1
233.30	387048.489	6675783.413	188.145	43.511	Filled fractures	1	1
235.54	387049.098	6675783.887	40.685	81.359	Unfilled fractures		3
235.98	387049.218	6675783.98	180.385	55.611	Unfilled fractures		1
237.42	387049.61	6675784.285	48.445	46.719	slickenside	3	1
237.46	387049.621	6675784.294	71.125	46.719	Filled fractures	1	1
238.38	387050.42	6675784.269	295.178	33.875	Tight fractures		
239.42	387050.705	6675784.488	283.228	31.805	Tight fractures		
240.56	387051.018	6675784.728	281.438	20.505	Filled fractures	1	2
240.71	387051.059	6675784.76	240.848	37.145	Filled fractures	1	1
241.71	387051.333	6675784.971	52.188	41.005	Filled fractures	1	1
242.85	387052.204	6675784.817	164.374	47.737	Tight fractures		
244.00	387052.522	6675785.058	60.494	51.263	Filled fractures	1	2
244.16	387052.567	6675785.091	62.284	68.033	Unfilled fractures		2
244.66	387052.705	6675785.196	31.834	40.103	slickenside	3	1
244.82	387052.749	6675785.229	57.514	61.653	Filled fractures	1	1
245.34	387052.893	6675785.338	45.574	48.673	Filled fractures	1	1
245.54	387052.948	6675785.38	74.224	54.523	Filled fractures	1	1
245.64	387052.976	6675785.401	182.284	40.367	Filled fractures	1	1
246.27	387053.15	6675785.533	64.674	45.003	Filled fractures	1	1
246.54	387053.225	6675785.589	50.344	34.873	Filled fractures	1	1
247.37	387053.455	6675785.763	211.834	87.157	Unfilled fractures		1
248.54	387054.077	6675785.539	89.496	58.957	Filled fractures	1	1
248.91	387054.18	6675785.616	51.286	46.867	Unfilled fractures		1

249.97	387054.475	6675785.835	57.856	57.527	Unfilled fractures		1
250.51	387054.625	6675785.947	110.986	47.767	Filled fractures	1	2
250.86	387054.722	6675786.02	217.856	48.953	slickenside	3	1
251.16	387054.806	6675786.082	106.206	52.097	Filled fractures	1	1
251.89	387055.008	6675786.233	49.496	47.767	Unfilled fractures		1
252.17	387055.086	6675786.292	41.736	77.637	Filled fractures	1	1
252.43	387055.159	6675786.345	50.086	82.037	Unfilled fractures		2
252.89	387055.635	6675786.163	183.02	46.578	slickenside	3	1
253.20	387055.721	6675786.227	55.86	58.232	Unfilled fractures		1
253.27	387055.741	6675786.241	55.86	58.942	Tight fractures		
253.72	387055.867	6675786.334	68.4	71.842	Filled fractures	1	1
255.32	387056.313	6675786.664	319.14	62.272	slickenside	3	1
256.12	387056.537	6675786.829	110.78	51.242	Filled fractures	1	1
258.34	387057.569	6675787.15	116.919	45.052	Filled fractures	1	1
263.85	387059.479	6675788.226	65.262	73.671	Unfilled fractures		1
265.26	387059.877	6675788.516	179.892	52.039	Filled fractures	1	2
265.50	387059.945	6675788.565	181.082	55.889	Tight fractures		
265.75	387060.015	6675788.616	175.712	45.729	Tight fractures		
266.14	387060.126	6675788.696	195.412	49.139	Filled fractures	1	1
266.48	387060.222	6675788.766	149.442	4.299	Unfilled fractures		1
268.61	387061.089	6675789.137	191.873	44.688	Tight fractures		
274.50	387062.969	6675790.177	144.93	3.269	Filled fractures	1	1
283.54	387065.992	6675792.062	192.796	17.373	Filled fractures	1	1
284.42	387066.244	6675792.243	282.346	49.103	Filled fractures	1	3
285.88	387066.661	6675792.542	59.656	76.527	Unfilled fractures		2
286.66	387066.884	6675792.701	313.986	0.233	Filled fractures	1	1
287.92	387067.497	6675792.855	234.742	47.303	Filled fractures	1	1
289.15	387067.85	6675793.106	350.262	1.797	Filled fractures	1	1
290.74	387068.305	6675793.431	59.812	60.607	Filled fractures	1	2
290.90	387068.351	6675793.464	252.052	27.153	Filled fractures	1	1
291.10	387068.408	6675793.505	138.022	14.413	Tight fractures		
291.33	387068.474	6675793.552	141.012	40.903	Tight fractures		
292.13	387068.703	6675793.715	56.232	43.357	Filled fractures	1	2
292.22	387068.729	6675793.734	163.692	26.093	Tight fractures		
292.41	387068.784	6675793.772	148.772	37.413	Filled fractures	1	3
292.62	387068.906	6675793.766	192.459	39.762	Filled fractures	1	1
292.79	387068.954	6675793.801	154.249	42.562	Filled fractures	1	1
292.89	387068.983	6675793.821	182.909	23.782	Filled fractures	1	2
293.02	387069.02	6675793.848	53.949	56.388	Tight fractures		
293.32	387069.106	6675793.909	53.359	57.138	Filled fractures	1	1
293.56	387069.175	6675793.958	182.309	54.242	Filled fractures	1	3
293.61	387069.189	6675793.968	182.909	54.002	Filled fractures	1	3
293.78	387069.238	6675794.003	238.429	10.322	Filled fractures	1	3
293.83	387069.252	6675794.013	242.009	7.732	Filled fractures	4	2
294.07	387069.321	6675794.062	243.209	14.352	Filled fractures	4	2
294.23	387069.367	6675794.095	197.829	21.352	Filled fractures	4	1

294.40	387069.416	6675794.13	181.119	46.402	Crushed zones		3
295.14	387069.628	6675794.281	188.279	47.072	Crushed zones		3
295.37	387069.694	6675794.328	171.559	13.582	Filled fractures	1	3
295.49	387069.728	6675794.352	243.799	38.892	Tight fractures		
296.00	387069.875	6675794.457	157.829	14.352	Filled fractures	1	1
296.56	387070.035	6675794.571	308.879	29.082	Filled fractures	1	1
296.80	387070.104	6675794.62	273.059	27.092	Filled fractures	1	2
297.34	387070.259	6675794.73	301.119	29.082	Tight fractures		
297.64	387070.443	6675794.635	227.656	26.083	Filled fractures	1	2
298.10	387070.575	6675794.729	47.066	10.387	Filled fractures	1	1
300.03	387071.129	6675795.122	311.246	38.943	Filled fractures	1	1
300.23	387071.186	6675795.163	240.796	41.403	Filled fractures	1	1
300.86	387071.367	6675795.291	317.806	82.827	Filled fractures	1	2
301.53	387071.559	6675795.427	305.276	41.403	Tight fractures		
316.75	387076.443	6675798.448	281.666	39.159	Filled fractures	1	2
317.93	387076.91	6675798.613	275.752	32.976	Filled fractures	5	1
318.19	387076.985	6675798.666	126.492	40.494	Filled fractures	5	1
319.20	387077.277	6675798.871	116.342	43.474	Unfilled fractures		2
325.64	387079.178	6675799.96	56.124	51.654	Filled fractures	2	1
326.44	387079.41	6675800.122	272.844	31.736	Filled fractures	1	1
327.00	387079.572	6675800.235	88.964	84.804	Filled fractures	1	3
327.37	387079.679	6675800.31	87.774	85.854	Filled fractures	1	3
327.62	387079.946	6675800.019	96.843	78.329	Filled fractures	1	3
327.77	387079.989	6675800.049	224.603	20.041	Filled fractures	1	2
328.42	387080.178	6675800.18	235.353	18.001	Filled fractures	1	2
328.53	387080.21	6675800.202	243.113	21.331	Filled fractures	1	1
328.73	387080.268	6675800.242	294.453	31.771	Filled fractures	1	2
330.63	387080.818	6675800.625	229.983	26.011	Unfilled fractures		1
330.69	387080.836	6675800.637	253.863	17.291	Filled fractures	1	3
330.93	387080.905	6675800.686	276.843	88.611	Filled fractures	1	3
331.63	387081.108	6675800.827	225.203	32.611	Filled fractures	1	2
331.72	387081.134	6675800.845	228.783	38.581	Filled fractures	1	1
332.12	387081.25	6675800.925	201.323	41.081	Filled fractures	1	1
333.00	387081.841	6675800.816	281.593	6.79	Filled fractures	1	2
333.15	387081.884	6675800.846	45.773	56.43	Unfilled fractures		1
333.51	387081.989	6675800.918	55.323	36.32	Tight fractures		
334.21	387082.193	6675801.059	228.453	15.07	Filled fractures	1	1
334.75	387082.35	6675801.167	263.083	21.31	Filled fractures	1	3
334.82	387082.37	6675801.181	272.633	24.32	Filled fractures	1	3
334.84	387082.376	6675801.185	277.413	22.55	Filled fractures	1	2
337.15	387083.048	6675801.649	271.443	43.64	Filled fractures	1	2
337.96	387083.496	6675801.504	236.37	8.549	Filled fractures	1	3
342.38	387084.784	6675802.387	305.02	33.759	Filled fractures	1	3
343.13	387085.163	6675802.166	82.841	10.48	Filled fractures	1	1
344.69	387085.619	6675802.476	119.561	54.9	Filled fractures	1	1
349.49	387087.224	6675803.228	235.544	2.106	Filled fractures	1	1

349.70	387087.285	6675803.269	306.594	22. 556	Tight fractures		
351.27	387087.745	6675803.58	295.844	24.896	Filled fractures	1	2
352.08	387087.982	6675803.741	274.944	53.376	Filled fractures	1	1
352.18	387088.011	6675803.76	277.334	32.996	Filled fractures	1	1
352.38	387088.069	6675803.8	275.544	11.126	Unfilled fractures		1
354.53	387088.898	6675804.041	301.312	29.961	Filled fractures	1	1
354.89	387089.003	6675804.113	278.032	30.861	Filled fractures	1	2
355.27	387089.115	6675804.188	264.302	27.031	Unfilled fractures		2
358.57	387090.231	6675804.686	318.177	74.77	Filled fractures	1	1
366.05	387090.231	6675804.686	225.092	52.807	Filled fractures	1	2
366.54	387090.231	6675804.686	173.142	19.317	Filled fractures	1	1
368.42	387090.231	6675804.686	269.26	12.71	Unfilled fractures		1
368.73	387090.231	6675804.686	213.14	28.03	Filled fractures	1	1
369.49	387090.231	6675804.686	213.14	30.85	Filled fractures	1	1

Fillings
1dark green
2 grey
3 slickenside filling, green
4 red, sticky
5 red, not sticky
6 two fillings, red and green
7 light green, not sticky

Roughness
1 smooth
2 moderately smooth
3 rough surfaces

APPENDIX III. The outcrop fractures

Outcrop	X	Y	Z	dip	azimuth	strike	Fracture surface	Fracture surface roughness	Fracture lenght	Aperture	Slickenside	Notes/ colour of the filling
1	386897.0	6675905.0	31.74	55.0	45.0	315.0	2	inaccessible	4			
1	386881.0	6675896.0	32.74	60.0	165.0	75.0	2	2	7	5	no	
1	386888.0	6675899.0	32.84			240.0	2	inaccessible	8,5			
1	386882.0	6675910.0	32.78	65.0	150.0	60.0	2	2	2	4	no	
1	386862.0	6675892.0	31.61			250.0	2	inaccessible	6			
1	386893.0	6675912.0	32.52			320.0	2	inaccessible	5			
1	386895.0	6675913.0	32.38	90.0	45.0	315.0	1	1	5	no other side	yes	
2	386985.0	6675736.0	26.93			230.0	2	inaccessible	4	3	can not be defined	
2	386979.0	6675736.0	26.86			260.0	2	inaccessible	2	10	can not be defined	
2	386976.0	6675734.0	26.78	70.0	170.0	80.0	2	2	2,5	3	can not be defined	
2	386976.0	6675722.0	25.76	50.0	310.0	220.0	1	2	1,5	5	can not be defined	
2	386970.0	6675723.0	25.65			215.0	2	inaccessible	11	9	can not be defined	
2	386969.0	6675721.0	25.51	65.0	180.0	90.0	2	2	6	3	can not be defined	
2	386968.0	6675726.0	25.75			175.0	2	inaccessible	6,5	4	can not be defined	
2	386992.0	6675731.0	26.07			40.0	2	inaccessible	2	1	can not be defined	
2	386963.0	6675718.0	25.58			240.0	3	inaccessible	3,5	4	can not be defined	

Outcrop	X	Y	Z	dip	azimuth	strike	Fracture surface	Fracture surface roughness	Fracture lenght	Aperture	Slickenside	Notes/ colour of the filling
2	386964.0	6675718.0	25.50			80.0	1	inaccessible	2.5	2	can not be defined	
2	386964.0	6675715.0	25.03			290.0	3	inaccessible	6	10	can not be defined	
3	386954.0	6675975.0	30.99	90.0	200.0	110.0	1	1	6	no other	yes	multicolour
3	386942.000000	6675981.0	30.98	65.0	230.0	140.0	1	1	1.5	no other side	yes	red
3	386952.0	6675975.0	31.03	60.0	170.0	80.0	2	1	4	2	no	green
3	386953.0	6675982.0	31.17	75.0	200.0	110.0	1	1	2.3	3	no	red-green
3	386946.0	6675987.0	31.05	60.0	260.0	170.0	1	1	1.5	no other side	no	red-green
3	386940.0	6675990.0	31.01	90.0	270.0	180.0	1	1	1.2	10	no	red-green
4	386958.0	6676190.0	17.61			340.0	2	inaccessible	7	4	can not be defined	
4	386953.0	6676143.0	15.63			10.0	1	inaccessible	1.3	7	can not be defined	
4	386951.0	6676201.0	17.18	80.0	150.0	60.0	3	2	2	1	can not be defined	
4	386952.0	6676201.0	17.21	80.0	165.0	75.0	1	inaccessible	1	0	can not be defined	
4	386961.0	6676203.0	16.96			310.0	3	inaccessible	4	3		
4	386978.0	6676210.0	14.82			80.0	1	inaccessible	2.9	0	can not be defined	
5	387160.0	6676269.0	13.86	45.0	300.0	210.0	1	inaccessible	only height	0		
6	387185.0	6676209.0	20.20	85.0	160.0	70.0	1	1	only height			

APPENDIX III. The outcrop fractures (continue)

Outcrop	X	Y	Z	dip	azimuth	strike	Fracture surface	Fracture surface roughness	Fracture lenght	Aperture	Slickenside	Notes/colour of the filling
6	387187.0	6676210.0	20.23	80.0	250.0	160.0	2			0		
6	387188.0	6676212.0	20.16	80.0	260.0	170.0	2	1	1.5	0	can not be defined	
6	387183.0	6676201.0	20.91	70.0	250.0	160.0	1	inaccessible	1.5	0	can not be defined	fault surface?
7	387200.0	6676195.0	19.00				1	inaccessible	1.0	0	can not be defined	crack
8	387302.7	6676083.6	19.10	70.0	180.0	90.0	1	inaccessible	only height	1	can not be defined	
8	387300.5	6676070.2	19.00	60.0	180.0	90.0	2	1	only height	0,5	no	red
8	387300.2	6676063.1	18.60	60.0	170.0	80.0	2	1	only height	no other side	no	red-green
8	387299.6	6676061.7	18.70	60.00	170.0	80.0	1	1	only height	1	no	red-green
9	387289.5	6676060.0	17.60				1	1	only height	1	no	red
10	387191.0	6675785.0	9.68	85.0	5.0	275.0	1	1	only height	1	can not be defined	
10	387158.0	6675730.0	10.40	45.0	30.0	300.0	1	1	only height	no other side	no	
10	387060.0	6675672.0	11.55	30.0	80.0	350.0	1	inaccessible	only height	0	can not be defined	
10	387045.0	6675673.0	14.24	70.0	10.0	280.0	1	inaccessible	only height	10	can not be defined	
10	387042.8	6675660.0	10.00	60.0	40.0	310.0	1	inaccessible	only height	1	can not be defined	
10	387041.3	6675658.9	10.00	55.0	40.0	310.0	1	inaccessible	only height	1	can not be defined	

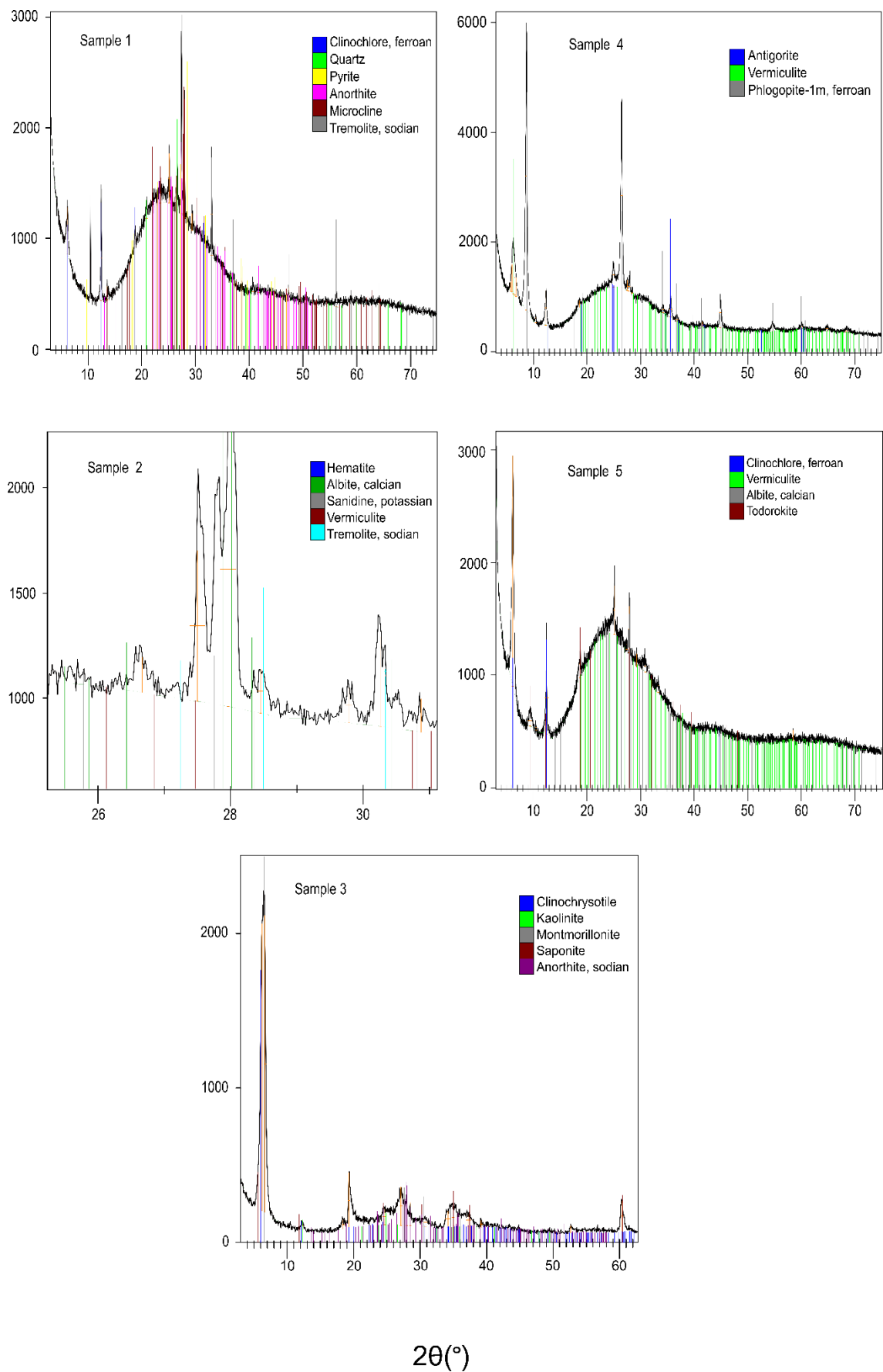# APPENDIX III. The outcrop fractures (continue)

Outcrop	X	Y	Z	dip	azimuth	strike	Fracture surface	Fracture surface roughness	Fracture lenght	Aperture	Slickenside	Notes/ colour of the filling
10	387040.4	6675657.1	10.0	50.0	40.0	310.0	1	inaccessible	only height	1	can not be defined	
10	387040.6	6675654.9	10.0	40.0	40.0	310.0	1	inaccessible	only height	1	can not be defined	

APPENDIX IV. The engineering geological values

Depth from	Depth to	Actual lenght	Over 10 cm parts	RQD	Jn	Jr	Fracture number	Fracture density
0	7.97	7.97	7.76	97.008	9	no data	12	1.506
7.97	8.81	0.84	0.55	94.493	4	no data	5	5.952
8.81	15.16	6.35	6.16	94.753	15	no data	19	2.992
15.16	18.61	3.45	3.26	95.848	12	no data	15	4.348
18.61	21.85	3.24	3.07	91.925	12	no data	10	3.086
21.85	24.74	2.89	2.77	96	6	no data	10	3.46
24.74	26.35	1.61	1.48	95.906	6	no data	8	4.969
26.35	28.6	2.25	2.16	94.213	6	no data	7	3.111
28.6	30.31	1.71	1.64	95.918	3	no data	6	3.509
30.31	38.95	8.64	8.14	100	15	2.11	26	3.009
38.77	43.18	4.41	4.23	99.383	6	1.46	9	2.041
43.18	47.68	4.5	4.5	100	4	1.5	6	1.333
47.68	50.92	3.24	3.22	100	12	2.06	10	3.086
50.92	53.94	3.02	3.02	99.387	4	1.3	5	1.656
53.94	56.39	2.45	2.45	98.525	6	2.75	4	1.633
56.39	64.55	8.16	8.11	96.951	15	1.5	13	1.593
64.55	67.94	3.39	3.34	100	6	1.78	9	2.655
67.94	72.86	4.92	4.77	99.01	15	1.27	16	3.252
72.86	75.72	2.86	2.86	96.923	6	1.36	7	2.448
75.72	83.8	8.08	8	98.328	15	1.72	18	2.228
83.8	87.05	3.25	3.15	98.38	4	2.58	6	1.846
87.05	90.04	2.99	2.94	94.631	6	1.42	6	2.007
90.04	94.36	4.32	4.25	96.035	6	1.17	10	2.315
94.36	100.32	5.96	5.64	88.485	15	1.62	14	2.349
100.32	107.13	6.81	6.54	0	15	1.83	23	3.377
107.13	108.78	1.65	1.46	89.753	2	2.71	6	3.636
108.78	109.21	0.43	0	88.194	20	4	2	0
109.21	122.19	12.98	11.65	89.349	15	1.7	57	4.391
122.19	123.63	1.44	1.27	99.533	3	2.23	12	8.333
123.63	125.32	1.69	1.51	96.121	6	1	6	3.55
125.32	127.46	2.14	2.13	99.034	3	1.3	5	2.336
127.46	132.1	4.64	4.46	95.433	9	1.63	12	2.586
132.1	147.62	15.52	15.37	97.892	15	1.82	24	1.546
147.62	160.54	12.92	12.33	98.577	15	1.64	33	2.554
160.54	164.81	4.27	4.18	100	4	1.67	7	1.639
164.81	181.67	16.86	16.62	96.685	15	1.36	35	2.076
181.67	186.72	5.05	5.05	98.693	15	1	4	0.792
186.72	188.53	1.81	1.75	98.829	3	1.7	5	2.762
188.53	191.59	3.06	3.02	100	6	1	6	1.961
191.59	200.13	8.54	8.44	100	6	1.77	13	1.522
200.13	205.37	5.24	5.24	69.444	9	2.5	3	0.573
205.37	208.4	3.03	3.03	91.026	3	1.63	4	1.32

Depth from	Depth to	Actual lenght	Over 10 cm parts	RQD	Jn	Jr	Fracture number	Fracture density
208.4	208.76	0.36	0.25	94.78	2	2.17	3	8.333
208.76	216.56	7.8	7.1	95.822	15	1.69	24	3.077
216.56	220.2	3.64	3.45	100	9	1.19	8	2.198
220.2	223.79	3.59	3.44	94.488	12	1.16	17	4.735
223.79	230.76	6.97	6.97	100	3	1	3	0.43
230.76	233.3	2.54	2.4	99.154	9	1.44	10	3.937
233.3	235.98	2.68	2.68	100	1	2	2	0.746
235.98	240.71	4.73	4.69	97.455	12	1	6	1.268
240.71	241.71	1	1	99.083	1	1	1	1
241.71	245.64	3.93	3.83	100	9	1.14	8	2.036
245.64	253.27	7.63	7.56	100	3	1.17	15	1.966
253.27	258.34	5.07	5.07	100	12	0.83	4	0.789
258.34	268.61	10.27	10.27	100	3	1.2	7	0.682
268.61	274.5	5.89	5.89	97.968	6	0	1	0.17
274.5	283.54	9.04	9.04	93.377	1	1	1	0.111
283.54	292.89	9.35	9.16	0	1	1.5	15	1.604
292.89	294.4	1.51	1.41	101.176	12	2.06	8	5.298
294.4	295.15	0.75	0	100	20	4	2	0
295.15	296	0.85	0.86	100	3	3	3	3.529
296	298.1	2.1	2.1	100	6	1.25	5	2.381
298.1	301.53	3.43	3.43	100	3	1.25	4	1.166
301.53	325.64	24.11	24.11	98.101	3	1.25	5	0.207
325.64	327.77	2.13	2.13	96.512	6	2.2	5	2.347
327.77	330.93	3.16	3.1	93.233	9	1.67	6	1.899
330.93	333.51	2.58	2.49	100	3	1.58	6	2.326
333.51	334.84	1.33	1.24	100	3	2.33	4	3.008
334.84	337.15	2.31	2.31	100	1	1.5	1	0.433
337.15	349.49	12.34	12.34	93.895	6	2	5	0.405
349.49	358.57	9.08	9.08	0	6	1.25	9	0.991
358.57	370.2	11.63	10.92	0	3	1.17	5	0.43

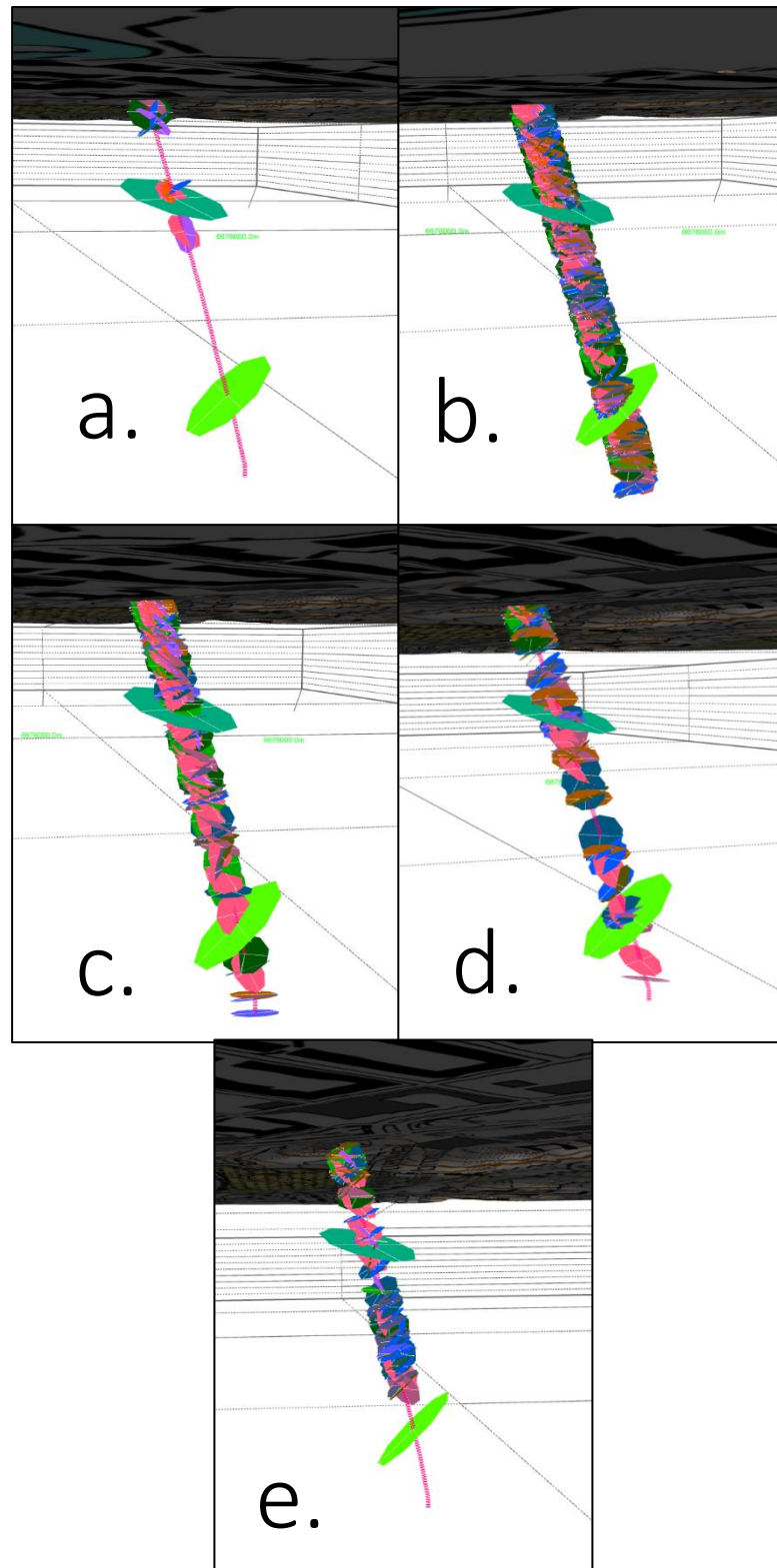## APPENDIX V: The XRD-diffractograms

From N to S

From NE to SW
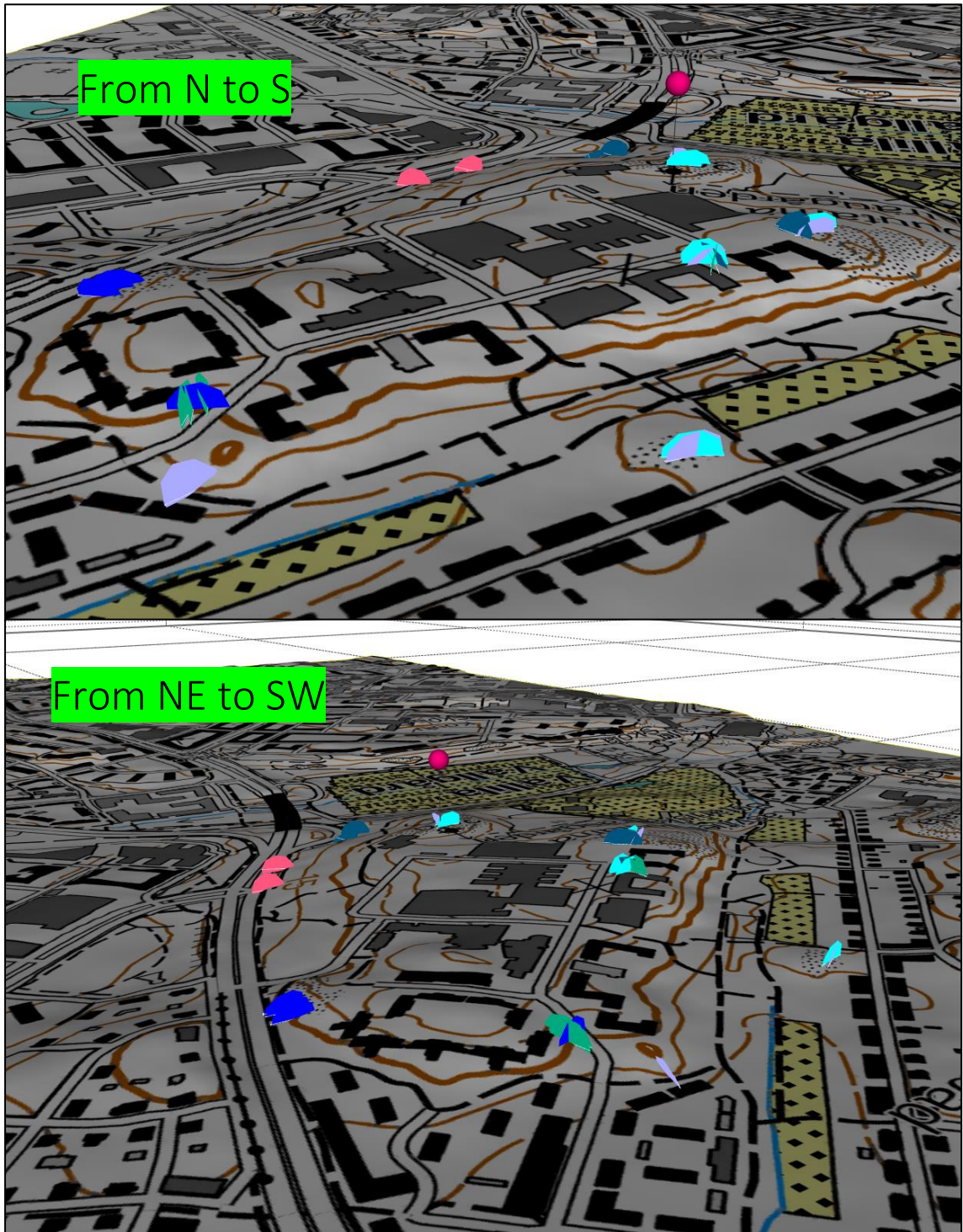
APPENDIX VI. The 3D-images from the drill hole and outcrops (continue)
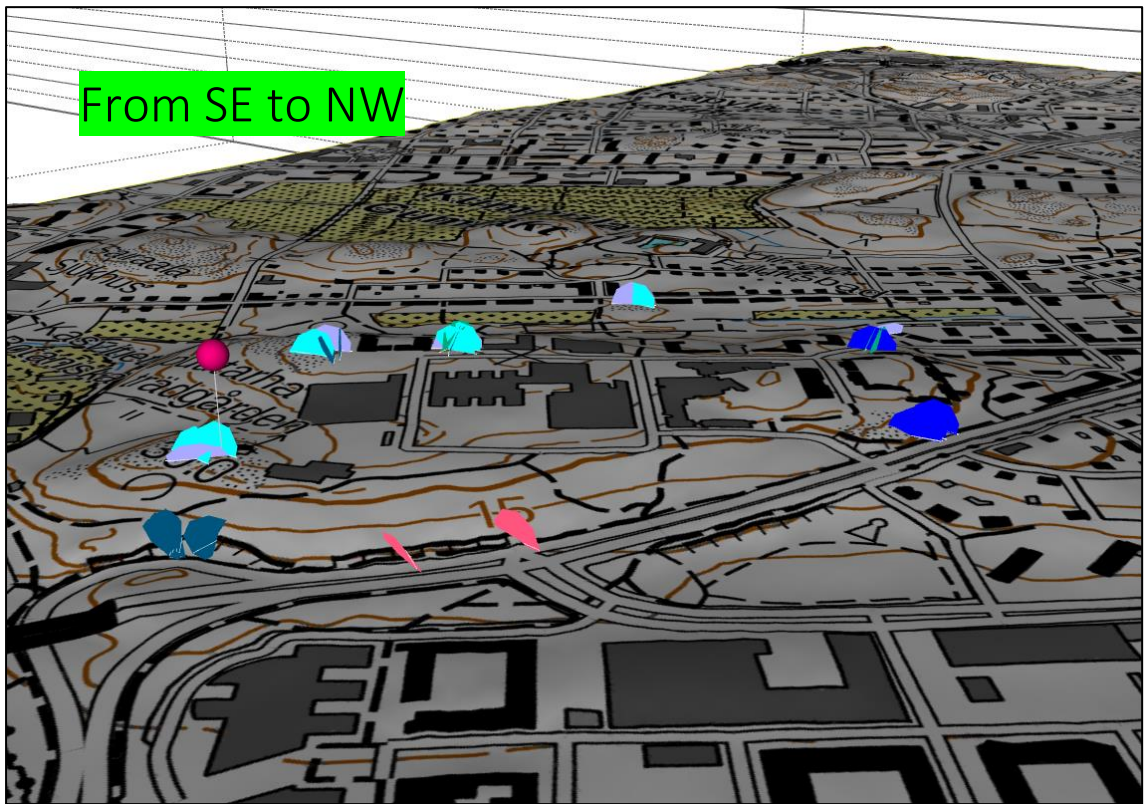
APPENDIX VII: The 2D-map of the crushed zones and 3D image from the crossing point of the crushed zones
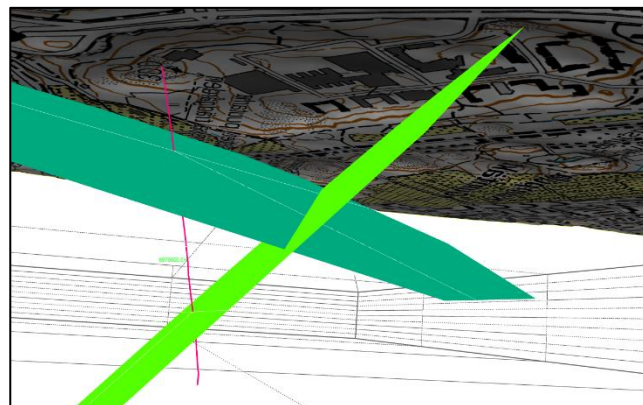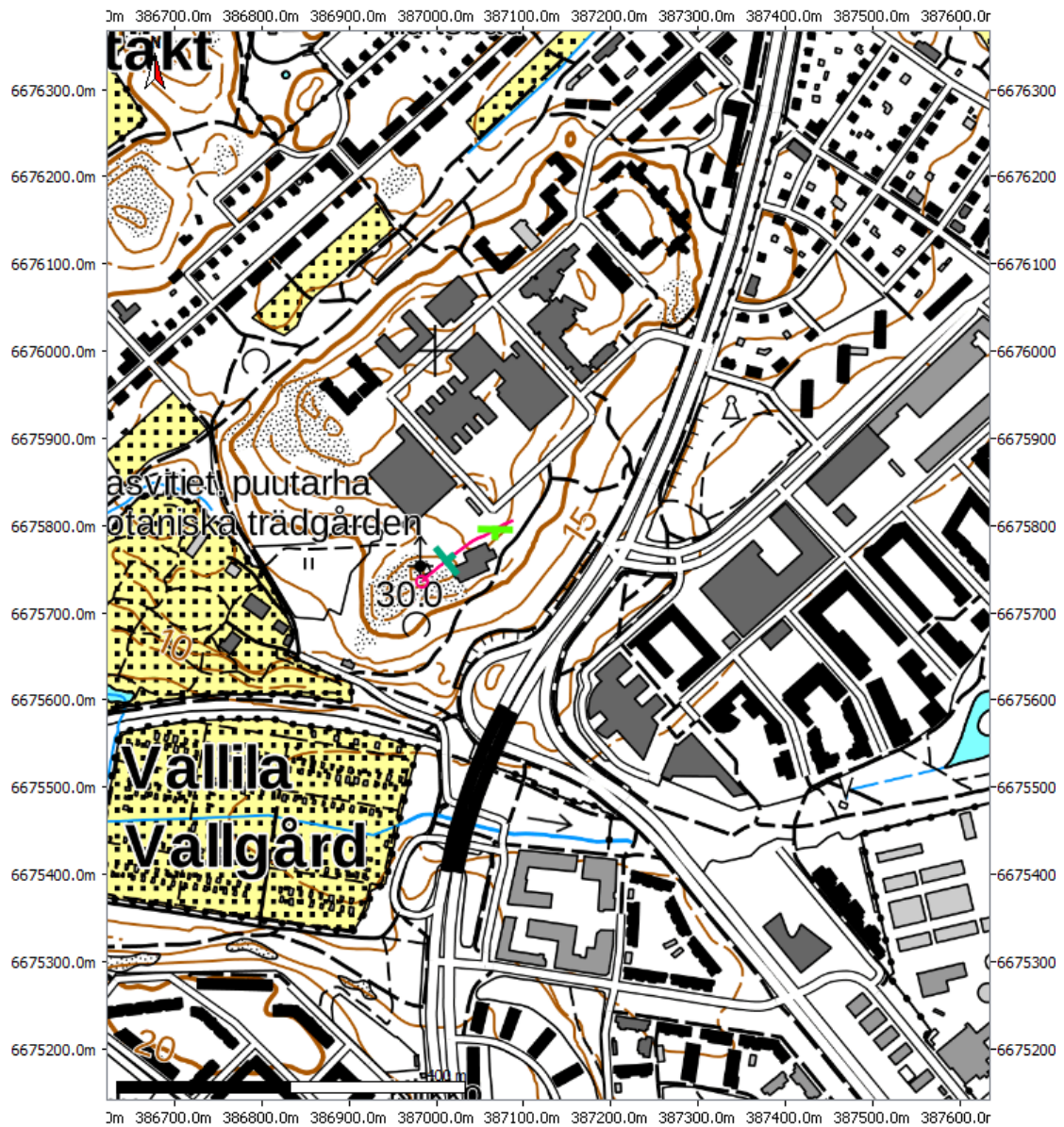
a. the crushed fractures. b. filled fractures. c. unfilled fractures. d. non-opened fractures and e. slickenside fractures